JPC 422

Report Number
TM-66-5

Transpiration Cooling - Its Theory and Application

by

J. B. Kelley

M. R. L'Ecuyer

Contract NsG 592

June 1966

JET PROPULSION CENTER
PURDUE UNIVERSITY

SCHOOL OF MECHANICAL ENGINEERING
LAFAYETTE, INDIANA

ERRATA SHEET

Page

vii — Line 9 . . . access . . . should be, . . . assess

13 — Line 7 . . . ballance . . . should be, . . balance

25 — Equation 2.23 should read

$$\rho_w v_w \frac{d\bar{u}}{dy} = \frac{d}{dy}\left(\mu \frac{d\bar{u}}{dy} - \bar{\rho}' \overline{v' u'}\right)$$

31 — Line 12 . . . is essence . . . should be, . . . in essence

37 — Equation after equation 2.52

$$Sc' = \frac{\epsilon_M}{\rho \epsilon_d}$$

71 — Lines 2 and 3 should read . . . the influence . . . could be isolated

72 — Line 20 should read . . . indicated by the dashed line

84 — Line 19 . . . serios . . . should be, . . . serious

87 — Line 21 . . . ovservation . . . should be, . . . observation

90 — Line 18 . . . pressue . . . should be, . . . pressure

91 — Equation 3.16 should read

$$St = \frac{c_f}{2} (Pr)^{-2/3}$$

92 — Colburn's equation should be

$$St = \frac{c_f}{2} (Pr)^{-0.67}$$

109 — Line 2 . . . Becuase . . . should be, . . . Because

Page	
118	Line 14 should read . . . of cross-sectional area open to flow
125	Line 19 should read . . . materials prepared by
127	Line 16 should read . . . The most obvious
129	Line 2 should read . . . warp wires
	Line 9 should read . . . diminishes chance
130	Line 17 should read . . . analysis are as accurate
141	Line 21 should read . . . March 1955.
	Line 37 should read . . . Water/Steam

PURDUE UNIVERSITY
AND
PURDUE RESEARCH FOUNDATION
Lafayette, Indiana

Report No. TM-66-5

TRANSPIRATION COOLING -- ITS THEORY AND APPLICATION

by

J. B. Kelley
M. R. L'Ecuyer

Technical Memorandum

Contract NsG 592

Jet Propulsion Center
Purdue University

June 1966

ACKNOWLEDGEMENTS

The literature review presented herein was supported by the National Aeronautics and Space Administration under Contract No. NsG 592 (PRF-3837-52-2889).

The authors wish to express their gratitude to Professor C. F. Warner for his suggestions regarding the contents of the subject report.

Appreciation is also expressed to Mrs. Christine Kelley for typing the original manuscript and to Mrs. Nancy Evans for typing the final manuscript.

TABLE OF CONTENTS

LIST OF TABLES

LIST OF FIGURES

ABSTRACT 30856

Transpiration from a porous surface is one of several mass transfer cooling concepts considered for applications in propulsion and related fields. The merits and feasibility of the concept have been demonstrated in numerous theoretical and experimental investigations. The material presented herein comprises a literature review of the various theories proposed and the experimental results obtained in the field of transpiration cooling of turbulent boundary layers.

The over-all objective of the review was to examine the extensive literature pertaining to transpiration cooling and to access the state of the art of this cooling scheme in the following subject areas:

(1) the theoretical analyses pertaining to the correlation of mass injection rates with surface temperature;

(2) the experimental investigations relating to the verification of existing theories and the development of empirical correlations for determining the effects of mass injection on surface heat transfer and skin friction;

(3) the theoretical and experimental studies regarding the characteristics of, and flow through, conventional porous materials.

The more prominent and applicable theories for the turbulent boundary layer with distributed injection are described and compared with the pertinent experimental data. Special emphasis is placed on the physical

(over)

processes involved in the reduction of heat transfer and skin friction due to transpiration from a porous surface. The theoretical and empirical solutions which, at this time, enable the most accurate predictions of mass injection rates for a specified surface temperature are recommended and sample calculations are presented in the appendix to illustrate a typical application.

The experimental investigations are discussed from the standpoint of establishing the influence of the various independent parameters on the skin friction coefficient and the rate of heat transfer. A correlation procedure based on the data is shown to agree with the analyses, the problems due to experimental error being considered. A table summarizing over twenty experimental investigations is included.

A solution for the prediction of mass flow rates through porous materials is recommended and the causes of deviations from these predictions are described qualitatively. The various types of porous materials available are discussed and compared on the basis of the most desirable properties.

Author

1. INTRODUCTION

1.1 General Discussion

Transpiration cooling is one of the more promising solutions to the material's problem imposed on high energy liquid, solid and nuclear rocket engines, atmospheric reentry vehicles and gas turbines by severe local heating. In general, it entails the use of a liquid or gaseous coolant initially separated from a high temperature environment by a porous material; the coolant is forced through the intervening medium by controlled regulation of the supply pressure and emerges in small vertical jets forming a continuous blanket of fluid over the wall. The severe environment encountered may be due either to extremely hot gases outside the boundary layer such as in rocket nozzle cooling applications or to viscous dissipation within the boundary layer as in reentry bodies.

It has been suggested (1)[1] that the definition of transpiration cooling be limited specifically to the case where the coolant and mainstream fluid have identical properties.[2] Others restrict the definition to the case of gas injection and apply the phrase "sweat cooling" (2) to liquids. To avoid confusion in this report, the term

---

[1] Numbers in parentheses refer to references listed in the Bibliography.

[2] Mass transfer cooling would then encompass foreign gas injection, ablation and film cooling.

"transpiration cooling" will not be limited to any particular coolant but will be distinguishable by the use of a porous injector. Downstream of the injector though, the process must be referred to as "film cooling."

Mass transfer techniques were originally proposed because it was realized in the earlier stages of rocket engine development that regenerative cooling could not adequately cope with the increased heat fluxes occurring with the advent of higher thrust chamber pressures and temperatures. There are three reasons for the over-all superior effectiveness of transpiration cooling over the more conventional regenerative cooling. They are: (1) since a large porous surface area is exposed to a relatively small coolant flow rate, the coolant and injector have considerable intimate contact making them an extremely efficient heat exchanger; (2) the coolant is believed to act as an insulator between the wall and freestream; and (3) injection alters the velocity and temperature distributions across the boundary layer in a manner conducive to a much lower heat flux.

The rocket engine cooling techniques which have been studied, and in some cases applied, are film cooling, radiation cooling, inert and endothermic heat sinks, ablation and regenerative cooling. Each has its own characteristic advantages and difficulties and consequently, selecting the most effective and economical method cannot be justified without first considering the particular application. The variety of methods proposed can be partially accounted for by the numerous and diverse space missions of the just as numerous space vehicles that have been designed and/or used. Probably the two most competitive

alternatives to the technique reviewed herein are film cooling and ablation in that both rely on direct contact of the coolant and heat source. Film cooling is more analogous to transpiration on the basis of the potential applications that have been considered because the equipment and coolants required are almost the same for both, the difference between the two being the method of injection. On the other hand, ablation and transpiration cooling have similar mathematical models with distributed injection peculiar to each. The former though is more limited by the application for which it can be used.

The difficulties encountered in experiments with film cooling are chiefly concerned with the problem of maintaining a stable coolant film between the hot gas and the wall. Complete wetting of the surface must be achieved to avoid "hot spots" which readily occur when the wall is not thoroughly protected. Injection is critical since any nonuniformities near the slot continue downstream exposing a considerable portion of the surface to a severe environment. Liquid film cooling has the additional problem of "droplet breakaway" characterized by partial or total destruction of the film by the turbulent shearing action of the boundary layer. Moreover, on the basis of the mass flow rate required to hold a surface at a particular temperature, transpiration cooling has been found more effective.

The two main difficulties with ablation which are intrinsic to its nature are: (1) the surface erodes away continually changing the amount of exposed area and thus the characteristics of the external

flow (a critical factor in nozzles); and (2) as soon as the ablating substance is completely released, protection no longer exists placing a time limit on the usefulness of the concept. The above limitations suggest that ablation would be more serviceable as a means for protecting reentry vehicles and this indeed has been the case. When compared to transpiration cooling on an effectiveness basis,[1] ablation is less efficient since the gases emitted by common ablative materials, in general, have a higher molecular weight than common transpiration coolants (it will be proven later that light gases are superior coolants). Two advantages of ablation cooling often neglected though are its relative economy (no auxiliary equipment such as pumps, regulators, and supply tanks are required) and its ability to be self-controlled (more mass is released automatically if heat rates increase). These are the primary reasons why ablation has been used more in practical systems than its two competitors. Nevertheless, far more experimental work has been conducted on transpiration and film cooling problems ostensibly because they are more amenable to such investigations. For ablation, new surfaces would be required for each individual test. Since the models for ablation and transpiration cooling are very similar, the analyses for the latter can, in general, be applied to the former. This provides an additional motivation for studies of transpiration and cooling and partially accounts for the extensive amount of work reported in the literature.

---

[1] The injection rate required to cool a surface to a specified temperature.

Because there are solid propellant rocket engines presently capable of raising nozzle throat temperatures to well above the limit necessary for maintaining the structural integrity of any material (about 3500 F), there is an immediate demand for supplemental cooling techniques to those in use. One that has been developed to serve in the interim until the difficulties of transpiration cooling are eliminated is cooling with composite materials. For this concept, a sintered metal such as tungsten is infiltrated with a liquid metal forming a "composite" structure when the liquid solidifies at ambient temperatures. Upon exposure to severe heating, the infiltrant (e.g. copper, manganese, silver, zinc, and lithium) boils or sublimes into a liquid or gas and escapes from the interstices of the material due to the increased specific volume. This method thus not only incorporates the advantages of transpiration cooling and ablation but eliminates an obvious difficulty with each, i.e., the need for auxiliary pumping equipment and the continually changing surface area. Unfortunately, there have been many problems[1] encountered with this system also.

1.2 The Scope of the Investigation

The approach employed in writing this report was to develop the state of the art of transpiration cooling as it exists today by reviewing those articles which have made the most significant contributions to the present understanding. There has been considerable

---

[1] cracking due to thermal shock, insert distortion, melting, etc.

work in specific related areas over the past twenty or more years but to the knowledge of the author, no comprehensive surveys have been prepared to evaluate the work of past investigations and to assess the need for future research. Because of this deficit, studies in the subject areas have proceeded in a somewhat random manner. Futhermore, identical problems have been solved by the separate and independent efforts of more than one person. To illustrate, there are at least four similar "mixing length solutions"[1] to the turbulent boundary layer problem with distributed mass injection and heat transfer present.

Although the transpiration cooling literature reviewed herein is rather broad, certain practical limitations were deemed necessary to fulfill the overall objectives of this report. Laminar flow was excluded from the survey because it is generally not encountered in rocket engine applications. Furthermore, blowing, which shall be used synomously with transpiration, induces transition to turbulence. One point which should hopefully become clear later is that very few experimental and analytical mass transfer studies have been directed toward obtaining an understanding of the effects of a pressure gradient upon heat transfer. This area was not excluded from the investigation but receives limited description because of this void in the literature.

This review has been divided into three separate categories under which virtually all articles pertaining to transpiration cooling tend to fall. They are: (1) the theoretical analyses; (2) the experimental

---

[1] See Chapter 3

work; and (3) flow through and characteristics of porous materials. The third major subject area is obviously distinct from the first two closely related categories. The theory and experimental work will be discussed separately in Chapters 2 and 3, respectively, and then compared in Chapter 3. The ultimate objective has been to find a simple and reliable method for predicting skin friction and heat transfer suitable for the design of transpiration cooling systems. An example is included in the appendix to illustrate a typical solution of the problem. In the chapter covering porous materials, the different materials available will be compared and methods for calculating flow rates through them will be outlined. The final chapter is devoted to conclusions and recommendations for future work.

2. REVIEW OF TRANSPIRATION COOLING THEORY

The ultimate objective of a theoretical analysis of transpiration cooling is to assess the influence of coolant injection upon the reduction in heat transfer, a fact which has been observed experimentally. More specifically the problem is to determine the flow rate per unit area necessary to achieve a desired wall temperature when the characteristic parameters of the mainstream,[1] the coolant properties, and reservoir temperature are given. The rate of injection is normally specified by a blowing rate parameter F, defined by the relation

$$F = \frac{(\rho v)_w}{(\rho u)_\infty} \qquad (2.1)^2$$

where

$(\rho v)_w$ = mass flux injected from the porous surface

$(\rho u)_\infty$ = mass flux of mainstream flow

The variable F was selected because it is dimensionless and permits simple comparison of theoretical predictions with experimental results. The starting point for all analyses considered has been the differential form of the boundary layer equations.

---

1 Molecular and turbulent fluid properties, flow rate per unit area, temperature, Mach number, Reynolds number and pressure gradient.

2 For a definition of the symbols, refer to the Nomenclature.

The first theoretical treatment (3) of the problem was published in 1947 and since that time, many improvements and changes have been made by numerous investigators. Nevertheless today there still exists discrepancies not only between theory and experiment but also, between the experimental data of the various investigators. Because a derivation for turbulent flow must utilize experimental data to evaluate unknown constants, at best the result can only be as good as the data it represents. Furthermore, as a consequence of the matching procedure at the wall and the interface of the boundary layer with the mainstream, any given analysis can be forced to fit the data.

In an attempt to elucidate a physical description of the turbulent boundary layer with mass injection, three general solutions to the problem shall be reviewed. They are the derivations due to Rannie (3), Rubesin (4), and Spalding, Auslander, and Sundaram (5). The simplifed analysis of Rannie has become a classic in the literature and represents the starting point for later work. More recent theories have modified that Couette flow analysis to approximate better the mechanism of turbulence in an actual boundary layer. The derivation of Rubesin, which is typical of the more recent theories, will be reviewed in Section 2.2. Following the trend of most present day works, it incorporates one of the phenomenological theories of turbulence, i.e., mixing length theory. The basic assumptions employed by Rubesin describe the most commonly accepted model for the turbulent boundary layer in the presence of mass addition; those assumptions will also be reviewed in detail.

A problem frequently encountered with an analysis such as Rubesin's is the extreme complexity of the equations and the inevitable difficulty in applying the results and obtaining numerical answers. Spalding, Auslander, and Sundaram (5) and Knuth and Dershin (6) have attempted to remedy this situation by approaching the problem from a more empirical point of view combining theory with data to find the equations which best fit the experimental data. For example, by using the data which is tabulated at the end of Reference 5, it is easy to calculate the required mass transfer rates knowing the following specified conditions: (1) density, pressure, temperature, and velocity outside the boundary layer; (2) the condition of the coolant in the reservoir (temperature and pressure); (3) the maximum permissible surface temperature. Hence, one of the more obvious advantages of their result is its simplicity and the relative ease by which answers can be obtained. The need for evaluating complex functions and integrating numerically is eliminated. An additional motivation for their analysis (5) was that the empirical equations could be forced to fit the general trend of the experimental data almost exactly. Other theoretical solutions are based on numerous heuristic assumptions, and consequently, the results become almost meaningless as almost any curve can be obtained if the appropriate assumptions are made. Most authors admit that mixing length theory has little theoretical or experimental basis and, in Reference 7 and 8, it is shown to be wrong. However, because a better approach does not exist, everyone proceeds to use it or some other phenomenological theory.

2.1 Theory of Rannie

At the outset it should be emphasized that the theory due to Rannie (3) represents an oversimplified model which, nevertheless, illustrates the general approach required for solving the problem. Friedman (9) arrived at a similar result by beginning with the same boundary layer model, but he used different experimental data to evaluate the constants introduced by the analysis. Crocco (10) extended the aforementioned analyses to a chemically reactive fluid. The subject investigations (3,9,10) represent the earliest attempts at finding an approximation to the reduction in wall temperature with mass transfer.

The model proposed by Rannie is represented in Figure 2.1 and is described by the following assumptions: (1) The boundary layer is divided into two distinct regions, a laminar sublayer and an outer turbulent region. (2) Fluid physical properties are constant in the laminar sublayer and are identical with those of the coolant; properties are also constant in the turbulent region though they are not necessarily equal to the sublayer values. (3) Derivatives in the x direction are negligible compared to those in the y direction. This is analogous to a fully developed flow in a pipe (without a pressure gradient). (4) Reynolds analogy for heat and momentum transfer is valid restricting the laminar and turbulent Prandtl numbers to unity. (5) The velocity distribution in the laminar sublayer is linear. (6) The skin friction coefficient is given by the relationship for a smooth pipe. (7) No radiation heat transfer occurs.

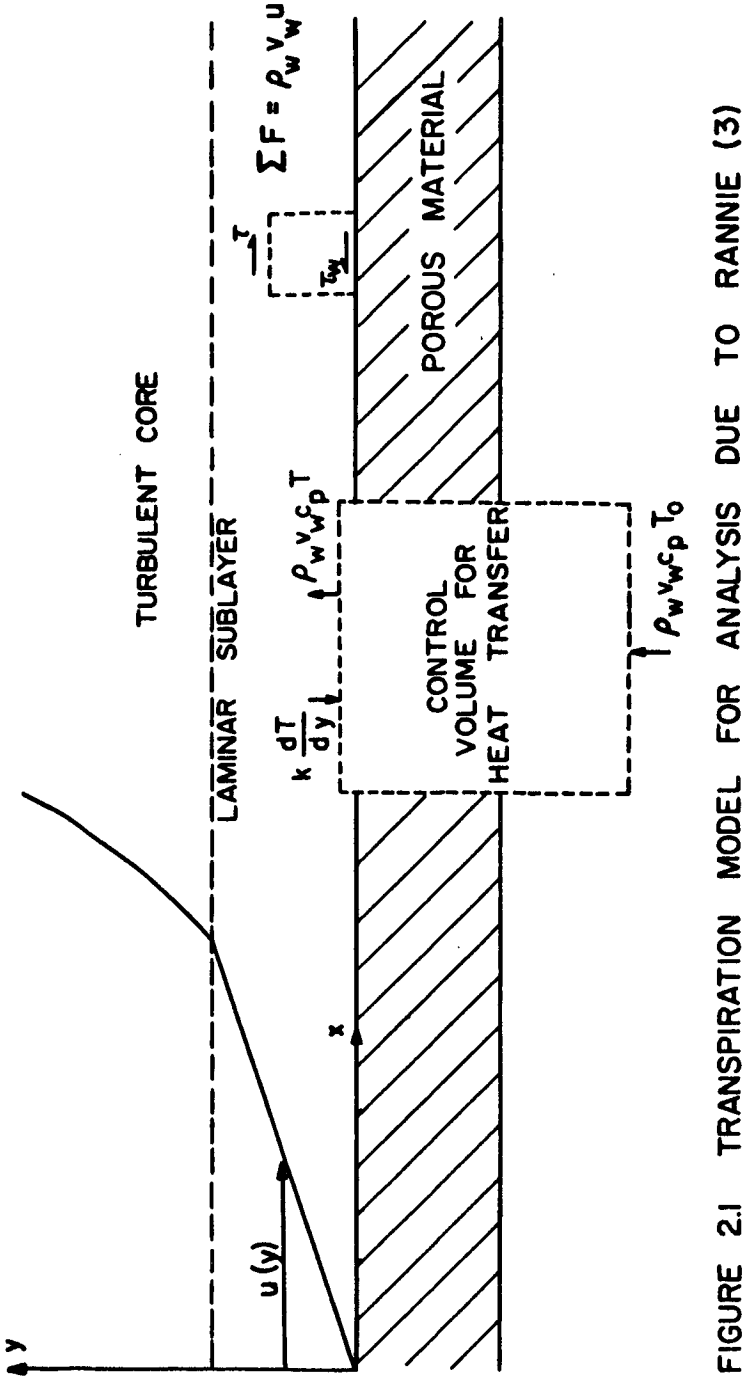

FIGURE 2.1 TRANSPIRATION MODEL FOR ANALYSIS DUE TO RANNIE (3)

With the above assumptions, it is relatively easy to obtain an expression for the surface temperature of the wall as a function of the mainstream and coolant supply temperatures, the blowing rate F, and the properties of the injected fluid. The steps in arriving at the desired result are reviewed briefly below.

Remembering that all variables are constant in the x direction, a momentum ballance for the control volume within the laminar sublayer yields

$$\tau = (\rho v)\ u + \tau_w \tag{2.2}$$

From assumption 3, the continuity equation reduces to

$$\frac{d\ (\rho v)}{d\ y} = 0 \tag{2.3}$$

which, after integrating, gives

$$\rho v = (\rho v)_w \tag{2.4}$$

By substituting the definition of the shear stress

$$\tau = \mu \frac{d\ u}{d\ y} \tag{2.5}$$

into equation 2.2 and integrating, the following relation for the velocity profile is obtained.

$$\frac{u}{u_a} = \frac{\exp\ (\rho_w v_w y/\mu) - 1}{\exp\ (\rho_w v_w y_a/\mu) - 1} \tag{2.6}$$

where the subscript "a" denotes a quantity evaluated at the interface of the turbulent boundary layer and laminar sublayer.

A similar result is obtained from the differential form of the energy equation

$$\rho_w v_w c_{pw} \frac{dT}{dy} = k \frac{d^2 T}{d y^2} \tag{2.7}$$

Integrating equation 2.7 across the laminar sublayer and substituting the appropriate boundary conditions,

$$q = \rho_w v_w c_{pw} (T - T_o)$$

$$T = T_w \quad \text{at} \quad y = o$$

yields the relationship

$$\frac{T - T_o}{T_w - T_o} = \exp\ \left(\frac{\rho_w v_w c_{pw} y}{k}\right) \tag{2.8}$$

Rewriting equation 2.8 in terms of the temperature, T_a, gives

$$\frac{T - T_w}{T_a - T_o} = \frac{\exp\ (Pr\rho_w v_w y/\mu) - 1}{\exp\ (Pr\rho_w v_w y_a/\mu) - 1} \tag{2.9}$$

Since the objective is to find the wall temperature, T_w, as a function of known properties of the mainstream, Rannie resorted to Reynolds analogy to extend the analysis into the outer turbulent region. The form of the analogy was taken directly from Reference 11 and is repeated below for convenience. At the interface between the sublayer and the outer turbulent region, the analogy becomes

$$\frac{q_a}{\rho c_p (T_\infty - T_a)} = \frac{\tau_a}{\rho (u_\infty - u_a)} \tag{2.10}$$

where the quantities q_a, τ_a, and T_a must be evaluated using their respective definitions and the sublayer equations, 2.6 and 2.8. Following this procedure, it is possible to show that

$$\frac{T_w - T_o}{T_\infty - T_o} = \frac{\exp(-Pr\rho_w v_w y_a/\mu)}{1 + \frac{c_p}{c_{pw}} \left(\frac{u_\infty}{u_a} - 1\right) (1 - \exp(-\rho_w v_w y_a/\mu))} \tag{2.11}$$

Although equation 2.11 is the required relationship for the wall temperature, the variables y_a and u_a appearing in that expression remain undetermined. The evaluation of these quantities is critical since regardless of the method employed, empirical approximations are required similar to the ones suggested below. In Section 2.2, it will be seen that Rubesin (4) encountered the same difficulty.

If it is assumed that the velocity profile in the laminar sublayer is linear, the distribution can be given by the expression

$$\frac{u}{u_a} = \frac{y}{y_a} \tag{2.12}$$

Using equation 2.12 for evaluating the shear stress gives

$$\tau_w = \mu \frac{d\,u}{d\,y} = \frac{\mu\, u_a}{y_a} \tag{2.13}$$

or

$$u_a = \frac{\tau_w\, y_a}{\mu}$$

In this manner, the velocity at the sublayer interface is obtained as a function of the shear stress at the wall (τ_w) and the sublayer thickness (y_a). Therefore, a solution using equation 2.11 is possible if the latter two quantities can be found.

To this end, Rannie defines the dimensionless distance y^+ in the usual manner

$$y^+ = \frac{\rho_\infty\, u_\infty}{\mu_\infty} (c_f/2)^{0.5}\, y \tag{2.14}$$

and evaluates it at y_a which yields with some manipulation

$$y_a = \frac{y_a^+\, \nu_\infty}{u_\infty} (2/c_f)^{0.5} \tag{2.15}$$

At the time, there was no existant data relating skin friction with the blowing rate. Consequently, it was necessary to employ the skin friction coefficient determined for a smooth impermeable pipe. Thus

$$c_f = \frac{0.046}{Re_d^{0.2}} \tag{2.16}$$

From more recent experimental results presented in Chapter 3, this is a poor approximation since for a moderate blowing rate, F, of less than 1 percent, the skin friction is reduced from its no blowing value by a factor greater than two.

The only unknown quantity remaining in equation 2.15 is the dimensionless thickness of the sublayer y_a^+. Prandtl found from an examination of velocity distribution data taken close to the wall of a pipe[1] that the dimensionless thickness of the sublayer is 5.6. Using this value for y_a^+ and equation 2.16, the final expression relating wall temperature with other known quantities is

$$\frac{T_\infty - T_w}{T_\infty - T_o} = 1 - \frac{\exp(-37\ Pr\ F\ Re_d^{0.1})}{1 + (1.18\ Re_d^{0.1} - 1)\ (1 - \exp(-37\ F\ Re_d^{0.1}))} \tag{2.17}$$

This is the desired result of the analysis. In Figure 2.2, the experimental results of Duwez and Wheeler (12, 13) are compared with the above equation for two different values of Reynolds number. Though equation 2.17 has no factor accounting for the influence of the properties of the porous wall material, the temperature ratio is seen to be significantly affected by the use of porous injectors of different materials. For a blowing rate (F) of 0.016, the percent difference between theory and experiment is on the order

---

[1] Internal pipe flow with no blowing

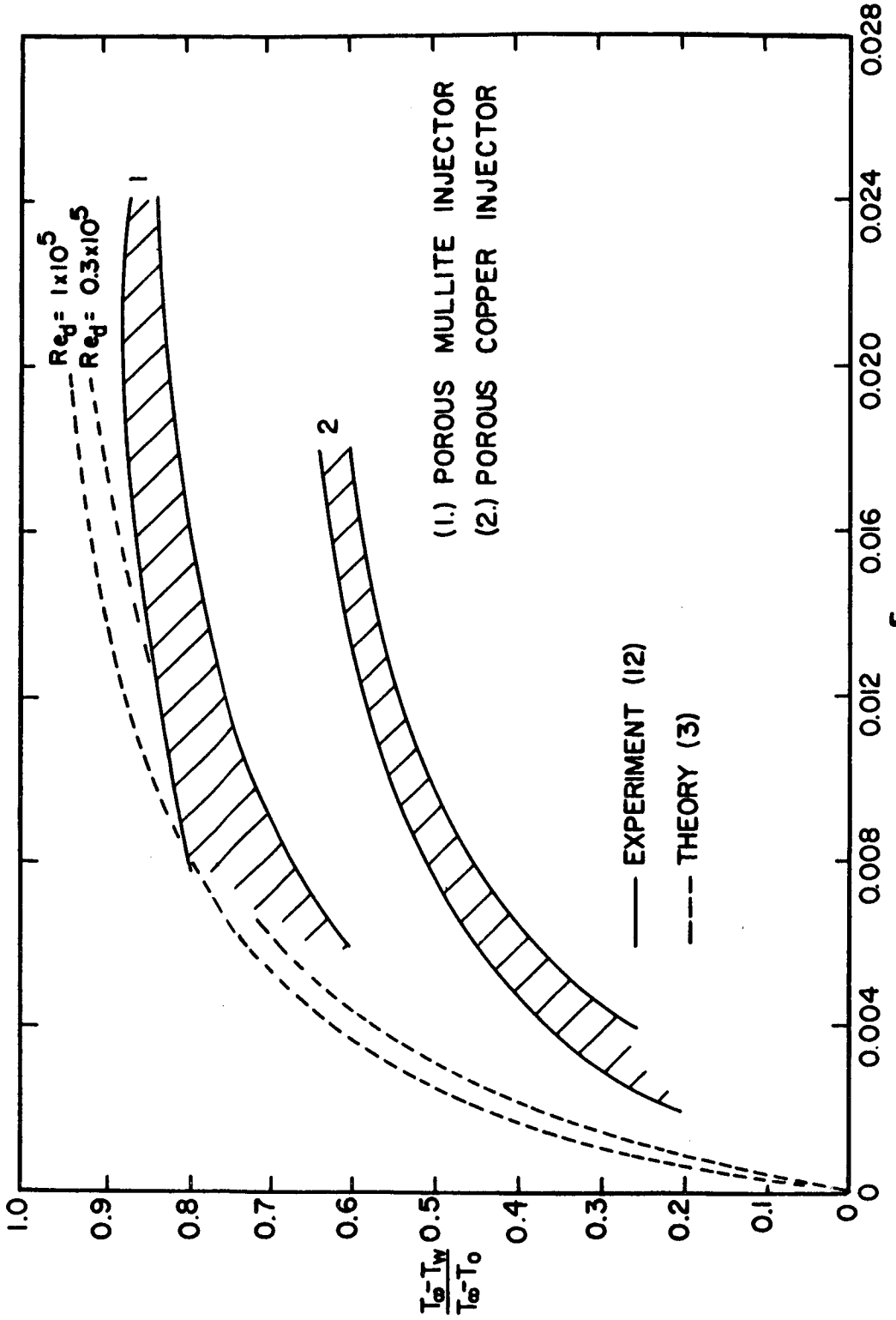

FIGURE 2.2 COMPARISON OF THEORETICAL PREDICTIONS OF RANNIE WITH EXPERIMENTAL RESULTS FOR REDUCTION IN WALL TEMPERATURE

of 10 percent for a porous mullite specimen, while for a copper specimen, the difference is 30 percent. This was expected since it was neceesary to assume that there was no external heat loss, and copper, which has the higher thermal conductivity, indicated the greatest error.

From this brief survey of Rannie's article, the need for a more rigorous solution can clearly be seen.

2.2 Theory of Rubesin

More recent investigators have attempted to account for the reduction of skin friction (and heat transfer) due to transpiration using either Prandtl's or von Karman's mixing length theory and the momentum integral equation with the effects of a finite wall velocity, v_w, included. Rubesin's (4) analysis of transpiration cooling for air injection into a turbulent boundary layer and a similar derivation due to Rubesin and Pappas' (14) for light gas[1] injection are typical of those theories. The modification of the former by the latter was necessitated by the wide variation in properties across the boundary layer. The foregoing works will be reviewed in this section in order to elucidate the techniques involved in determining the rate of mass injection necessary to achieve a desired wall temperature. A more detailed comparison of the various analytical treatments has been presented by Spalding, et. al. (5). In concluding this section, the subject papers (4, 14) are compared with other analyses to indicate the alternate approaches which are possible.

---

[1] Helium or hydrogen

One of the main contributions of the analysis due to Rubesin is that it describes more accurately the physics of the turbulent boundary layer in the presence of mass transfer; the final equations are unwieldy and because there exists simpler empirical expressions, the result of the mixing length approach is not recommended. A comparison of the various analytical solutions with experiment indicates that none possess any distinct advantage in accuracy[1] (5).

2.2.1 The Model

The analysis of Rubesin applys to flow over a flat plate with zero or negligible streamwise pressure gradient. The theoretical model for the analysis of the compressible turbulent boundary layer with transpiration cooling employs mixing length theory and is based upon the following.

Assumptions[2]

(1) Only the case of a flat plate is considered.

(2) The flow is steady.

(3) Derivatives in the x direction can be neglected in comparison with those in the y direction.

(4) Similar to Rannie's model, the boundary layer is divided into two regions; a thin laminar sublayer adjacent to the wall where molecular transport processes predominate and an outer turbulent region where they are negligible.

(5) "Reynolds analogy" is valid for the outer turbulent region.

---

1 This is due primarily to the scatter in experimental data; see Figure 3.7 in Chapter 3.

2 These assumptions are common to the numerous analyses employing mixing length theory (4, 5, 14, 15, 16, 17, 18).

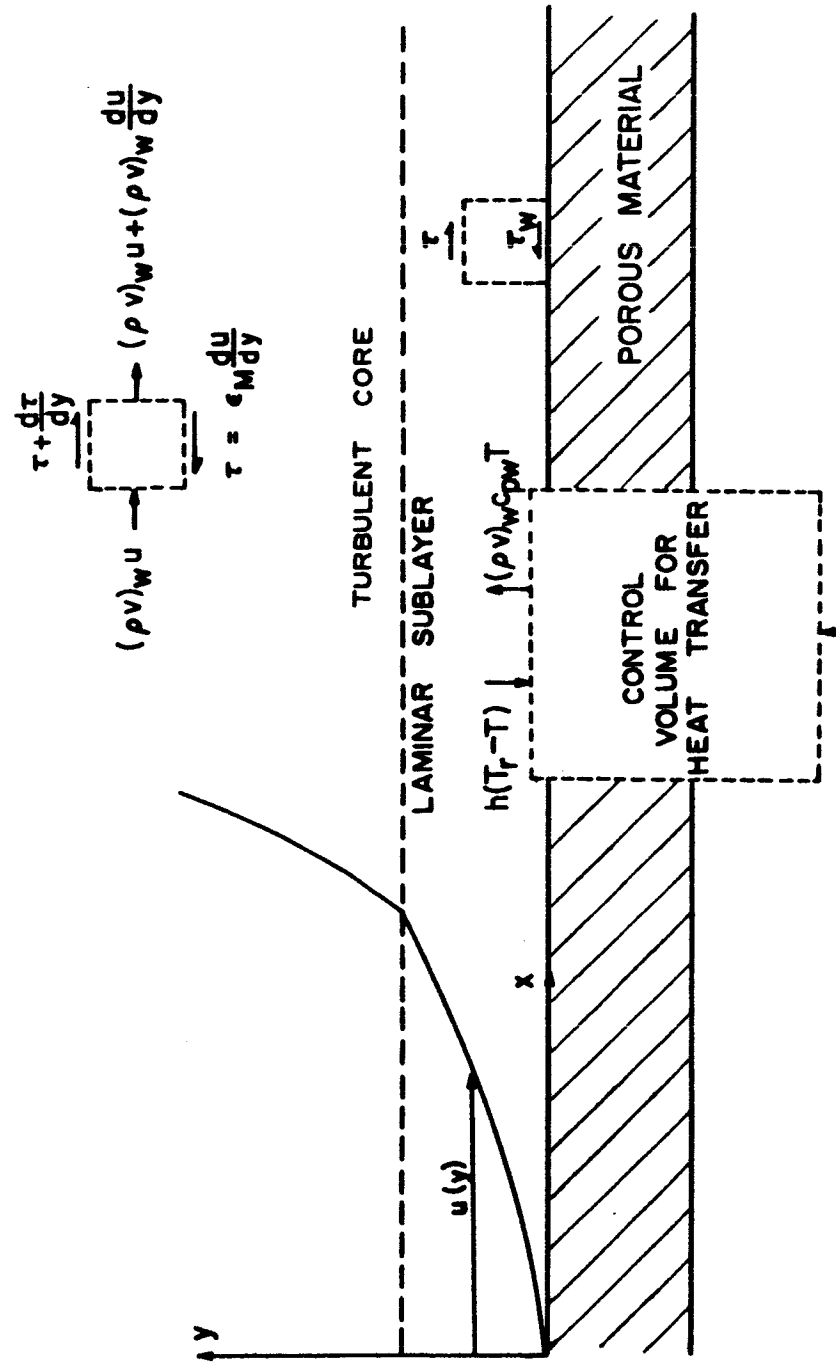

FIGURE 2.3 TRANSPIRATION MODEL FOR ANALYSIS DUE TO RUBESIN (4)

Discussion. Assumption (1) is tantamount to saying that the steamwise pressure gradient is zero or negligible and outside the turbulent boundary layer, the mainstream velocity is constant. There are no theoretical solutions to the knowledge of the author which account for the effects of pressure gradient in the turbulent mass transfer problem. Reference 19 evaluated the effect of pressure gradient experimentally and found that although it significantly affected skin friction results, it had little influence if any on the heat transfer. For this reason, an analysis such as Rubesin's can be applied to rocket nozzles.

Assumption (3) is necessary because the boundary layer equations contain partial differentials with independent variables x and y. Since little success has been achieved with similarity solutions of turbulent flow, the partial differential equations must be reduced to an ordinary form in some other manner. Fully developed flow on a flat plate is impossible but, nevertheless, changes in the y direction well downstream of the leading edge and within the boundary layer will always be much greater than changes in the x direction, a fact borne out by experimental studies of incompressible flow over an impermeable flat plate (7). It is assumed by the authors (4, 5, 14, 16, 17, 18) reviewed in this chapter that this can be extended to the problem of transpiration cooling of a compressible boundary layer without invoking any serious difficulties.

By necessity, a sharp division of the boundary layer is made because the turbulence level drops very rapidly close to the wall. To approximate the physics of this phenomena, the eddy viscosity and eddy thermal conductivity must be neglected in the sublayer; but beyond the interface

of the two regions, the turbulent properties must predominate over their molecular equivalents. This permits separate integration of the momentum equation yielding the velocity distribution at any cross-section when the solutions are matched. Since experimental data are used to evaluate the constants of integration, it is not surprising that this procedure gives good results (20). Turcotte (21) offers an alternate approach for finding a relationship for the reduction in skin friction on a transpired surface by employing Rannie's (22) empirical formula for the variation of the turbulent eddy viscosity close to the wall. Knuth and Dershin (6) later make a slight improvement on this expression. These alternate approaches of References 6 and 21 will be discussed in Section 2.2.4.

The final assumption (5) of the preceding section must be used twice in the solution to the problem. As will be domonstrated later, a solution would not be possible without the relationships between skin friction, heat transfer and mass transfer which the Reynolds analogy provides. Furthermore, an expression is required relating the density gradients which occur for compressible flow with known parameters of the boundary layer. This then permits the double integration of the momentum equation in the turbulent region with the eddy viscosity expressed in terms of mixing length. The numerous possible forms of the "modified Reynolds analogy" is one of the points at which many authors disagree and partially accounts for the different solutions. Rubesin's form of the analogy will be compared with other forms in the concluding section of this chapter.

2.2.2 Injection of Air into Air

Rubesin (4) divides his analysis into two parts making different and sometimes contradictory assumptions in each. The objective of the first portion of this derivation is to determine the effect of mass transfer on the skin friction coefficient when the molecular and turbulent Prandtl numbers are equal to one. The second half of the analysis is directed to finding a relationship between heat transfer and skin friction for any Prandtl number. Thus, a simultaneous solution of the two results is contingent upon the assumption that the skin friction is independent of the Prandtl number (23).

The derivation begins with the simplification of the momentum and energy equations. The general Navier Stokes equation written for the boundary layer in the streamwise direction cannot be integrated for two reasons: (1) it contains derivatives in both the x and y directions, i.e., it is a partial differential equation; and (2) because there are six unknowns: $\bar{u}$, $\bar{v}$, u'; v'; $\bar{\rho}$ and ρ'. Neglecting derivatives in the x direction and taking the time average, the x momentum equation gives

$$(\bar{\rho}\,\bar{u} + \overline{\rho' v'})\,\frac{d\bar{u}}{dy} = \frac{d}{dy}\left(\mu\,\frac{d\bar{u}}{dy} - \bar{\rho}\,\overline{u' v'}\right) \tag{2.18}$$

The continuity equation similarly becomes

$$\frac{d\,(\bar{\rho}\,\bar{v} + \overline{\rho' v'})}{dy} = 0 \tag{2.19}$$

This is essentially the starting point for most mixing length analyses. In proceeding to review Rubesin's analysis, it is instructive to clarify the purpose for beginning with the boundary layer equations. By integrating the x momentum equation, the u or streamwise velocity is found as a function of y. Recalling that the von Karman integral momentum equation relates skin friction with momentum thickness (which, in turn, is a function of the velocity distribution), an expression for c_f may be obtained once θ is known. These steps will now be reviewed in more detail.

The continuity equation is integrated directly to give the relationship

$$\bar{\rho}\,\bar{v} + \overline{\rho' v'} = \text{constant} \tag{2.20}$$

The boundary condition at the wall (y = 0) is

$$\overline{\rho_w' v_w'} = 0 \tag{2.21}$$

Therefore, equation 2.20 becomes

$$\rho_w v_w = \bar{\rho}\,\bar{v} + \overline{\rho' v'} \tag{2.22}$$

Substituting this expression back into the momentum equation (2.18) results in the following

$$\rho_w v_w \frac{d\bar{u}}{dy} = \frac{d}{y}\left(\mu \frac{d\bar{u}}{dy} - \bar{\rho}' \overline{v' u'}\right) \tag{2.23}$$

The eddy viscosity may be defined as

$$\epsilon_M = - \frac{\bar{\rho}\,\overline{v' u'}}{d\bar{u}/dy} \tag{2.24}$$

which, upon substitution into equation 2.23, gives

$$\rho_w v_w \frac{d\bar{u}}{dy} = \frac{d}{dy}\left(\mu \frac{d\bar{u}}{dy} + \epsilon_M \frac{d\bar{u}}{dy}\right) \tag{2.25}$$

Equation 2.25 can be integrated without the need for additional substitutions. Thus

$$\rho_w v_w u = \mu \frac{d\bar{u}}{dy} + \epsilon_M \frac{d\bar{u}}{dy} + \text{constant} \tag{2.26}$$

This expression, however, is intractable unless the variation of the dynamic and eddy viscosity can be determined for any cross-section. At this point, it is necessary to appeal to assumption (4) that the flow is divisible into a laminar sublayer adjacent to the plate and an outer turbulent region. Consequently, if appropriate approximations for the value of ϵ_M exist, the velocity profile may be found separately for each layer and then the distributions matched at the interface.

In the laminar sublayer, one observes that by the definition of laminar flow, both of the fluctuating velocity components are identically zero. Thus

$$\rho\,\overline{u' v'} = 0 \tag{2.27}$$

Since the eddy viscosity is therefore equal to zero for this region, equation 2.26 can be written as follows

$$\rho_w v_w u = \mu \frac{du}{dy} + \text{constant} \tag{2.28}$$

The constant in equation 2.28 is evaluated utilizing the no slip condition at the wall; i.e.,

$$u_w = 0$$

$$\tau_w = \mu \left(\frac{du}{dy}\right)_w$$

$$\tau_w = \text{constant} \tag{2.29}$$

Rearranging equation 2.28 and using the boundary condition, $u = 0$ at $y = 0$, gives

$$y = \int_0^u \frac{\mu \, du}{\rho_w v_w u + \tau_w} \tag{2.30}$$

Since the variation of the dynamic viscosity across the boundary layer is not known until the temperature distribution is known, it is assumed that μ is constant and equal to the value at the wall. Thus

$$\mu = \mu_w$$

After performing the indicated integration (2.30) and obtaining y as

a function of u, the expression can be nondimensionalized by defining the new parameters y^+ and u^+ in the form

$$y^+ = \frac{\rho_\infty u_\infty}{\mu_\infty} \sqrt{\frac{c_f}{2}}\ y \tag{2.31}$$

$$u^+ = \frac{u}{u_\infty} (2/c_f)^{0.5} \tag{2.32}$$

In this manner, a universal velocity profile for the sublayer is obtained.

$$y^+ = \frac{1}{F} (c_f/2)^{0.5} \frac{\mu_W}{\mu_\infty} \ln (1 + Fu^+ (2/c_f)^{0.5}) \tag{2.33}$$

It is important to note that the dimensionless distance y^+ introduces the dynamic viscosity evaluated at the outer edge of the turbulent boundary layer. In apparent contradiction to the approximation made earlier, the value of μ in the freestream is not considered to be equal to the value at the wall. Rubesin assumed that the accuracy of the results would be improved if this were done. The viscosity ratio in equation 2.33 is evaluated with the following expression

$$\frac{\mu_\infty}{\mu_W} = \left(\frac{T_\infty}{T_W}\right)^\omega \tag{2.34}$$

In a similar manner, the velocity distribution in the outer turbulent region is determined by using equation 2.26 in the simplified form

$$\rho_w v_w \overline{u} = \varepsilon_M \frac{d\overline{u}}{dy} + \text{constant} \tag{2.35}$$

where as stated earlier, $\varepsilon_M >> \mu$. Unfortunately, the eddy momentum diffusivity depends upon the flow field and varies too widely to be treated as a constant. One of the assumptions leading to the boundary layer equations was that the laminar sublayer is very thin compared to the turbulent region; this permitted treating viscosity as a constant for the purpose of integrating the laminar form of the momentum equation. In the turbulent region though, it is necessary to employ mixing length theory or some other phenomenological theory to obtain an expression for ε_M in terms of velocity u and distance y. Thus employing the Prandtl mixing length concept, ε_M is given by

$$\varepsilon_M = \rho L_p^2 \frac{du}{dy} \tag{2.36}$$

$$L_p = Ky \tag{2.37}$$

A strict application of equations 2.36 and 2.37 should be limited to the inner turbulent region which accounts for only about 10 percent of the boundary layer thickness. Beyond that point,[1] the mixing length theory has been found to be less accurate (24). Nevertheless, for simplicity, the mixing length equations are usually extended to include

---

[1] The outer turbulent region is commonly called the velocity defect layer.

the entire turbulent region on the basis that: (1) they provide a good approximation to the defect layer though they are not as accurate as the more complicated defect expressions; (2) simpler results are obtained by using one equation for both regions; and (3) approximately 50 percent of the momentum defect occurs in the 10 percent of the boundary layer called the inner turbulent region.

Because the velocity and shear profiles must be continuous through the laminar and turbulent regions, the constants of integration of equations 2.28 and 2.35 must be the same and equal to the shear stress at the wall.[1] Integrating equation 2.33 by using the appropriate mixing length expressions defined earlier results in the relationship

$$y = y_a \exp \int_{u_a}^{u} \frac{K \rho^{\frac{1}{2}} \, du}{\sqrt{\rho_w \nu_w u + \tau_w}} \tag{2.38}$$

where the subscript "a" denotes the interface between the laminar sublayer and turbulent region. The parameters at the interface, y_a and u_a, are unknown and must be evaluated from experimental data. Procedures for this are discussed in detail by Rubesin (4).

With the velocity profiles for the sublayer and turbulent region known, it is possible in theory to determine the momentum thickness defined by the expression.

$$\theta = \int_0^1 \frac{\rho}{\rho_\infty} \, z \, (1 - z) \, \frac{dy}{dz} \, dz \tag{2.39}$$

---

[1] As shown earlier from the boundary conditions for the laminar sublayer

where

$$z = \frac{u}{u_\infty}$$

The local skin friction coefficient, c_f, is subsequently found from the momentum integral equation. One difficulty in evaluating θ, which should become immediately apparent, is the determination of an expression for the density ratio ρ/ρ_∞ as a function of the velocity or coordinate distance y. To obtain such a relationship, it is necessary to resort to a modified form of Reynolds analogy. If it is assumed that the laminar and turbulent Prandtl numbers are unity, it can be shown (4) that the energy equation reduces to

$$\rho_w v_w \frac{d}{dy}\left(c_p T + \frac{u^2}{2}\right) = \frac{d}{dy}\left((\mu + \varepsilon_M)\frac{d}{dy}\left(c_p T + \frac{u^2}{2}\right)\right) \qquad (2.40)$$

Comparing equation 2.40 with the x momentum equation (2.35), the identical forms of the two expressions indicate that the following must be true

$$c_p T + \frac{u^2}{2} = a\,u + b \qquad (2.41)$$

where "a" and "b" are constants. This is essence is a statement of the modified Reynolds analogy. By employing the boundary conditions

$$T = T_w \text{ and } u = o \text{ at } y = o$$

one can show that

$$\frac{T}{T_w} = 1 + B_1 z - B_2^2 z^2 \tag{2.42}$$

where, as shown in Reference 4, B_1 and B_2 are functions of the Mach number, specific heat ratio of the mainstream gas, and the ratio of the mainstream to wall temperature. Thus for a particular transpiration cooling problem with given conditions, B_1 and B_2 can be treated as constants. By introducing the perfect gas law, equation 2.42 can be used to relate density and velocity by eliminating temperature.[1] Thus

$$\frac{\rho}{\rho_\infty} = \frac{T_\infty}{T} = \frac{T_\infty}{T_w} \left(\frac{1}{1 + B_1 z - B_2^2 z^2}\right) \tag{2.43}$$

With this functional relationship, the value of the momentum thickness can be determined by integrating equation 2.39 by parts. The integration can be simplified somewhat by assuming that the turbulent region extends to the wall. Since the laminar sublayer is very thin, the error incurred by this assumption is small. Equation 2.44 below results from following the foregoing procedure if the Reynolds number based on the momentum thickness Θ is introduced; with some manipulation, one has

$$Re_\Theta = y_a^+ \left(1 + \frac{2F}{c_f}\right)^{\frac{1}{2}} \exp \int_{z_a}^{1} \frac{(\rho/\rho_\infty)^{\frac{1}{2}} \, dz}{(F z_a + c_f/2)^{\frac{1}{2}}} \tag{2.44}$$

It is now possible to use the von Karman momentum integral equation in conjunction with equation 2.44 to find the skin friction coefficient. The momentum integral equation in terms of the Reynolds number is

---

[1] The transverse pressure gradient is zero from the y momentum equation.

$$\frac{c_f}{2} + F = \frac{d\ Re_\theta}{d\ Re_x} \tag{2.45}$$

where F accounts for the effects of blowing at the wall. Noting that the two preceding expressions contain two unknowns (momentum thickness and friction coefficient), they may be solved simultaneously to determine c_f. The solution requires a transformation of variables and the evaluation of an elliptic integral of the first kind. The expression obtained for the skin friction before integration is

$$\ln \left(\frac{K}{y_a^+} \left(\frac{c_f}{2}\left(\frac{c_f}{2} + F\right)\right)^{0.5} Re_x\right) = \int_{z_a}^{1} \frac{K\ (\rho/\rho_\infty)^{0.5}\ dz}{(F\ z + c_f/2)^{0.5}} \tag{2.46}$$

In order to solve for c_f using equation 2.46, the values of the dimensionless velocity z_a and distance y_a^+ at the interface between the laminar sublayer and turbulent region must be obtained. Since these are assumed to be universal values for a given mainstream fluid and coolant, though not entirely independent of the blowing rate (4), they may be found by experiment and used as constants for any calculations if the same fluids are used. The determination of these constants is described in detail by Rubesin (4). The important point to emphasize here is that the accuracy of the theoretical results is limited by the accuracy of the experimental data used to evaluate the constants K, y_a^+, and u_a^+. This then is one of the primary drawbacks in employing mixing length theory to solve the heat transfer problem with transpiration cooling.

Once the skin friction is known, the heat transfer coefficient can be determined using Reynolds analogy (this subsequently permits a solution to either the mass transfer rate or surface temperature). For the second portion of the analysis, the Prandtl number is not restricted to unity for reasons explained below. The heat transfer coefficient is a function of the Prandtl number as indicated by the functional heat transfer relationship

$$Nu = a\, Re^{b} Pr^{c} \tag{2.47}$$

where

$$b,\ c > o$$

As discussed earlier, Rubesin has shown (23) that the skin friction coefficient is nearly independent of Prandtl number in the range $0.7 < Pr < 2.0$. The coolants most frequently employed for transpiration cooling experiments (e.g., air, steam, nitrogen and helium) have Prandtl numbers in this prescribed range (25). With this as a basis, the impetus for the remainder of the analysis is provided; for if the skin friction coefficient just found for $Pr = 1.0$ can be generalized to any Prandtl number, and if an analogy can be deduced relating the heat transfer coefficient with the skin friction coefficient, the injection rate necessary to cool a surface to a particular temperature can be determined by a simultaneous solution of the two equations. Hence, the final portion of the analysis is assumed to be valid for any Prandtl number (4).

The x momentum equation was earlier simplified to the form

$$\rho_w v_w u + \tau_w = (\mu + \varepsilon_M) \frac{du}{dy} \tag{2.48}$$

Similarly the energy equation may be shown to be

$$\rho_w v_w \left(c_p(T-T_w) + \frac{u^2}{2}\right) - q_w = \left(\frac{\mu}{Pr} + \frac{\varepsilon_M}{Pr'}\right) \frac{d(c_p T)}{dy} + (\mu + \varepsilon_M) \frac{udu}{dy} \qquad (2.49)$$

If equation 2.49 is divided by equation 2.48 and the result integrated, with considerable algebraic manipulation, one finds that

$$\frac{2St}{c_f} = \frac{F}{\left(\frac{c_f}{2}\right)^{\frac{1-Pr}{}} \left(1 + \frac{c_f}{2}\right)^{Pr-Pr'} \left(F + \frac{c_f}{2}\right)^{Pr'} - \frac{c_f}{2}} \qquad (2.50)$$

where the Stanton number is defined in the usual manner

$$St = \frac{q_w}{(T_r - T_w)\, \rho_\infty\, u_\infty\, c_{p\infty}} = \frac{F\,(T_w - T_o)\, c_{pc}}{(T_r - T_w)\, c_{p\infty}} \qquad (2.51)$$

Therefore, for the case of a specified blowing rate and with the skin friction coefficient known from equation 2.46, the Stanton number may be determined using equation 2.50. The surface temperature then follows from the above definition (2.51) of the Stanton number. If the maximum wall temperature is given instead of the blowing rate F, the foregoing equations may be solved by trial and error.

The analysis of Rubesin illustrates the technique involved in applying mixing length theory to a turbulent boundary layer with the injection of air. In Chapter 3 of this report, the predictions of Rubesin will be compared with the more pertinent experimental results.

In the following section, the method used by Rubesin (4) is extended by Rubesin and Pappas (14) to light gas injection into a mainstream of air or a similar gas with a molecular weight near that of air.

2.2.3 Extension by Rubesin and Pappas to Light Gas Injection

It has been shown analytically (5, 14) and experimentally (26,27) that,when compared on a pound mass basis, light gases (those with low molecular weights) are more effective as transpiration coolants than heavy gases. The analysis of Rubesin and Pappas (14), which is an extension of the previous analysis of Rubesin (4), considers the injection of light gases (e.g., helium into air) and includes the effects of binary diffusion. Their procedure is very similar to that of Rubesin although the results will be noticeably different, primarily because of the presence of a foreign gas which considerably alters the properties across the boundary layer.

The analysis is based upon the model of Section 2.2.1 and the following additional assumptions which account for the two component gas.

(1) Diffusion of species will be considered to be due to concentration gradients only.

(2) The boundary layer is approximately isothermal.

(3) In the laminar sublayer, the Schmidt (Sc), and Prandtl (Pr), equivalent Prandtl number $(Pr)^*$ and the ratio μ/μ_a are constant and equal to the average value in the sublayer. These quantities are defined below.

$$Pr = \frac{c_p \mu}{k}$$

$$Pr^* = \frac{c_{pc} \mu_\infty}{k}$$

$$Sc = \frac{\mu}{\rho D_{12}} \tag{2.52}$$

(4) Similarly in the turbulent region, the turbulent Schmidt (Sc') and Prandtl (Pr') numbers are constant and equal to unity. They are defined by

$$Sc' = \frac{\varepsilon_v}{\rho \varepsilon_d}$$

$$Pr' = \frac{\varepsilon_M c_p}{\varepsilon_k}$$

where

ε_d = eddy diffusion coefficient

ε_M = eddy viscosity

ε_k = eddy thermal conductivity

Again the analysis can be divided into two parts: (1) a solution of the momentum equation to obtain an expression for the skin friction coefficient as a function of the blowing rate and molecular properties; (2) the determination of an expression for the rate of heat transfer (Stanton number) by employing Reynolds analogy and the solution for c_f.

The starting point for the analysis is the boundary layer equations. The momentum equations for the laminar sublayer and outer turbulent region are identical to Rubesin's equations 2.28 and 2.35 and therefore will not be repeated here. Considering diffusion only due to concentration gradients and neglecting derivatives in the x direction, the equations for mass transport in the laminar sublayer and outer turbulent region are, respectively

$$\rho_w v_w \frac{df}{dy} = \frac{d}{dy}\left(\rho D_{12} \frac{df}{dy}\right) \tag{2.53}$$

$$\rho_w v_w \frac{df}{dy} = \frac{d}{dy}\left(\rho \varepsilon_d \frac{df}{dy}\right) \tag{2.54}$$

where "f" is the mass fraction of the foreign gas.

Before the boundary layer equations can be integrated, it is necessary to derive an expression for the transverse density gradient. Using the perfect gas law to find the ratio of the binary mixture density at a point within the boundary layer to the density in the freestream, it is easy to show that

$$\frac{\rho}{\rho_\infty} = \frac{W\, T_\infty}{W_\infty\, T} \tag{2.55}$$

where W is the molecular weight of the mixture at the point considered and W_∞ is the molecular weight of the freestream gas. In order to simplify the problem, the authors (14) assumed the boundary layer is approximately isothermal which permitted the cancelation of the ratio

T_∞/T in equation 2.55. This is in reality a poor assumption since even for supersonic flow where temperature gradients are due to compressibility effects, the ratio T/T_∞ is on the order of 1.5 to 2.0 (28).

The molecular weight is defined by the expression

$$\frac{1}{W} = \frac{f}{W_1} + \frac{1 - f}{W_\infty} \tag{2.56}$$

Substituting 2.56 and regrouping terms gives

$$\frac{\rho}{\rho_\infty} = \frac{1}{(W_\infty/W_1 - 1)\, f + 1} \tag{2.57}$$

Recalling that in order to integrate the momentum equation, one needs density as a function of velocity and not mass fraction, it is now necessary to resort to a form of Reynolds analogy. In the solution due to Rubesin (4), the analogy between momentum and energy was employed since the density was expressed in terms of temperature. However, because in this case mass fraction appears instead of temperature, a relationship must be found by appealing to the momentum and mass transfer equations. This procedure is illustrated by the following.

The diffusion equation (2.54) for the turbulent region can be integrated once directly because, as previously shown, $\rho_w v_w$ = constant. Dividing the result by the momentum equation (2.35) for the turbulent region gives

$$\frac{\rho_w v_w\,(f - 1)}{\tau_w v_w u + \tau_w} = \frac{\rho\, \varepsilon_d\, (df/dy)}{\varepsilon_M\, (du/dy)} = \frac{1}{Sc'}\,\frac{df}{du} \tag{2.58}$$

The authors then use assumption (4), discussed earlier in this section, that the Schmidt number is constant and equal to one. Finally, integrating equation 2.58 and using the definition of skin friction coefficient in terms of the wall friction and freestream velocity, the following expression is obtained

$$1 - f = \frac{F z + c_f/2}{F + c_f/2} \tag{2.59}$$

This provides a correlation between velocity and mass fraction which, when used in conjunction with equation 2.57, gives density as a function of velocity. The functional relationship may be written as

$$\frac{\rho}{\rho_\infty} = \frac{1}{m - nz} \tag{2.60}$$

where m and n depend on molecular weight (W , W_1), blowing rate (F), and skin friction (c_f). For a particular value of x, there is only one blowing rate and value of the local skin friction; thus, the two quantities m and n can be treated as constants for the purpose of integration with respect to y.

A relationship for the velocity profile in the outer turbulent region can be determined by again resorting to the momentum equation (2.35). It is possible to integrate both sides of that expression if: (1) the eddy momentum coefficient is written in terms of Prandtl's mixing length formula; and (2) equation 2.60 is substituted for the density.

The procedure followed is exactly the same as presented in the preceding section and the resulting expression again is a complex relationship involving hyperbolic functions and natural logarithms. It is of the form

$$y = y(y_a, z_a, K, c_f, z) \tag{2.61}$$

The above functional relationship for the velocity distribution in the outer turbulent region may be used to find the momentum thickness in terms of the parameters F and c_f. This is necessary for the solution of the von Karman momentum integral equation yielding c_f as a function of F, the desired result. The momentum thickness is readily obtained from 2.61 since all of the independent parameters in that equation are themselves independent of y. As noted in the previous section, because the laminar sublayer is very thin compared to the outer turbulent region, the thickness of the laminar layer may be neglected by changing the lower limit of the integral for the momentum thickness to y_a and letting this variable approach zero. In effect, the turbulent region is extended to the wall.

Similar to the analysis of Rubesin (4), the only problem remaining is the evaluation of the variables u_a, y_a, and K. If y_a and u_a are expressed in dimensionless form, they may be treated as constants and taken directly from experimental data. The values of those constants were found from Reference 4 with K = 0.392. In fact, the only difference in the procedure of Rubesin and Pappas (14) and that of Rubesin (4) was

in the evaluation of the viscosity μ. Rubesin and Pappas employed a value for the dynamic viscosity equal to the average value in the sublayer.

Knowing the momentum thickness from the integral of the turbulent velocity distribution, the von Karman momentum integral equation gives

$$Re_x = \frac{R_{ya}\, g}{K\sqrt{\frac{c_f}{2} + F}} \tag{2.62}$$

where g is a complex function of the form

$$g = g(k, F, m, n, c_f/2, z_a)$$

Equation 2.62 is the desired result of the first portion of the analysis. Since all quantities are known in equation 2.62, c_f may be found for a specified value of F. Due to the complexity of the result, the skin friction coefficient must be determined by a trial and error solution.

With the skin friction coefficient known for a given set of conditions, the authors utilize Reynolds analogy to evaluate the Stanton number. The final expression is obtained by dividing the energy equation by the momentum equation and integrating the result. For convenience the Prandtl and Schmidt numbers are set equal to unity. Furthermore, it is assumed that the equivalent Prandtl number, Pr^*, is constant. The resulting equation is

$$\frac{2St}{c_f} = \frac{2F/c_f}{\frac{F(1-z_a)}{Fz_a + c_f/2} + \frac{c_{pa}}{c_{p\infty}}\left[\frac{F + c_f/2}{Fz_a + c_f/2}\right]\left[\left[\frac{Fz_a + c_f/2}{c_f/2}\right]^{Pr^*} - 1\right]} \tag{2.63}$$

The heat transfer coefficient can be determined from equation 2.63 if the blowing rate is specified and if the skin friction coefficient is known from the first part of the analysis. Typical results of such computations are graphically compared with experimental results in Chapter 3. From the foregoing analysis, Rubesin and Pappas have drawn the following conclusions: (1) in general, the injection of helium and hydrogen reduce the skin friction by 2.5 and 5.0 times, respectively, as much as air; (2) similarly, helium and hydrogen reduce the Stanton number by 2.4 and 5.2 times, respectively, as much as air.

It is instructive to compare the analytical results for air and the light gases in order to determine why the latter are considered more effective on a per pound basis. The effects of light gas injection on the skin friction coefficient can be illustrated using the momentum integral equation in the form

$$\frac{c_f}{2} = \frac{d\theta}{dx} - F \qquad (2.64)$$

If the momentum thickness is known as a function of x for given mainstream conditions and coolant properties, a simple comparison of the skin friction coefficient for selected values of molecular weight and equal blowing rates is possible. Rubesin and Pappas did find an expression for the rate of change of momentum thickness with x, but qualitatively the difference between the effects of light gases and air cannot be seen from the equation. Nevertheless, by studying the parameters which logically could have a significant effect, molecular weight can be deduced as the variable which

accounts for the difference. The other parameter which might be considered is the dynamic viscosity. However, by applying the method suggested by Wilke (29) to the turbulent boundary layer, it is seen that the average viscosity at a point increases for increasing mass fractions of helium in a helium-air mixture and decreases for an increasing mass fraction of hydrogen in a hydrogen-air mixture; thus, generalizations as to the influence of viscosity of light gases can be ruled out.

Molecular weight affects the skin friction coefficient indirectly by altering the characteristics of the boundary layer in two ways: (1) it changes the actual thickness of the boundary layer; and (2) it changes the properties of the flowing gas. The first effect can be deduced by noting that at equal blowing rates for air and light gas injection, the light gas will have the higher specific volume. This tends to increase the boundary layer thickness (and the momentum defect) due to the additional volume occupied by the coolant (30). If this were the only factor, skin friction would be greater for the injection of light gases due to a larger value of θ[1]. Thus, since the results of previous investigations (19, 26, 27) indicate that the foregoing is not true, it can be assumed that the second factor predominates over the first. Though all properties of the boundary layer are influenced by the introduction of a foreign gas or liquid, density is the only one that appears in the definition of momentum thickness and for this reason, it will be considered to be the most important. To illustrate its effect, the equation for density variations

---

[1] See equation 2.64

across the boundary layer (2.57) can be used to show that ρ/ρ_∞ for helium injection is less than one half for values of z up to approximately 0.7.[1] For the injection of air into air, the ratio is one for the assumptions[2] made by Rubesin and Pappas. Thus since density is much less for light gases, θ must also be less. Finally, if it can be assumed that the rate of growth of momentum thickness ($d\theta/dx$) must similarly be smaller in order for the corresponding lower value of θ to occur, it follows that c_f will have a greater reduction with the injection of light gases.

The greater reduction in heat transfer achieved by light gas injection, relative to that realized by heavy gases, is more readily understood. In describing the mechanism of transpiration cooling, the reduction in heat transfer is partially ascribed to the blanketing effect of the coolant. In general, the lower the molecular weight, the higher will be the specific heat, and thus more heat will be absorbed in the laminar sublayer and less transferred to the wall. To show that the properties of the boundary layer are considerably influenced by the coolant properties, the following illustration is given. For a moderately low injection rate of F = 0.001 with either helium or hydrogen,[3] the mass fraction of the injected gas at the interface of the laminar sublayer with the turbulent core will be approximately 0.5 and at the wall approximately 0.7. Thus it is safe

---

1 Evaluated at a typical value of F = 0.00125 and $Re_x = 1x10^7$

2 Isothermal and constant pressure boundary layer

3 Also, with $c_f/2 = 5x10^{-4}$ and $Re = 1x10^7$

to assume that the properties of the gas in the laminar sublayer are chiefly determined by the properties of the coolant for injection rates within a practical range. For helium, the specific heat at constant pressure is over five times as great as the value for air.

2.2.4 Comparison with Other Analytical Theories

In this section, the numerous analyses of the turbulent boundary layer in the presence of mass transfer will be described in a general way to define the objectives of the various solutions; then, a comparison will be made of the more relevant analyses in those specific problem areas most pertinent to transpiration cooling. The subject areas for which there is little agreement occur in: (1) approximating the velocity distribution across the boundary layer (phenomenological theories); (2) evaluating the density variations for a compressible boundary layer; and (3) evaluating Reynolds analogy for heat, momentum, and/or mass transfer. Finally, the semi-empirical technique due to Turcotte (21) will be presented since his unique assumptions simplify the analysis.

References 4, 14, 15, 16, 17, 18, 31, and 32 have all attempted to find a suitable expression for the turbulent velocity distribution with a nonzero component of velocity at the wall which, as seen earlier, is necessary for the evaluation of skin friction and heat transfer. Tennekes (32) and Stevenson (33) have reviewed most of the above references to demonstrate the different possible techniques available to obtain the velocity profile. It is noted here that the more accurate expressions are also the most complex. Some (4, 14, 16, 17, 18, 31) of these analyses have been extended to include the effects of mass transfer

on heat transfer. Others (14, 17, 31) have gone even further to evaluate the effects of foreign gas addition. Alternate empirical approaches (5, 6, 21) have been proposed to not only approximate the experimental data but to simplify the form of the result. The analysis of Turcotte (21) is best classified as semi-empirical and it represents the most formidable challenge to mixing length theory as a means for evaluating the turbulent shear stress. However, it also has been strongly criticized (34).[1] In the final section of this chapter, the unique empirical analysis due to Spalding (5) will be reviewed.

Most authors (5, 6, 14, 16, 21, 32, 33) state before attempting to solve the turbulent mass transfer problem that there is insufficient understanding of the mechanism of turbulent flow to obtain an accurate expression for the velocity profile. They agree that mixing length theory as proposed by Prandtl and von Karman has no firm experimental basis. Finally, it is argued that until there are more experimental data and better agreement among the data, the problem cannot be adequately solved by any means. However, the theories which exist today are believed to give answers of reasonable engineering accuracy. This, in part, is due to the occurrence of one "free parameter" (21) which can be evaluated somewhat arbitrarily, forcing the analysis to agree more closely with existing data. The remainder of this section shall be devoted to discussing the points mentioned earlier for which different techniques are used to evaluate certain expressions.

In the last ten to fifteen years, considerable work has been directed to obtaining a universal velocity profile for turbulent flow over impermeable

---

[1] See final portion of this section

surfaces by dividing the boundary layer into four regions which alledgedly have different physical characteristics. The division made by Danberg (24) for Re = $2x10^3$ is given in Table 2.1.

Table 2.1 A Typical Arbitrary Division of the Boundary Layer

Layer	Location	Percent Contribution to Momentum Thickness
Laminar Sublayer	$0 \leq y \leq 5\ \nu_w/u^*$	0.6%
Buffer Layer	$5\ \nu_w/u^* \leq y \leq 30\ \nu_w/u^*$	6.8%
Turbulent Layer	$30\ \nu_w/u^* \leq y \leq 0.2\delta$	50.0%
Velocity Defect Layer	$0.2\delta \leq y \leq \delta$	42.6%

Whether such a rigorous division of the boundary layer is advisable for the purpose of analyzing the reduction in heat transfer with transpiration cooling is questionable. In fact, all of the aforementioned authors concerned with transpiration cooling theory extend the turbulent region to include both the buffer and velocity defect layers. The important point to observe from Table 2.1 is that almost 60 percent of the momentum defect occurs in the region where the greatest concentrations of injected or foreign gas exist, thus corroborating the argument presented earlier that light gases reduce θ by the sizable factor ρ/ρ_∞.

In choosing a phenomenological law to evaluate ε_M, the majority of investigators (4, 14, 15, 16, 35) have employed Prandtl's mixing length and only a few (17, 31) have used the von Karman form of the expression, presumably because the former is easier to apply. Whether one form is more accurate than the other is questionable. For incompressible flow, the two alternate expressions yield the same

velocity distribution (24). On the other hand, for compressible flow, the profile obtained using Prandtl's mixing length equation has a higher initial slope ($(du/dy)_a$) but, nevertheless, the same value of c_f results if higher order terms are neglected in the von Karman form.

Probably the main point at which some authors differ occurs in the evaluation of ρ/ρ_∞. Only Clarke, Menkes, and Libby (16) assume that the boundary layer is incompressible. Others begin with the equation

$$\frac{\rho}{\rho_\infty} = \frac{W}{W_\infty}\frac{T_\infty}{T} \tag{2.65}$$

where, of course, for the injection of like gases, one has

$$\frac{W}{W_\infty} = 1$$

Differences usually arise because little agreement exists for finding the ratios on the right hand side of equation 2.65 in terms of velocity (or distance from the wall), mass fraction and molecular weight. Rubesin and Pappas (14) assume that the boundary layer is isothermal and thus cancel the ratio T_∞/T. Lapin (17) considered a nonisothermal boundary layer with foreign gas injection but made another far reaching assumption that the Prandtl number and Schmidt numbers are equal to one, insuring similar velocity, enthalpy and concentration profiles.

For injection of air into air, Dorrance and Dore (15) and Rubesin (4) follow the procedure of Lapin by assuming that the transport of momentum is proportional to the transport of heat (inferring that the turbulent Prandtly number is one). This is the Reynolds analogy assumption which all must make if a compressible boundary layer is considered.

An analogy between heat and momentum transfer must be employed again to obtain a relationship between skin friction and heat transfer. References 15, 16, 17 and 31 assume that the ratio $2St/c_f$ is equal to one. Others proceed in the same manner as Rubesin (4) and determine an expression by manipulating and integrating the momentum and energy equations.

An alternate method for solving the momentum equation without the use of mixing length theory has been suggested by Turcotte (21). For this analysis, the velocity profile for an incompressible boundary layer is approximated from which a simple and unique expression for skin friction results. The basic hypothesis is that Rannie's (22) expression for the eddy viscosity, ε_M, in turbulent pipe flow[1] is valid for injection if it is modified with an appropriate parameter b. Rannie's expression then becomes

$$\frac{\varepsilon_M}{\nu} = \sinh^2 (by^+/13.89)$$

Combining the above and the momentum equation (with derivatives in the x direction negligible compared to those in the y direction), Turcotte integrates the result and evaluates the expression at the interface of the laminar sublayer with the turbulent region giving

$$\tau_a = \tau_w \exp \left(\frac{13.89G}{b}\right)$$

---

[1] Originally proposed for the region very close to the wall

where G is defined by

$$G = \frac{\nu_w}{u^*}$$

Another far reaching assumption is now made that the effect of injection is limited to the laminar sublayer. This is the basis of the derivation due to Turcotte. For if this is true, then the shear stress at the interface of the sublayer with the turbulent core must be independent of the injection rate; since the shear stress is constant across the sublayer for no blowing, it is concluded that

$$\tau_a = \tau_{ao} = \tau_{wo}$$

i.e., the interface shear stress with injection can be replaced by a more easily evaluated quantity, the wall shear stress without injection. The final equation is then

$$\frac{\tau_w}{\tau_{wo}} = \exp \frac{(-13.89G)}{b}$$

The various possible values for the parameter b were determined by Turcotte without resorting to experimental results. He believed that one of the advantages of his solution was the elimination of the free parameters introduced by mixing length solutions. Leadon (20), however, used experimental data to show that several errors are involved in the assumptions of Turcotte, the most notable being that injection does affect the velocity distribution outside the laminar sublayer.

2.3 Theory of Spalding, Auslander and Sundarum

A third approach to the solution of the heat and mass transfer problem is best represented by the attempt of Spalding, Auslander and Sundarum (5) to obtain empirical correlations which fit the heat transfer data. As mentioned earlier, the final equations are easy to use and the authors claim that calculations can be performed in minutes, yielding answers with an accuracy to within one percent of the experimental results. The analysis is actually an extension of a more limited earlier work by Spalding and Chi (37) for the turbulent boundary layer without mass transfer. The final results of Reference 5 are valid for compressible and incompressible fluids, subsonic and supersonic flows,[1] and non-reacting and reacting coolants. As illustrated below, Spalding, et. al. did not eliminate the need for evaluating complex functions and integrals but, nevertheless, their expressions were manipulated in such a form that they could be integrated numerically; the equations were then programmed on a computer. The results of the numerical integrations have been tabulated (5) for hydrogen, helium and air and thus numerical values for the various functions may be taken directly from the report if the mainstream conditions, coolant supply conditions and surface temperatures are specified.

The analysis is based on the observation by Spalding and Chi (37) that the use of mixing length theory and the von Karman momentum integral equation for finding the skin friction on a flat plate with a turbulent boundary layer leads to an equation of the functional form

---

[1] The authors believe however that the accuracy of the results decrease for lower Mach numbers

$$\left(\frac{c_f}{2}\right) F_c = \psi_x \left(Re_x F_{Rx}\right) \tag{2.66}$$

regardless of the presence of heat and/or mass transfer. F_c, ψ_x, and F_{Rx} are initially undetermined functions which were introduced to account for the influence of the independent variables. By comparing the above expression (2.66) with the results of mixing length theory due either to Prandtl or von Karman, the authors deduced that the following must be true

$$F_c = F_c \left(M_\infty, T_w/T_\infty, 2F/c_f\right)$$

$$F_{Rx} = F_{Rx} \left(M_\infty, T_w/T_\infty, 2F/c_f\right)$$

An initial simplification can be made if it is assumed that the skin friction is a function only of Reynolds number for the case of no heat or mass transfer and a very small Mach number ($M << 1$); for then F_c and F_{Rx} must reduce to one. This permits a solution for the function ψ_x without prior knowledge of the other two functions; i.e., using experimental data, the term "$c_f/2$" in equation 2.66 can be plotted against ψ_x (Re_x) for the condition, $F_c = F_{Rx} = 1$. In effect then, equation 2.66 has been solved graphically. If the solution is generalized to permit heat and mass transfer at any Mach number, the same functional relationship must hold. However, before a value for c_f can be determined from the graph of equation 2.66 for the more general case, expressions for F_c and F_{Rx} must be found. If solutions for these functions exist, the foregoing approach becomes justified.

The function F_c is deduced by rearranging the result obtained by integrating the von Karman form of the momentum equation (equation 2.44 of Rubesin is one form). Spalding, et. al. (5) arrive at the following similar form

$$\frac{c_f}{2}\left[\int_0^1 \frac{(\rho/\rho_\infty)^{0.5}}{(1+\frac{2Fz}{c_f})^{0.5}}\,dz\right]^{-2} = \frac{K^2}{(\ln(KE'\,Re_\Theta))^2} \qquad (2.67)$$

where

$E' \approx$ constant

Since two independent functions are included in equation 2.66, it is convenient to arbitrarily force the function F_c to be equal to the coefficient of $c_f/2$ in equation 2.67. Thus

$$F_c = \left[\int_0^1 \frac{(\rho/\rho_\infty)^{0.5}}{(1+B_u z)^{0.5}}\,(dz)\right]^{-2} \qquad (2.68)$$

where B_u is defined as

$$B_u = \frac{2F}{c_f} \qquad (2.69)$$

For a particular coolant and mainstream fluid, the integral (2.68) can be solved numerically by employing Reynolds analogy. This has been done and the results tabulated by Spalding, et. al. (5) for hydrogen, helium and air.

This leaves only the function F_{Rx} to be evaluated empirically. With values of c_f and Reynolds number known from experiment, particular values F_{Rx} can be found using equation 2.66 and the function F_c from equation 2.68. Finally, plotting another curve of F_{Rx} against the blowing parameter B_u, it is noted that the equation

$$F_{Rx} = \frac{\mu_\infty}{\mu_w} \frac{(1 + F/St)}{F_c}^{-0.5} \tag{2.70}$$

matches the results as well as any other. The equation used for determining the ratio F/St appearing in this expression (2.70) will be presented below.

In a recent book by Spalding (38), he discusses a unique method for finding the ratio of blowing rate to Stanton number (F/St) which he calls the driving force for heat transfer or B_h. Because it requires considerable background from the introductory chapters of Reference 38 and because it is merely a convenient definition, the derivation of the equation will be omitted. The following was obtained for a chemically inert coolant

$$B_h = \frac{F}{St} = \frac{c_{p\infty} (T_\infty - T_w) + ru_\infty^2/2}{c_{pc} (T_w - T_o) + q_{rad/\dot{m}}} \tag{2.71}$$

where $c_{p\infty}$ is the specific heat of the mainstream fluid and c_{pc} is the specific heat of the coolant. The radiation heat ransfer is usually neglected. All the variables on the right hand side of equation 2.71 are specified for a particular problem except the recovery factor. From experimental results, its value may be approximated by the expression

$$r = (Pr)^{1/3} (1 + B_h)^{-0.04} \tag{2.72}$$

Thus equations 2.71 and 2.72 must be solved simultaneously for r and B_h. However, since neither F or the Stanton number are known or specified though the ratio is, they cannot, as yet be found.

Again experimental data is utilized and a Reynolds analogy is postulated to be of the form

$$\frac{c_f}{2} = St\ (Pr)^{2/3} \tag{2.73}$$

or

$$B_u = (Pr)^{-2/3} B_h \tag{2.74}$$

where B_u is the driving force for mass transfer. With the skin friction coefficient known, it is possible to solve for the mass transfer rate from the definition of B_u (equation 2.69).

The procedure for calculating the mass transfer rate from the specified conditions of the problem were summarized by Spalding, et al. and are reviewed briefly below.

(1) Solve equations 2.71 and 2.72 simultaneously for B_h (i.e., F/St) and r, the recovery factor.

(2) Determine B_u from equation 2.74.

(3) Find the value of the function F_c in the tables presented in Reference 5.

(4) Calculate F_{Rx} using equation 2.70.

(5) The skin friction coefficient can now be found directly from the graph (5) of equation 2.66, and the mass flow rate follows from the definition of B_u (2.69).

The only criticisms that can be made of the foregoing solution is that there is insufficient data at the present to insure an accurate empirical result. Also, the derivation does not consider the physics of the boundary layer.

Knuth and Dershin (6) present a similar technique but were not able to arrive at conclusive results due to the insufficient data necessary to justify their approach. They established a curve based on constant properties (e.g., air into air) for the skin friction coefficient as a function of the blowing rate. Attempts were then made to generalize the results by developing equations based on reference state conditions for the more general case of variable properties.

In conclusion, the author recommends the solution due to Spalding, et. al. (5) for the design of transpiration cooling systems. The analysis was based on both past theory and experiment and accurately represents the data existing at the time of publication. Those experimental results and others reported since are discussed in Chapter 3. While the correlation of Spalding, et. al. adequately represents existing data more accurately than any theory, there are still some discrepancies at subsonic Mach numbers which are not accounted for and which to date have not been reconciled. Finally, as emphasized earlier, the most noteworthy advantages of the solution are its general applicability and simplicity.

3. REVIEW OF EXPERIMENTAL WORK

3.1 Introduction

Before proceeding with a review and evaluation of the more recent experimental work on transpiration cooling that is relevant to rocket nozzle cooling, it is helpful to discuss the history and development of the state of the art as it exists today. The parameters of interest and the independent variables which have been found to have the greatest influence on heat transfer will then be discussed to reveal the problems arising in determining the significant parameters for data correlation and to justify the basis for much of the existing data today. Finally, some of the more pertinent experimental work will be reviewed in detail to indicate what has been accomplished and the areas requiring future experimental work. A table has been prepared to briefly summarize the range of parameters that have been investigated and the experimental objectives of most of the unclassified literature concerned with transpiration cooling of a turbulent boundary layer. In addition, several graphs will be presented comparing existant data with the analyses of Chapter 2.

Work in the field of transpiration cooling has continued since 1929 when Oberth (39) first recognized sweat cooling as a potential method for rocket engine cooling. The following year, Goddard (40) conducted the first successful transpiration cooling experiment employing a four inch diameter rocket engine with a porous ceramic insert as the injector.

The test lasted only a few seconds but it was labeled a success and provided the motivation for experimentation to follow. The first experimental work reported in the literature was conducted by Meyer-Hartwig (41) in 1940 to determine the effectiveness of transpiration cooling in reducing the heat transfer to a porous copper wall subjected to gas temperatures up to 4500 F. These first tests, which are discussed further in References 2 and 42, demonstrated the feasibility of this unique cooling idea.

The most extensive and systematic investigation into this area was initiated in 1940 by Pol Duwez and co-workers at the California Institute of Technology (3, 12, 13, 42, 43, 44, 45, 46, 47, 48, 49). This program continued into the early 1950's and included the following aspects of transpiration cooling: (1) a study of the manufacture and flow properties of porous materials; and (2) the theoretical and experimental developments of the cooling technique. Experimental investigations were conducted on the cooling of cylindrical porous ducts of materials such as copper, stainless steel and ceramics, employing nitrogen, hydrogen and water as coolants. One of the more noteworthy conclusions of the investigations was that the cooling efficiency of the transpiration process is due more to the excellent heat transfer from the wall to the coolant than to the insulation provided by the mass injection of the wall.

Concurrent with the work at C.I.T., Young (50) carried out independent tests for Aerojet General Corporation from 1944 to 1946 to determine the effectiveness and problems entailed with using water as the coolant. As will be discussed in Chapter 4, Young discovered that if boiling occurs locally, i.e., at one particular point along the

test section, it will subsequently spread to adjacent areas. The propagating nature of this phenomena is due mainly to the local increase in surface temperature; for the result is an increase in kinematic viscosity and thus, a lower rate of injection. By spreading in this manner, the entire test section soon becomes saturated with steam and the lower mass flow rate becomes erratic. Despite this problem, Young was able to conduct a stable experiment for three minutes using water and a porous nickel liner. Since that first experiment, very limited attention has been focused on using water as the transpiring fluid (27, 51, 52, 53, 54). This is probably largely due to the superior cooling effectiveness of light gas injection into a boundary layer when compared to a heavy gas, as discussed in Chapter 2. However, the latent heat of a liquid makes it the chief competitor to the system employing a light gaseous coolant.

Another application for transpiration cooling was opened in 1946 when Moore and Grootenhuis (55) suggested this technique for the cooling of gas turbine blades. Most of the problems in this area are associated with fabrication of complicated geometries and deposition of solid impurities on the blade surface.

The study of transpiration cooling increased considerably in the 1950's and today, there exists a large number of articles dealing with not only the nozzle and turbine blade problem, but supersonic vehicle cooling, prevention of icing on lead sections of airplane wings, electric arc cooling; and further, the analogous technique of suction has received moderate attention as a potential means of boundary layer control for flow past airplane wings.

Experiments have been conducted in more recent years on such widely diverse geometries as flat plates, cones, wedges, spheres, nozzles, channels and turbine blades for selected coolants and selected values of free stream temperature, Mach number, Reynolds number, and blowing rate. Table 3.1 summarizes the range of parameters considered in the pertinent investigations and illustrates that each study is unique from the standpoint of having a particular range of test conditions. Considerable difficulty is encountered in comparing the results of various investigations since the method of data correlation has not been standardized, partly because of the lack of agreement as to the most influential parameters and partly because of the differences in taking the data. It is not surprising then that the range of applicability of the data for each individual experiment is extremely limited. Furthermore, though a tremendous amount of data has been accumulated since Goddard's first experiment, there still exists a need for additional experimental investigations encompassing a more systematic and wider variation of the parameters involved.

3.2 Determination of Significant Parameters

3.2.1 Dimensionless Correlations

In general, the determination of the skin friction coefficient and/or the heat transfer coefficient is the primary objective of all transpiration cooling measurements. From the former quantity along with the run conditions, the total drag is readily calculated and from the latter, the temperature of the wall or the blowing rate. Skin friction will be considered in detail in this report (as has been done in most

recent investigations to be discussed) because it must be determined first before the heat transfer coefficient can be determined through the Reynolds analogy. In fact, Reynolds analogy becomes after many simplifying and heuristic assumptions

$$St = \frac{c_f}{2} \tag{3.1}$$

Thus, the general trends displayed by one should be followed closely by the other and this indeed has been shown to be true (24). Skin friction by itself is of primary importance to the aerodynamicist whose concern is with external flow over blunt bodies. The temperatures in the mainstream over an aerodynamic profile are frequently ambient and thus high heat fluxes are due mainly to the viscous dissipation in the boundary layer. However, the problems of the rocket nozzle, airfoil, or reentry vehicle designer are essentially the same for in any of the cases, the same parameters (as outlined in the preceding chapter) must be considered to solve the problem. If the pressure gradients in both the axial and transverse directions are negligible, the problems are in fact identical.

Since many discrepancies exist in much of the data, one of the most important considerations after experimentally determining the two parameters c_f and St is to find the most effective method of plotting the results. An additional motivation for determining a universal and satisfactory correlation is to develop an alternate approach for solving the transpiration problem; i.e., as discussed in Chapter 2, because most of the analyses require lengthy numerical solutions, it would appear expedient to experimentally obtain a dimensionless correlation which could be used in place of the more involved analytical equations.

The skin friction and heat transfer coefficients are influenced the most significantly by the rate of mass injection (generally written in terms of the dimensionless blowing rate F). Other variables having some effect on c_f and St are the Reynolds number, Mach number, the ratio of mainstream to wall temperature, and properties of the coolant. The objective then is to determine an effective manner of correlating the data which would eliminate as much of the influence of the free parameters as possible.

Stewart (56) conducted a preliminary study of this problem and arrived at a relationship which gives answers within the range of accuracy of the theoretical predictions (4, 14). The most obvious method of plotting results is to use blowing rate as the independent variable but, unfortunately, this leaves the influence of the aforementioned independent variables (M, Re, T/T_w) unaccounted for. Though he was not the first person, he suggested dividing the dependent variable of interest (c_f or St) and the blowing rate F, by the zero mass transfer value of the parameter measured (c_{fo} or St_o), reasoning that Mach number, Reynolds number, and temperature ratio should have the same influence on the dynamics of the boundary layer regardless of the mass transfer; thus, it is intended that the influence of the independent variables cancel by expressing the reductions in heat transfer and skin friction coefficients in terms of a dimensionless ratio. To adjust the result for foreign gas injection, Stewart also recommended multiplying the independent variable by the factor

$$c_p^* = \left(\frac{c_{pc}}{c_{p\infty}}\right)^{0.6} \qquad (3.2)$$

which was found empirically to improve the correlation for several gases.

Thus, for the presentation of skin friction data, c_f/c_{fo} should be plotted against $Fc_{pc}^{0.6}/(c_{fo}c_{p\infty}^{0.6})$ and for the heat transfer data, St/St_o against $Fc_{pc}^{0.6}/(St_o c_{p\infty}^{0.6})$. In section 3.3 of this chapter, some typical experimental results will be compared with theory and using Stewart's coordinates, the data and analyses are shown to lie virtually on the same line. The specific heat was chosen as a correction factor because it is inversely proportional to molecular weight as well as a function of temperature. An obvious disadvantage of this technique is that the reference condition (the mainstream fluid) is not always the same (usually air). Brunner (27), for example, subjected a porous cone to the products of combustion of oxygen and alcohol and found that on the basis of Stewart's correlation, his results were off by a factor of 9.0 percent; however, considering the discrepancies of typical transpiration cooling results, this is not significant.

3.2.2 Measurement Techniques

Skin Friction In general, there are two fundamental ways by which skin friction can be determined in mass transfer experiments but unfortunately, the same equipment is not required for each technique precluding an easy comparison of the data. The first method to be described is the simplest and the most frequently used for external flow. It requires the measurement of the drag on a model which, as described below, can readily be related to the skin friction. References 26 and 57 effectively demonstrated the usefulness of this technique in their evaluation of the effects of

blowing on the surface skin friction of a cone. By attaching a strain gage to the strut support of their models and with help of static pressure measurements at various points along the surface, they were able to ascertain the total drag by means of a force balance. From the total drag force, the shear stress and thus the skin friction coefficient were calculated. Since the average value of shear stress was found, the fact that c_f must also be an average value is self-evident. This is a major shortcoming of this method since the local skin friction distribution cannot be found from the data taken.

An alternate method for determining the skin friction coefficient which has been frequently employed (19, 20, 24, 26, 58, 59, 60) requires boundary layer measurements of the static pressure profile yielding after some calculation, the velocity distribution for any particular cross-section. Considerable equipment is required since a pitot traverse must be made at selected points along the test section. From the velocity profiles, the displacement and momentum thicknesses can be determined by graphical or numerical integration. With these quantities known at several points, their respective derivatives in the direction of flow follow directly. Furthermore, if a streamwise pressure gradient exists, the variation in freestream velocity can be found easily from the boundary layer measurements and the momentum equation. Knowing these quantities, the von Karman momentum integral for a nonzero wall velocity gives the skin friction; for turbulent flow, it is

$$\frac{d\theta}{dx} - \frac{(\rho v)_w}{(\rho u)_\infty} + \frac{\theta}{u_\infty}\left(\frac{\delta^*}{\theta} + 2\right)\frac{du_\infty}{dx} = \frac{c_f}{2} \qquad (3.3)$$

where Θ is the momentum thickness, δ^* the displacement thickness and c_f the local value of skin friction. The sole assumption invoked by adopting equation 3.3 is that the terms involving the product of fluctuating components of velocity are negligible. Mickley and Davis (20) argued that no serious errors could result if the blowing rate is "sufficiently high."

Heat Transfer Coefficient Again there are essentially two ways to determine the heat transfer coefficient and thus the Stanton number. An energy balance can be written for a control volume enclosing the porous surface and boundary layer. The appropriate equation is

$$q_{wall} = q_{coolant} + q_{cond} + q_{rad} \qquad (3.4)$$

The term on the left hand side represents the energy loss from the fluid in the freestream and boundary layer and the three terms on the right hand side account for the enthalpy rise of the coolant across the porous wall, the conduction of heat through the porous material and radiation from the plate to the surroundings. To simplify the experiment as much as possible, the plate is normally coated on the outside with a substance having a low emissitivity, thus permitting the radiation term to be neglected. As demonstrated by Bartle and Leadon (28), the conduction term can be made negligible by heating the outside wall of the test section to the inside wall temperature with auxiliary electrical equipment. Adjusting the temperatures requires considerable precision since the steady state is disrupted by the additional energy

input. An alternate technique (61) permits conduction losses but requires a series of thermocouples accurately placed to measure the lateral and transverse temperature gradients. Assuming that conduction and radiation effects can be neglected, equation 3.4 becomes

$$h(T_w - T_r) = (\rho v c_p T)_o - (\rho v c_p T)_w \tag{3.5}$$

Introducing the Stanton number defined as

$$St = \frac{q_w}{\rho_\infty u_\infty c_{p\infty}(T_r - T_w)} \tag{3.6}$$

and assuming that the product, $\rho v c_p$ remains constant for the coolant from the reservoir to injection, the following relation for the Stanton number is obtained.

$$St = \frac{(\rho v c_p)_o \ (T_o - T_w)}{(\rho u c_p)_\infty \ (T_w - T_r)} \tag{3.7}$$

All of the terms in the above expression can be determined from a single experiment except the adiabatic wall temperature. To complete the evaluation of St, T_r must be found as follows. The wall and coolant temperatures are first measured for given mainstream conditions and blowing rate. Then, with the same mainstream conditions and blowing rate, the coolant supply is heated until it reaches the wall temperature. This procedure eliminates all energy losses from the freestream gas and guarantees that the wall temperature will be at its recovery or adiabatic value. The steady state

is altered when this is done but there must be a condition for which the supply and wall temperatures are constant and equal. With all terms on the right hand side of equation 3.7 known, the Stanton number can be calculated.

The alternate method of determining the Stanton number is analogous to the second technique described for finding the skin friction coefficient. This involves measurements of the thermal boundary layer and the use of the energy integral equation which can be written as

$$\frac{d\phi}{dx} + \frac{\phi}{u_\infty}\frac{du_\infty}{dx} - \frac{c_{pc}}{c_{p\infty}} F = St \qquad (3.8)$$

where ϕ is the energy defect of the boundary layer defined by

$$\phi = \int_0^{\delta_T} \frac{\rho u(T_\infty^o - T^o)\, dy}{\rho_\infty u_\infty (T_r - T_w)} \qquad (3.9)$$

By measuring the boundary layer velocity and temperature profiles at various points along the plate, ϕ can be determined numerically and from it, the gradient of the energy loss, $d\phi/dx$. The local Stanton number is then determined from equation 3.8.

3.3 Results

Due to the accumulation of data in the literature over the past fifteen years, a definite need exists for a comprehensive comparison of the work that has been accomplished in specific areas of transpiration

cooling. In Table 3.1, over twenty investigations are presented and compared on the basis of the independent variables measured, the apparatus used and the techniques involved. This table was limited to turbulent flow since when blowing is introduced into a normally laminar boundary layer, it tends to become unstable and transition occurs soon thereafter. Therefore, though transpiration cooling may reduce the heat transfer by a more significant factor than transition to turbulence tends to increase it, the advantages of the end result for normally laminar flow are greatly diminished (62).

Rather than discuss all the investigations included in the table, only those reports most pertinent to rocket thrust chamber cooling are considered in detail. Though the choice is somewhat arbitrary, the experiments which seem to be of greatest importance are those due to Mickley and Davis (20), Tewfik (59), Pappas and Okuno (26), Romanenko and Kharchenko (19), Bartle and Leadon (28), Green and Nall (42), Danberg (24), and Brunner (27). The experimental work shall be discussed from the standpoint of the apparatus required for the individual measurements and the most significant results and contributions of each study.[1]

3.3.1 Pertinent Experimental Work

Mickley and Davis Probably the most extensive and precise work performed to determine skin friction as a function of blowing rate and Reynolds number can be attributed to Mickley and Davis (20). The effect

---

[1] The less extensive work of Hacker (64) will not be discussed, but his data will be presented later.

TABLE 3.1 GENERAL COMPARISON OF EX

Reference	Coolant	Test Section Geometry	Porous Material	Skin Friction Calculated	Temperature Measurements	Bounda Measur
Friedman (9)	Air	Cylinder	Nickel	No	Yes	No
Duwez and Wheeler (94)	N_2, H_2	Cylinder	Copper, Nickel, Stainless Steel	No	Yes	No
Brunner (27)	N_2, He, H_2O	Cone	Sintered Inconel	No	Yes	No
Rubesin, Pappas, and Okuno (61)	Air	Flat Plate	Sintered Stainless Steel	No	Yes	No
Chauvin and Carter (51)	N_2, He, H_2O	Cone	Sintered Stainless Steel	No	Yes	No
Eckert, Diagualla, and Donoughe (93)	Air	Flat Plate	Sintered Bronze	Yes	No	Pressu
Leadon and Scott (67)	Air, He	Flat Plate	Sintered Stainless Steel Wire	No	Yes	No
Tendeland and Okuno (57)	Air	Cone	Copper Wire Mesh	Yes	No	No
Mickley and Davis (20)	Air	Flat Plate	Wire Cloth	Yes	No	Pressu
Brunk (36)	Air	Flat Plate	Sintered Bronze	No	Yes	No
Barrow (58)	Air	Flat Plate	**	Yes	No	Pressu
Green and Nall (42)	N_2	Nozzle	Sintered Stainless Steel	Yes	Yes	No
Pappas and Okuno (26)	He, Air, Freon-12	Cone	Treated Fibrous Glass	Yes	No	No
Hacker (64)	Air	Flat Plate	**	Yes	No	Pressu
Walton and Rashis (92)	N_2, He	Cone	Sintered Stainless Steel	No	Yes	No
Rashis (71)	N_2, He	Double Wedge	Sintered Stainless Steel	No	Yes	No
Bartle and Leadon (28)	N_2	Flat Plate	Sintered Stainless Steel	No	Yes	Pressu Temper
Romanenko and Kharchenko (19)	He, Freon-12, CO_2, Air	Flat Plate	Porous Copper	Yes	Yes	Pressu Temper
Tewfik (59)	Air	Cylinder	Wire Cloth	Yes	No	Pressu
Danberg (24)	Air	Flat Plate	Sintered Stainless Steel	Yes	Yes	Pressu Temper
Olson and Eckert (60)	Air	Cylinder	Porostrand Wire Cloth	Yes	No	Pressu

* Stagnation Temperature

** Not Specified

PERIMENTAL INVESTIGATIONS

ry Layer ments	Range of Blowing Rate	Range of Reynolds Number	Mach Number	Freestream Temperature (°F)	Remarks
	**	2.5×10^4 to 2.5×10^5	0	800 to 1300	
	0 to 0.025	1.5×10^3 to 1.0×10^5	0 to 1.0	1100 to 4200	
	0.002 to 0.06	1.4×10^6	2.5	2040 *	
	0.001, 0.002, 0.003	1.5×10^6 to 7×10^6	2.7	150 *	
	0 to 0.0014	8×10^6	2.05	563 to 640 *	
re	0 to 0.017	3×10^6 to 6×10^6	0	ambient	
	0 to 0.004	4×10^6	3.0	42.5, 73.6	
	0 to 0.0028	6.25×10^6 to 8.56×10^6	2.71	ambient	
re	0 to 0.01	4×10^4 to 3×10^6	0	ambient	Flow in channel with $dP/dy = 0$
	0 to 0.016	1×10^6 to 16×10^6	0.6	215 *	Stanton number not calculated
re	**	**	0	ambient	Velocity profile measurements
	0.001 to 0.02	1×10^6 to 10×10^6	$M > 1.0$	ambient, 500 *	
	0 to 0.00285	0.9×10^6 to 5.9×10^6	0.3, 0.7, 3.5, 4.7	ambient	
re	0 to 0.01	**	0	ambient	Studied separation
	**	12×10^6	$M < 4.08$	$T_\infty^\circ \leq 1390$	Tests in hot jet and free flight
	0.0003 to 0.003	5.78×10^5 to 8.2×10^6	2.0	1295 to 2910 *	
re and ature	0 to 0.0016	1×10^6 to 5×10^6	2.0, 3.2	42.5, 73.6	
re and ature	0.0001 to 0.007	1×10^5 to 5×10^5	0	350, 530	Pressure gradient effects included
re	0 to 0.00312	1×10^5 to 1.1×10^6	0	ambient	External flow; flow parallel to axis
re and ature	0 to 0.0025	8×10^6 to 19×10^6	6.7	527 *	
re	0.00246 to 0.0584	2.8×10^4 to 8.2×10^4	0	ambient	Velocity profile measurements

of Mach number and wall to freestream temperature was purposefully eliminated in their work so that the influcence of Reynolds number could is isolated, thus enabling a study of c_f as a function of the blowing rate F with Re_x as the free parameter. Since all run conditions were established at $M \approx 0$ and $T_w/T_\infty = 1.0$, their results become extremely limited in regard to practical applications; nevertheless, because the data is extensive, it may be used to verify the numerous theoretical analyses of other authors.

The work of Mickley and Davis was conducted to clarify a previous investigation by Mickley, Ross, Squyers and Stewart (63) when it was discovered that the latter had used defective equipment which gave some incorrect results. The procedure and equipment of Mickley and Davis was much the same as that of the former study (63). The mainstream air was supplied by a centrifugal fan to a calming chamber where vorticity and turbulence was reduced. The calming chamber led into a convergent nozzle followed by a rectangular test section. Only the upper wall of the one foot wide and ten foot long channel was porous. The bottom plate was adjustable to enable the establishment of a zero Euler number and pressure gradient, thus approximating the flow over a flat plate. To insure boundary layer development beginning at the leading edge, provisions were made for suction at the upstream edge of the porous injector.

As indicated in Table 3.1, air was not only used for the bulk flow but for the injected fluid as well. The mainstream velocity ranged from 17 to 60 fps, the blowing rate F from zero to 0.01 and the Reynolds number based on x from 4×10^4 to 30×10^5. The model

intended for the investigation could be described as turbulent, steady, subsonic flow with zero pressure gradient. The blowing rate F had a constant local value for the entire length of the test section. An impact probe was used to measure the velocity distribution at nine stations along the plate. The precision of these measurements were estimated at

$$\frac{\Delta u}{u^2} = \frac{1.8}{u^2} \tag{3.10}$$

As explained earlier, the velocity profiles permitted the calculation of the displacement and momentum thicknesses and their gradients in the axial direction. Thus, the skin friction coefficient follows from the momentum integral equation.

Mickley and Davis found that for the conditions which they considered in their experimental investigation, the skin friction and velocity distribution are a function only of the blowing rate and a Reynolds number based on the distance from the leading edge. This is in agreement with Spalding's hypothesis of Chapter 2. A comparison of their results with previous data (63) indicated an error of 15 to 30 percent in the earlier data. In Figure 3.1, the results of Mickley and Davis are presented with the skin friction coefficient plotted as a function of the Reynolds number with blowing rate as a parameter. The theoretical predictions of Rubesin (4), which are indicated by the solid line in Figure 3.1, are in general agreement with the over-all trend of the experimental results although the latter are as much as 15 percent low. It is virtually impossible to prove which is more exact and in fact, it seems to be relatively unimportant when Reynolds number is the independent

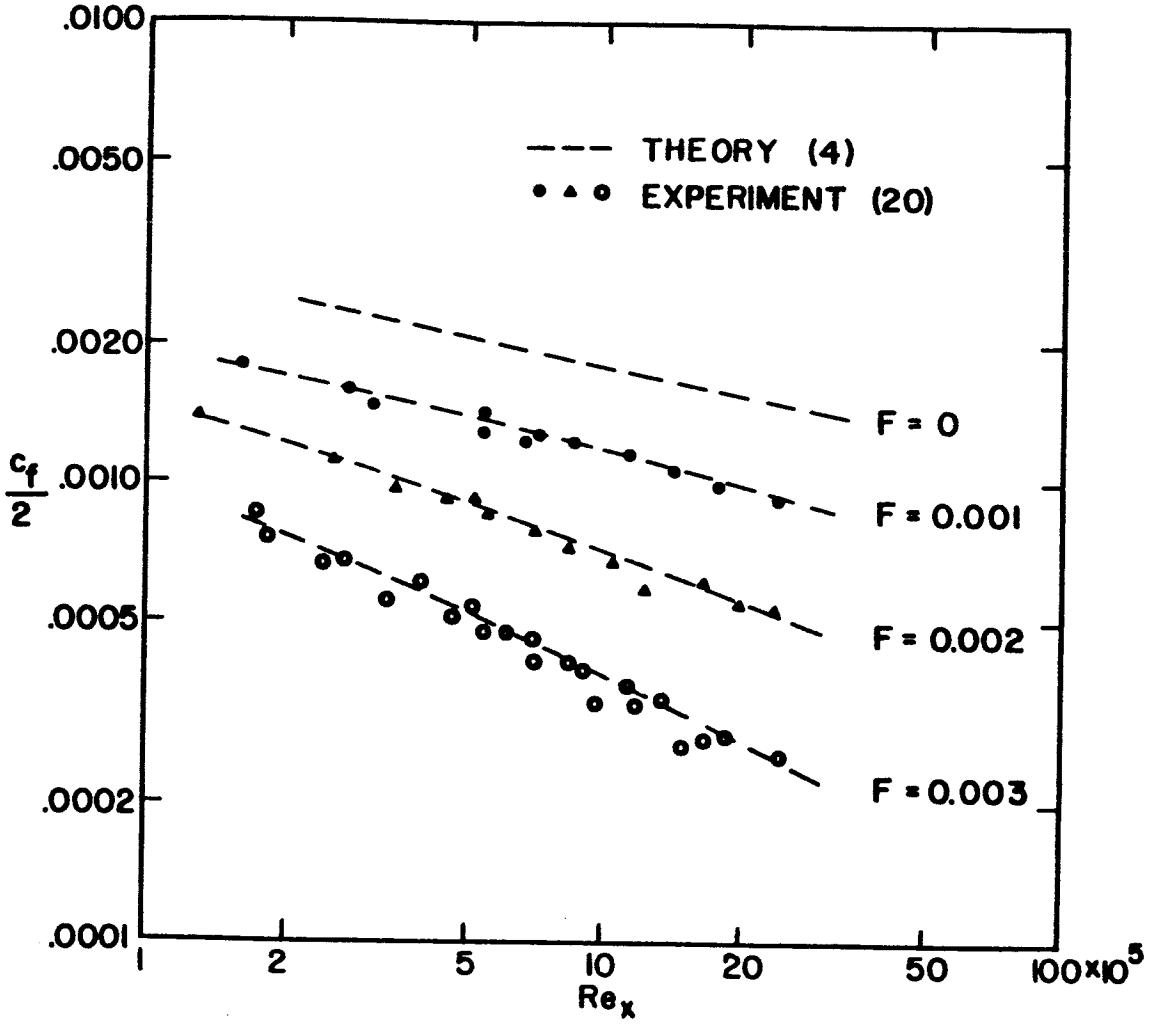

FIGURE 3.1 VARIATION OF LOCAL SKIN FRICTION COEFFICIENT WITH REYNOLDS NUMBER (20)

variable; for Mickley and Davis used the distance x as the characteristic length and although the model was intended to approximate flow over a flat plate, it was actually internal flow. The hydraulic diameter is normally considered to be the characteristic dimension for flow through pipes or ducts.

Although it is difficulat to assess the accuracy of the theoretical solutions beyond indicating the limitations of the assumptions involved, it is relatively easy to uncover the problems incurred by the measurements of Mickley and Davis (20). For example, though suction was employed at the leading edge, the velocity profile in the center of the channel was already approaching fully developed flow. The theoretical analyses reviewed in the preceding Chapter were of course for flow over a flat plate. Further, serious errors, as pointed out by Tewfik (59) and described below, are involved in the calculation procedure of Reference 20.

The momentum integral equation for a turbulent boundary layer with injection and a freestream pressure gradient is

$$\frac{d\Theta}{dx} + \frac{\Theta}{u_\infty}\left(\frac{\delta^*}{\Theta} + 2\right)\frac{du_\infty}{dx} - F = \frac{c_f}{2} \qquad (3.11)$$

The subject experimental results (20) show that the terms involving the gradient of momentum thickness and the blowing rate parameter are both comparatively large and of the same order of magnitude; thus, their difference is small. Even though the pressure gradient term may be small, it cannot, in general, be neglected when compared to the difference of the two aforementioned terms. Unfortunately, Mickley and Davis did not

recognize this, reasoning that since the freestream velocity varied only slightly, the entire pressure gradient term could be considered negligible. Because of this omission of the pressure gradient term in calculating c_f, Tewfik (59) found that the values for the skin friction coefficient calculated by Mickley and Davis were 15 percent too small at the highest value of F. Further questions arise regarding the validity of the data when it is noted that the values of the skin friction coefficient for no blowing agree very well with the equation for a smooth impermeable flat plate. One would expect a porous plate to behave more like an extremely rough surface with a sizeable roughness factor, ε/d.

In the final section of this Chapter, the data of Reference 20 are compared with other existing results on the basis of the fractional reduction in skin friction and with blowing rate as the independent variable. See Figure 3.7.

Tewfik Tewfik (59) conducted experimental investigations of his own because of the problems he discovered with the skin friction results of Mickley and Davis. His work will be discussed briefly because of the significant disagreement of his results with other subsonic data (19, 20, 26, 64). A comparison of the various results will be deferred to the final section of this Chapter.

His experiments were concerned with external flow over a 2 in. (outside diameter) circular cylinder with the flow parallel to the axis of symmetry. The velocity of the freesteam was 110 fps and thus the Mach number was approximately zero. Air was injected at blowing rates of 0.00107, 0.00202, and 0.00312. Boundary layer measurements of the

static pressure profile were made from which the skin friction was determined from equation 3.11.

The following conclusions were the result of his (59) experimental work. (1) The density-velocity product (ρv) is not constant across the boundary layer (as assumed in the theoretical analyses of the preceding Chapter) but changes by a factor of three from the wall to the outer edge of the turbulent region. (2) The momentum equation in the form

$$\tau = \tau_w + (\rho v)_w u$$

is a "poor" approximation beyond the inner "tenth" of the boundary layer. (3) The effect of Mach number on the ratio c_f/c_{fo} is negligible. (4) The results for the skin friction coefficient ratio agree with the analysis of Rubesin (4) but disagree significantly with the solution due to Turcotte (21). (5) All boundary layer thicknesses were increased by injection. Only conclusion (3) is objected to here, primarily because of the following study due to Pappas and Okuno (26).

Pappas and Okuno The work of Pappas and Okuno (26) is included because it is not only recent but encompasses a larger range of parameters than the other investigations reviewed. Again, the interest was primarily in measuring the skin friction coefficient of a compressible turbulent boundary layer though considerable attention was given to the influence of blowing rate, Mach number and the effect of foreign gas injection, i.e., molecular weight.

A 10 in. cone with a total included angle of 15^o was employed as the porous injector in the exhaust of a 2 ft x 2 ft transonic wind

tunnel. The injector was manufactured from a mat of glass fibers treated with uncurred phenolic resin. Skin friction measurements were based on a force balance for the cone as described earlier. Eleven pressure taps with an orifice diameter of 0.020 in. were distributed over the porous surface and on the base of the cone to determine the external pressure distribution. It was discovered that the difference in pressure between the exterior surface of the cone and the base was on the same order of magnitude as the total shear stress. Calculations of the total drag on the model were possible using a strain gage attached to the cone support. The total frictional force and thus the average friction coefficient, $\bar{c}_f$, was determined from the external pressure distribution, the coolant injection rate, the total drag and the wind tunnel stagnation temperature pressure.

To insure a turbulent boundary layer beginning at the leading edge of the cone, garnet paper was attached in front of the nose cone to serve as a boundary layer trip. The authors conjectured that the influence of mass injection on the boundary layer growth may have been somewhat reduced because the porous surface did not begin for approximately 2 in. downstream of the nose. Experiments were conducted for freestream Mach numbers of 0.3, 0.7, 3.5, and 4.7 and a Reynolds number varied from 0.9×10^6 to 5.9×10^6. The Reynolds number for the subsonic portion of the experiment was based on the freestream conditions, whereas for the supersonic portion, the surface conditions after the shock wave for a hypothetical inviscid flow were selected. In each case, the characteristic length of the cone was 10.5 in., the total length. This then presents an initial difficulty

in comparing the subsonic results of Pappas and Okuno (26) with Mickley and Davis (20) and Tewfik (59) since the latter investigations (20, 59) employed a Reynolds number based on the distance from the leading edge and found a local value of skin friction coefficient.

Another difficulty in comparing the results of Pappas and Okuno with other investigations arises because the skin friction coefficient does not necessarily have the same value on a cone as it does on other geometries under the same mainstream conditions. To obtain a relationship for skin friction coefficient under the condition of zero blowing, Mickley and Davis adopted the Blasius equation given by

$$c_{fo} = 0.0592\ Re_x^{-0.2} \tag{3.12}$$

which they verified experimentally. To obtain the equivalent equation for a cone, the constant must be changed to 0.0754, the characteristic length x to L, and the local value of skin friction to the average value. Thus

$$c_{fo} = 0.0754\ Re_L^{-0.2}$$

If the data for the flat plate and cone are compared on the basis of the ratio of the skin friction coefficient with blowing to the skin friction coefficient without blowing, then it is generally believed (26, 65) that the effects due to differences in Reynolds number and geometry will cancel out. In other words, plotting c_f/c_{fo} against $2F/c_{fo}$ for a flat

plate should be analogous to plotting $\bar{c}_f/\bar{c}_{fo}$ against $2F/\bar{c}_{fo}$ for a cone and if so, the curves should, in fact, be coincident. This is another reason for most authors correlating their data in the manner specified above.

A second objective of the investigation conducted by Pappas and Okuno was to assess the influence of Mach number on $\bar{c}_f/\bar{c}_{fo}$. The subsonic results of Reference 20 suggest that the various theories for a turbulent boundary layer with mass injection (4, 5, 14, 16, 17, 66) do not properly account for the influence of Mach number on the relative reduction in skin friction (c_f/c_{fo}). In fact, Rubesin's theory, which is typical of most, indicates that a change in Mach number from zero to 4.0 has an insignificant effect on the reduction. Moreover, this effect of Mach number is probably within the range of accuracy of their predicted results. Pappas and Okuno found that the higher the blowing rate, the more pronounced the effect of Mach number becomes. For example, at a blowing rate of $2F/\bar{c}_{fo} = 0.2$ for helium, the change in the ratio $\bar{c}_f/\bar{c}_{fo}$ is less than 5 percent for a Mach number change from 0.3 to 3.0. However, for a blowing rate of $2F/\bar{c}_{fo} = 2.8$, the change in $\bar{c}_f/\bar{c}_{fo}$ for the same Mach number change is on the order of 40 percent. The data of Mickley and Davis (20), Pappas and Okuno (26) and Danberg[1] (24) are presented in Figure 3.2 to illustrate the influence of Mach number on the skin friction coefficient. It should be noted that between a Mach number of 2.5 and 5.0, the effect is relatively insignificant. In the subsonic regions of the curves, the effect becomes somewhat more pronounced.

---

[1] The results of Danberg will be discussed in detail later in this section.

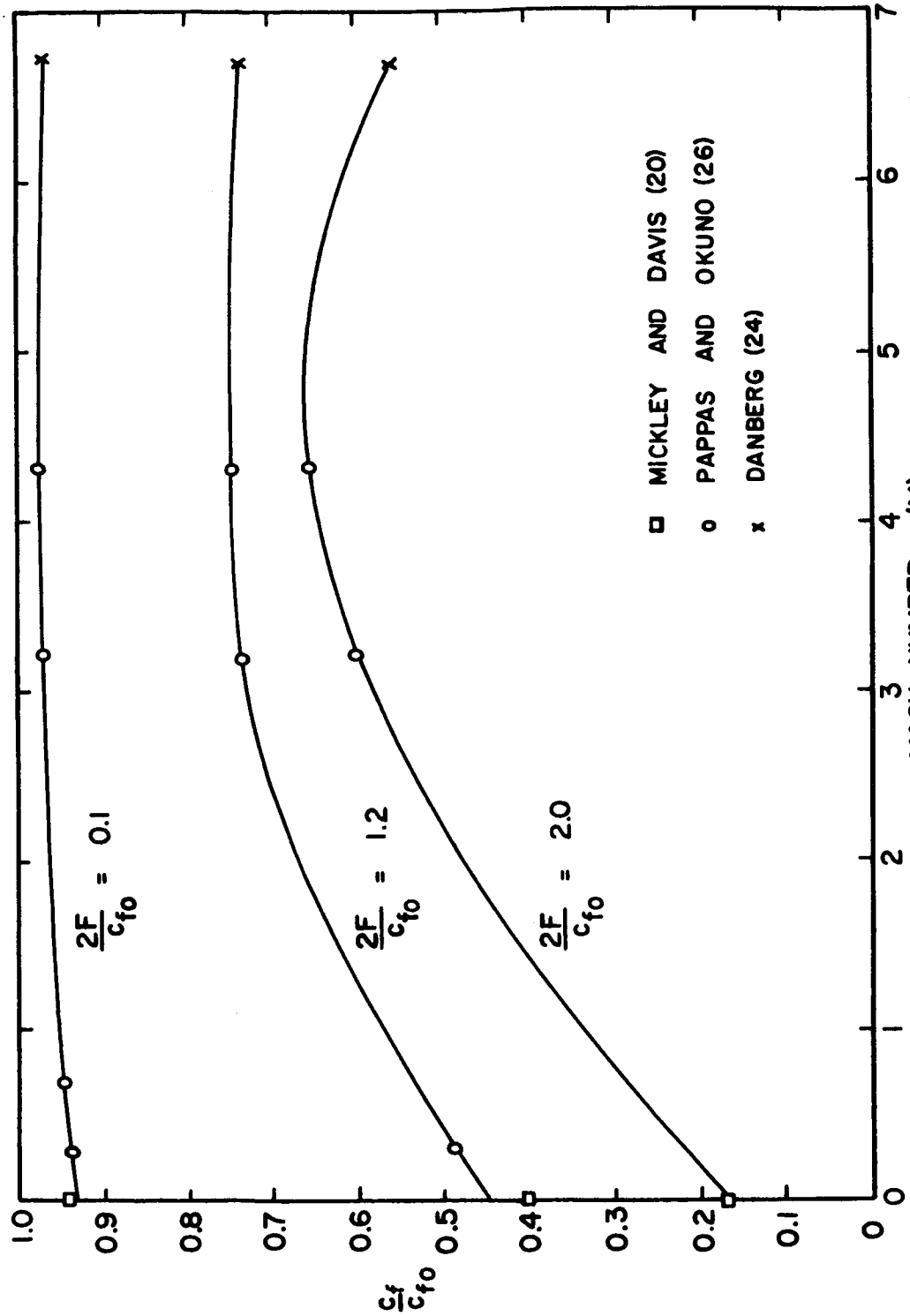

FIGURE 3.2 EFFECT OF MACH NUMBER ON THE REDUCTION IN SKIN FRICTION WITH AIR INJECTION

A final objective of the parametric study of Reference 26 was to compare the effects of the injection of a light gas (helium) and a heavy gas (freon-12) with the effects of the injection of air into air. Helium was chosen because it is inert and freon-12 because its molecular weight is about the same as the gas emitted by common ablating heat shield materials. A comparison of the effectiveness of helium, air, and freon-12 is presented in Figure 3.3 in the form of the skin friction reduction realized for selected values of blowing rate with the Mach number held constant at approximately zero. The experimental results are in general agreement with the theoretical predictions of Rubesin and Pappas (14) as shown, which indicates helium to be the most efficient, air the second best, and freon-12 the least effective. Reductions of the skin friction coefficient due to blowing of up to 80 percent were realized with helium without inducing boundary layer separation.

Romanenko and Kharchenko The investigation of Romanenko and Kharchenko (19) is one of the more significant recent contributions to the understanding of transpiration cooling problems for three reasons: (1) their unique experimental techniques (see below) made their approach more accurate; (2) both the nonzero and constant pressure gradient cases were considered; and (3) the effects due to blowing on both the skin friction coefficient and heat transfer, i.e., Stanton number, were investigated.

The apparatus employed in the experimental study was similar to that used by Mickley and Davis (20) in that the tests were conducted in a

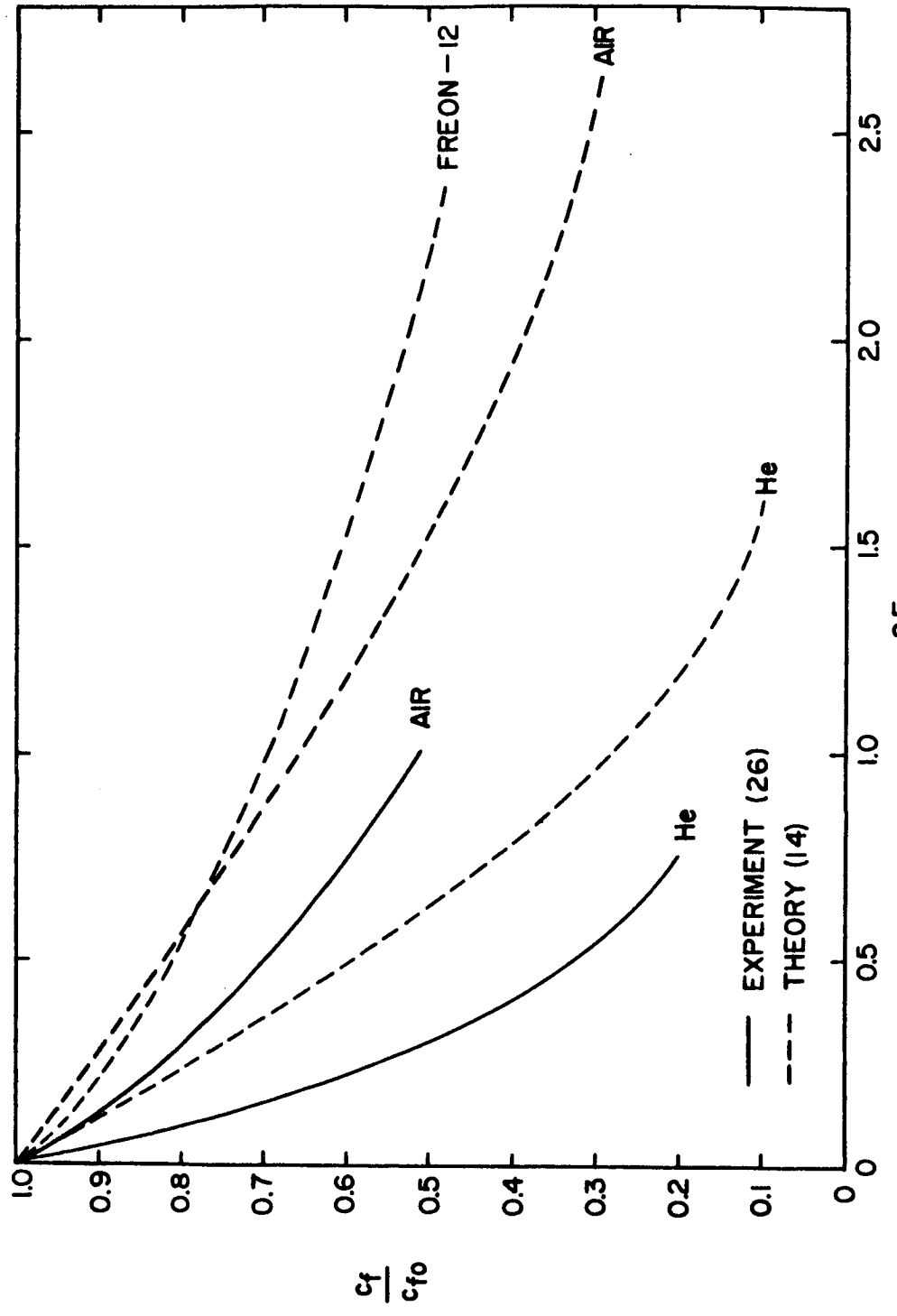

FIGURE 3.3 COMPARION OF THE EFFECTIVENESS OF AIR AND He IN REDUCING SKIN FRICTION

rectangular duct with suction provided near the leading edge. A 11.8 in. x 2.36 in. porous plate was imbedded in the bottom wall of the test section and the side walls were made adjustable to hold the pressure gradient at the desired value. The following conditions were maintained throughout the experiment:

$$10^5 < Re < 5x10^5$$

$$M = 0.0$$

$$82 \text{ fps} < u_\infty < 250 \text{ fps}$$

$$350 \text{ F} < T_\infty < 530 \text{ F}$$

$$0.0001 < F < 0.007$$

The coolants used were freon-12, carbon dioxide, air and helium. Boundary layer measurements were made to determine the velocity and temperature distributions normal to the plate.

One reason that their results are extremely important is that two different methods were used for determining not only the skin friction coefficient but the heat transfer coefficient as well. This feature enabled them to double check each point on any given curve. In Figure 3.7, to be discussed in detail in Section 3.3.2, their results for skin friction are shown to lie within the range indicated for all other subsonic results (20, 26, 64) except Tewfiks (59). Thus, the premise that Mach number has a significant effect on the relative skin friction ratio is given added support. The skin friction coefficient without blowing and for the zero pressure gradient portion of the experiment was determined by three separate methods. They were: (1) the integral momentum

equation; (2) the Klauser method; and (3) the Blasius equation given by the relation

$$\frac{c_{fo}}{2} = 0.0296\ Re_x^{-0.2}$$

Good agreement was obtained by all techniques.

The heat transfer experiments were conducted in a similar manner. Both the energy integral equation and a heat balance were used to obtain the Stanton number. Some error could have been introduced in determining the Stanton number with zero blowing for only the empirical equation

$$St_o = \frac{0.0296\ Re_x^{-0.2}}{1 + .87\ A_1\ Re_x^{-0.1}(Pr-1)} \qquad (3.13)$$

where $A_1 = 1.5Pr^{-0.167}$ was used. The data from their measurements are plotted in Figure 3.8 (Section 3.3.2) along with similar results and again, further discussion will be deferred until the other pertinent investigations (24, 27, 28) have been reviewed. But assuming that the error introduced by using equation 3.13 is not great, it may be concluded (19) that the effect of Mach number on heat transfer data is not significant when plotted in the indicated manner (St/St_o vs. F/St_o). A further surprising conclusion of their investigation was that a pressure gradient does not significantly affect the results. Thus the heat transfer results of Romanenko and Kharchenko may be generalized to any Mach number or pressure gradient without serios error. On the

other hand, the skin friction results were considerably influenced by both the aforementioned parameters. The authors (19) present a detailed method for determining the skin friction coefficient for flow with a pressure gradient and thus it shall not be reviewed here.

Bartle and Leadon The number of experimental investigations specifically concerned with the combined effects of heat and mass transfer which can be compared with the theories presented in Chapter 2 are limited. Bartle and Leadon (28) conducted what is believed to be one of the more accurate experiments involving boundary layer measurements. Earlier experiments by Leadon and Scott (67) were of an exploratory nature and tended to verify the then existing theories of References 4, 15, and 63. The objective of the investigation of Bartle and Leadon was to supplement the data of the former report (28) with more exact measurements to attempt to discern any discrepancies which may exist between theory and experiment. Their interest then was in the reduction of heat transfer achieved with gas injection into a compressible turbulent boundary layer.

The test section was formed by sintering 5 microinch stainless steel powder into a 5.5 in. x 16 in. porous plate and it was used as the bottom plate of a wind tunnel. Thermocouples were implanted at a distance of 0.025 in. from the inside wall for measuring the surface temperature. An isothermal wall was maintained by varying the rate of injection along the test section. A variable axial injection rate was possible by regulating the flow through individual coolant manifolds supplying successive portions of the porous test section. Experimentation to realize the isothermal wall condition indicated a required axial variation of the injection velocity somewhat greater than $v_w \propto x^{-0.2}$, which is indicated by turbulent boundary layer theory (28).

To simplify the experiment as much as possible, an attempt was made to minimize extraneous energy losses to the surroundings due to radiation from the outer wall and conduction due to lateral and longitudinal temperature gradients. To this end, the interior surfaces facing the porous plate were coated with a chem-nickel liner and auxiliary guard heaters were used to maintain the plate at a uniform temperature.

Experiments were conducted for nitrogen injection into air for a freestream Mach number of 2.0 and 3.2 and a corresponding mainstream static temperature of 73.6 F and 42.5 F, respectively. The heat transfer to the surface was mainly due to viscous dissipation in the boundary layer and consequently, an accurate evaluation of the recovery and wall temperatures was an important procedure in determining St or h.

A heat balance identical to the one described in Section 3.2.2 (equation 3.5) was written for a control volume defined by the porous plate. It was found that the independent variable which minimizes the effects of Mach number the most significantly is F/St_o, which is in agreement with other recent work (19, 24, 27, 65). The dependent variables studied by Bartle and Leadon were the Stanton number in the form St/St_o, the recovery factor (r/r_o), and the design temperature ratio defined by

$$R = \frac{T_w - T_o}{T_{ro} - T_o} \tag{3.14}$$

Their results for Stanton number follow the predicted trends indicated by theory (4, 15, 66). As for the case of skin friction coefficient, a significant dependence of the Stanton number ratio (St/St_o) on Mach number resulted when F/St_o was used as the independent variable. The results

lie slightly above and below the predictions of Rubesin (4) for Mach numbers of 3.2 and 2.0, respectively. The data for the latter (M = 2.0) are plotted in Figure 3.8. Finally, it was observed that the design temperature ratio is virtually independent of Mach number as shown in Figure 3.4. Use of this curve is recommended by the author when the recovery temperature without blowing is given or can be determined.

Green and Nall. Several experiments on transpiration cooling have been performed with nozzles having porous inserts at or near the throat (68, 69). Unfortunately, the interest has been primarily in the effects of injection on the heat transfer downstream of the porous insert. This problem is analogous to that of gaseous film cooling (70). The only investigation (unclassified) reported specifically concerned with the effects of transpiration cooling on the heat transfer to a nozzle is that of Green and Nall (42).

The experimental apparatus consisted of a two dimensional nozzle, the bottom plate of which was fabricated from sintered stainless steel plate. Plates having three different values of permeability were employed in the investigation. The two dimensional nozzle had a constant channel width of 0.5 in. and was shaped to a divergence half-angle of 15^{o} and an expansion ratio of ten. The side walls were fabricated from glass and quartz crystal to enable ovservation by spark schlieren photography.

Nitrogen was employed as the mainstream fluid and the coolant as well. Experiments were conducted for two mainstream stagnation temperatures: 500 F and a temperature corresponding to ambient conditions; mainstream stagnation pressures ranged from approximately 200 to 400 psia.

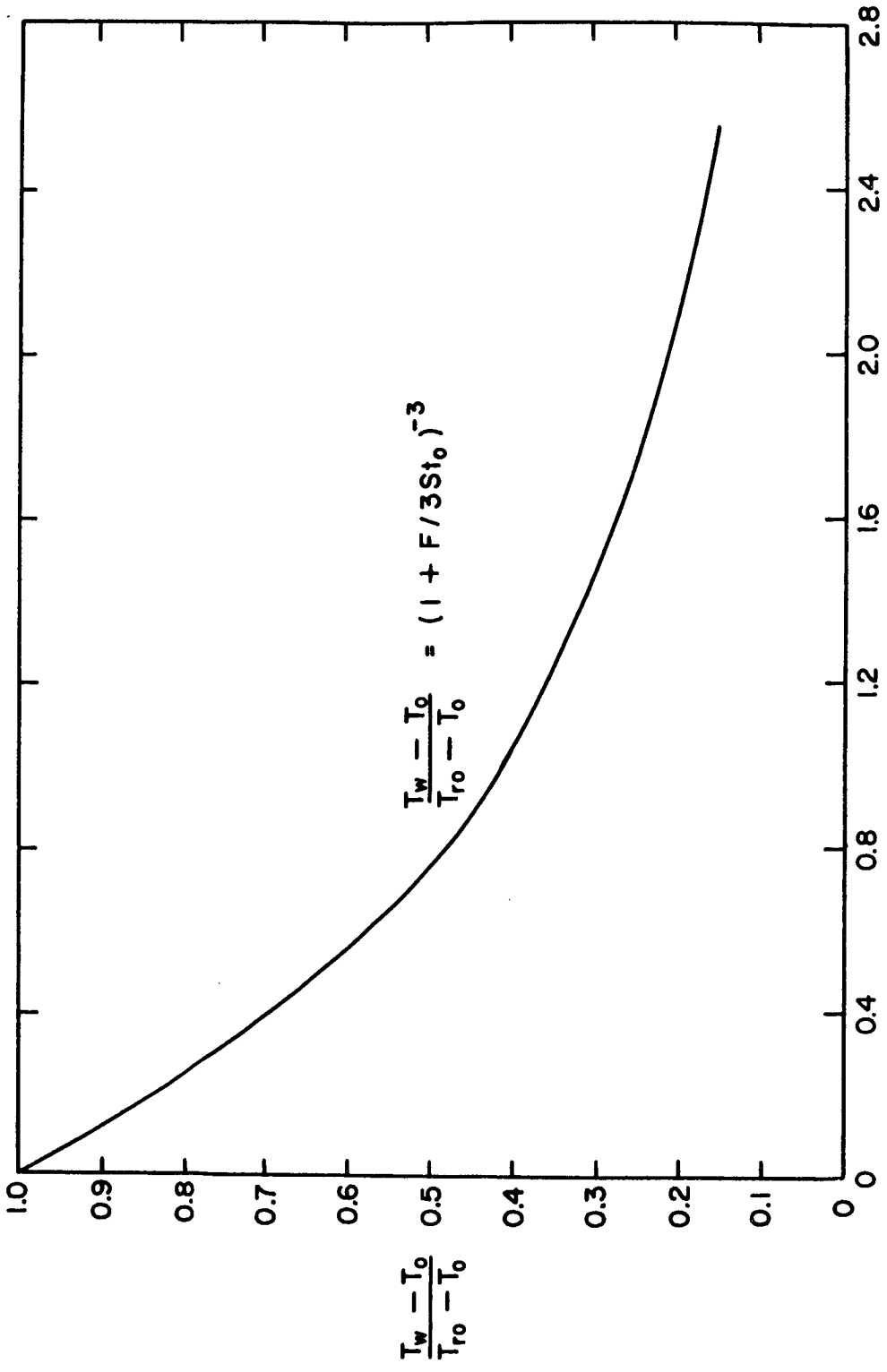

FIGURE 3.4 EXPERIMENTAL RESULTS OF BARTLE AND LEADON FOR THE DESIGN TEMPERATURE RATIO AT M = 2.0, AND M = 3.2

The two main objectives of the subject investigation were to study the effect of injection upon boundary layer separation as it relates to thrust vector control and to determine the effects of transpiration cooling on the heat transfer to the nozzle wall. With regard to the former objective, it was concluded that the point of optimum separation[1] for maximum thrust was approached with an increasing blowing rate. For the test conditions, the local injection rate parameter F varied from 0.005 to 0.03 at the separation point. Further, it was discovered that the stagnation temperature did not influence the effectiveness of the separation significantly. Though this was only a preliminary investigation, it demonstrated that injection can be used successfully as a means of thrust vector control if the inlet manifold is compartmented. The latter is necessitated by the variable static pressure distribution along the inner wall surface requiring a similar variation in pressure in the several compartments. In the tests conducted in Reference 42, a deflection of the exhaust jet of 10^{o} was obtained for the maximum injection rate.

The experiments designed to study the effects of mass transfer on the rate of heat transfer were primarily concerned with the region upstream of the point of jet detachment. The results demonstrated that the effectiveness of transpiration cooling is not diminished in the diverging section of a nozzle where a large positive Euler number exists. In fact, for the range of injection rates employed ($0.005 > F > 0.003$), the reduction in heat transfer due to blowing was greater than one order of magnitude. The Stanton number ratio (St/St_{o}) was found to decrease

---

[1] Point along the wall where the static pressure equals one atmosphere (42)

from 1.0 to 0.2 for an increase in the dimensionless blowing rate (F/St_0) from zero to 3.0 while for a blowing rate change from 3.0 to 10.0, the Stanton number ratio decreased from only 0.2 to approximately 0.04. These results are also only preliminary since insufficient measurements were made to calculate the heat transfer without the assistance of Rubesin's (4) equations.

Danberg One of the most recent and significant contributions to existing data in the area of transpiration cooling is that due to Danberg (24). In addition to obtaining data for skin friction and heat transfer reductions due to transpiration cooling, he accomplished the following: (1) verified the Reynolds analogy for the case of mass injection; (2) studied and illustrated graphically the effect of injection on the boundary layer thickness and the velocity and temperature profiles; and (3) extended the existing range of data to higher Mach numbers.

Tests were conducted on a porous flat plate, 1.94 ft. long and 0.833 ft. wide, in a hypersonic wind tunnel with a Mach number of 6.7. The supply temperature was maintained at 530 F throughout the experiments while the supply pressue was varied from fifteen to thirty atmospheres. Boundary layer measurements were made for the velocity and temperature profiles to facilitate a comparison of the skin friction and heat transfer with blowing. The pressure term in the momentum integral equation was neglected in the calculations because it affected the results by only 1.5 percent whereas the scatter in the data for selected run conditions ranged from 10 to 15 percent.

The most pertinent result of Danberg's study was his verification of the validity of the Reynolds analogy in the presence of mass transfer.

This is illustrated by Figure 3.5 in which the experimentally determined Stanton number is plotted against the skin friction coefficient for wall to freestream temperature ratios of 4.5, 5.2 and 7.6. It can be seen that for the injection of air into air, Reynolds analogy in the form

$$St = \frac{c_f}{2} \tag{3.15}$$

represents a better approximation to the data than the modified Reynolds analogy due to Colburn, i.e.,

$$St = \frac{c_f}{2} (Pr)^{2/3} \tag{3.16}$$

Equation 3.15 was also shown to be a better approximation for the case of no mass injection.[1]

Earlier in this section, it may be recalled that Pappas and Okuno (26) found that the effect of Mach number diminished at hypersonic speeds and in all cases for F/c_{f_0} = constant, c_f/c_{f_0} either decreased slightly or approached a constant as M was increased above 4.5. Danberg's results, as illustrated previously in Figure 3.2, indicated that this indeed is the case. This, in part, explains why there is general agreement of data for the reduction in heat transfer and skin friction for supersonic

---

[1] It should be emphasized that the choice of the analogy to be employed can have a pronounced influence on the prediction of the blowing rate required for a given situation. This is particularly important in regard to the evaluation of St_0. The sample calculations in Appendix B illustrate this point.

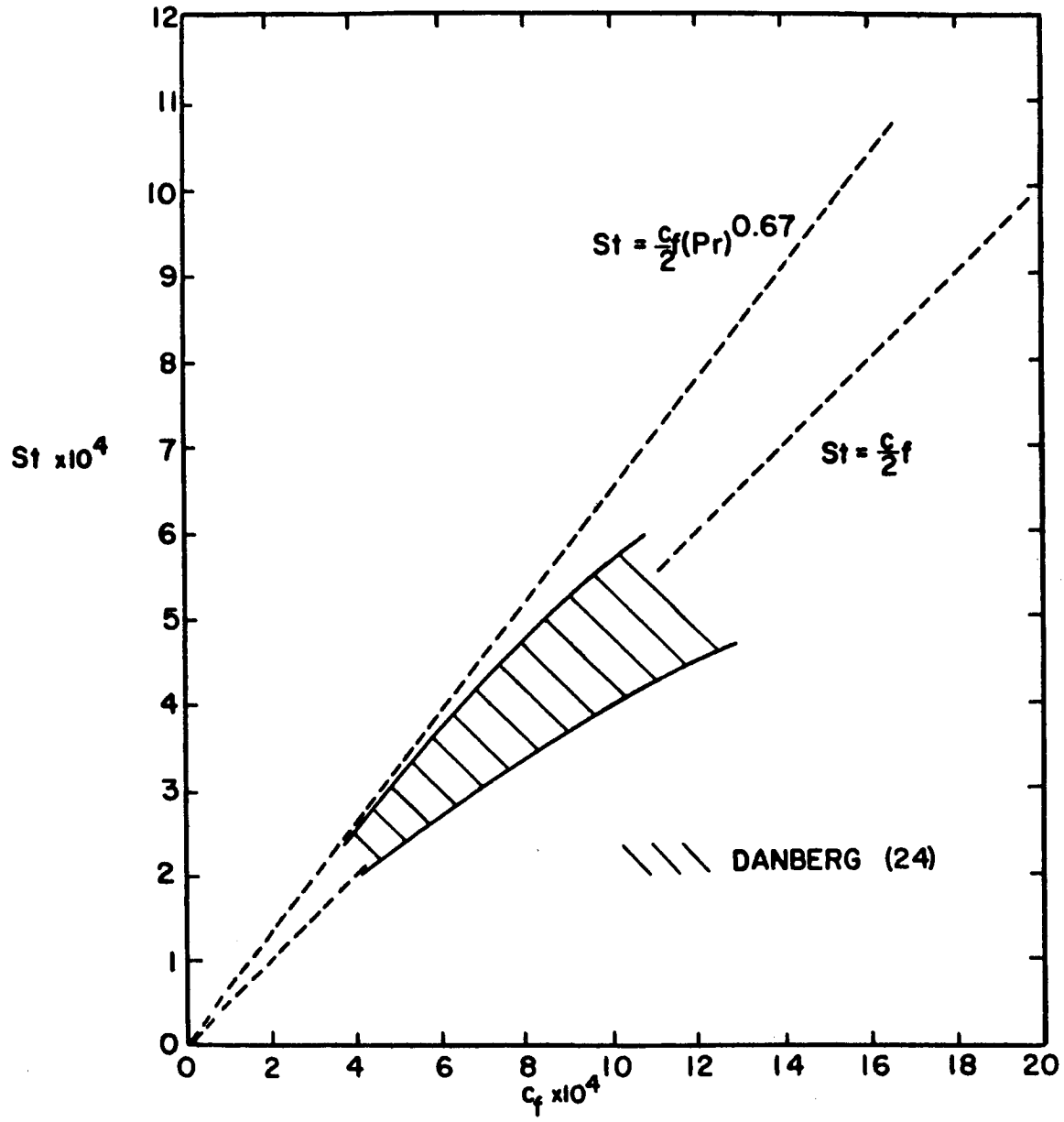

FIGURE 3.5 REYNOLDS ANALOGY FOR AIR INJECTION AT M=6.7

Mach numbers. However, for subsonic Mach numbers, discrepancies among the data still exist. This latter point will be illustrated further in the section entitled "Comparison of Theory with Experiment."

Brunner The primary objectives of the final investigation (27) reviewed in this section were threefold: (1) to provide a verification of the existing transpiration cooling data for the reduction in Stanton number; (2) to extend that data from a value of $F/St_o = 3.0$ to $F/St_o = 10$; (3) to verify the correlation of Stewart (56) for the reduction in Stanton number with mass injection (see equation 3.17).

The tests for the determination of heat transfer were performed on a 20^o cone similar to the one used by Pappas and Okuno (26) for durations of approximately one minute. A heat balance was written for the model which gave the Stanton number from the experimental measurements. Nitrogen, helium, and water were used as the coolants, enabling easy comparison of the effectiveness of a "heavy gas," a light gas, and water.[1] The following conditions were maintained during the tests: $M = 2.5$, $T^o = 5600$ R, $P = 110$ psia, and $0.002 < F < 0.060$. The conical model was placed directly in the path of a rocket exhaust which had an effective molecular weight of 25.08. It was intended that the heat fluxes to the surface of the cone (estimated at 1500 Btu/sq ft sec) be on the same order of magnitude as those encountered by an actual reentry vehicle. The authors (27) noted that without cooling, the model would have been destroyed in less than a second and even with ablation, it is believed that it would have lasted only ten seconds.

---

[1] Although not explicity stated in the paper (27), when water was employed as a coolant the flow rates were regulated such that evaporation of the water did not occur within the porous material. The phase change for the water occurred at or above the porous surface (95).

The heat transfer results of Brunner (27) for transpiration cooling with helium, nitrogen, and water have been reasonably well correlated as shown in Figure 3.6 The figure is plotted in the dimensionless manner recommended by Stewart (56) and with these coordinates, the data points for the three coolants are reasonably well represented by the same curve. The results are represented by Stewart's equation

$$\frac{St}{St_o} = \left(1 + \frac{2}{9} F\, c_p^*/St_o\right)^{-3} \qquad (3.17)$$

to within -10 percent. Brunner suggested that the slight error is due to the difference in environments between that for which equation 3.17 was intended (air) and the combustion gases used in the actual tests. From his investigation, Brunner concluded that helium is more effective than water when compared on a pound mass basis. Nitrogen, on the other hand, was less effective than water.[1] The tests also demonstrated that any of the aforementioned coolants provide a feasible transpiration cooling system for reentry purposes.

3.3.2 Comparison of Theory with Experiment

The purpose of this final section will be to summarize the subject experimental investigations and to compare the results with theoretical predictions. Some conclusions shall be made based on the foregoing discussion and those areas which require further investigation will become clear.

---

[1] See Section 3.3.2 for further discussion and clarification of the relative effectiveness of light gases and water.

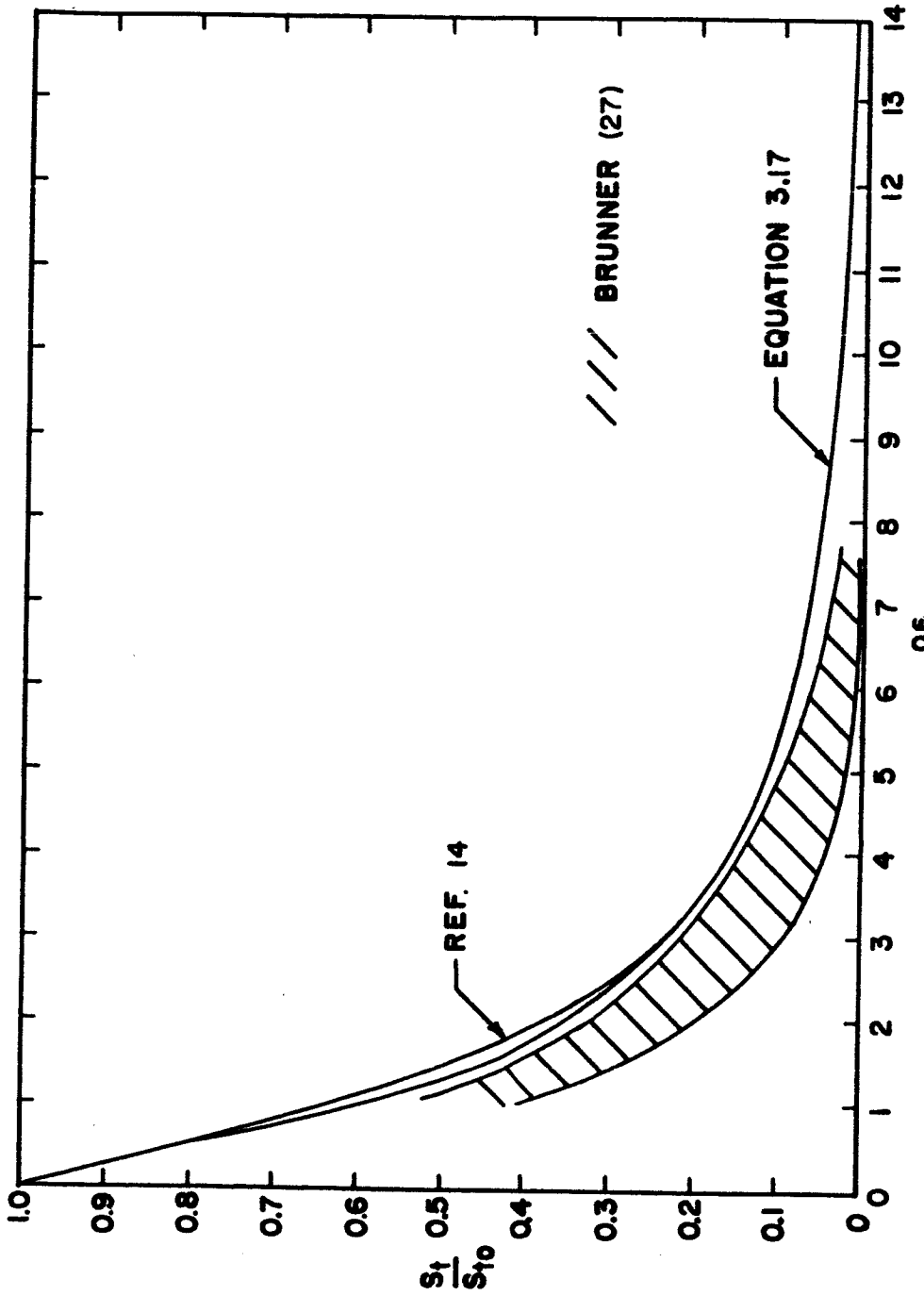

FIGURE 3.6 COMPARISON OF EXPERIMENTAL HEAT TRANSFER RESULTS (27) FOR N_2, He, AND H_2O COOLANTS WITH THEORY

In Figure 3.7, the effect of injection upon skin friction is illustrated by comparing the experimental results of References 19, 20, 24, 26, 57, 59, and 64 with the theoretical predictions of References 4, 15, and 18. The results are presented in terms of the dimensionless groups c_f/c_{fo} and F/c_{fo} in order to minimize the influence of the independent parameters (M, Re, T_w/T_∞) which differ because the various tests were not conducted for the same steady state conditions. The first and most obvious point which should be observed from such a comparison is that the theoretical predictions do not indicate any significant effect of Mach number upon c_f/c_{fo} whereas the experimental results exhibit a noticeable influence of the Mach number. The experimental results of Mickley and Davis (20), Hacker (64), Romanenko and Kharchenko (19) and Pappas and Okuno (26), for a Mach number much less than one, lie below the predictions of Rubesin (4), Dorrance and Dore (15), and van Driest[1] (18), for the case of $M \approx 0$. On the other hand, the experimental results of Tendeland and Okuno (57), Pappas and Okuno (26), and Danberg (24), for a Mach number greater than one, lie well above the theoretical predictions (4, 15, 18) for Mach numbers of the same magnitude. The analysis of Spalding, et. al. (5) does not account for the influence of "M" on c_f/c_{fo} because the authors were not familiar with the work of Reference 26 when they derived their empirical equations. It may be concluded that it appears that mass injection reduces the skin friction more significantly for subsonic flow than for supersonic flow. However, due to the controversial subsonic results of Tewfik (59), the magnitude of this reduction cannot be accurately estimated until more data are obtained.

---

[1] The results of van Driest agree almost exactly with those of Rubesin

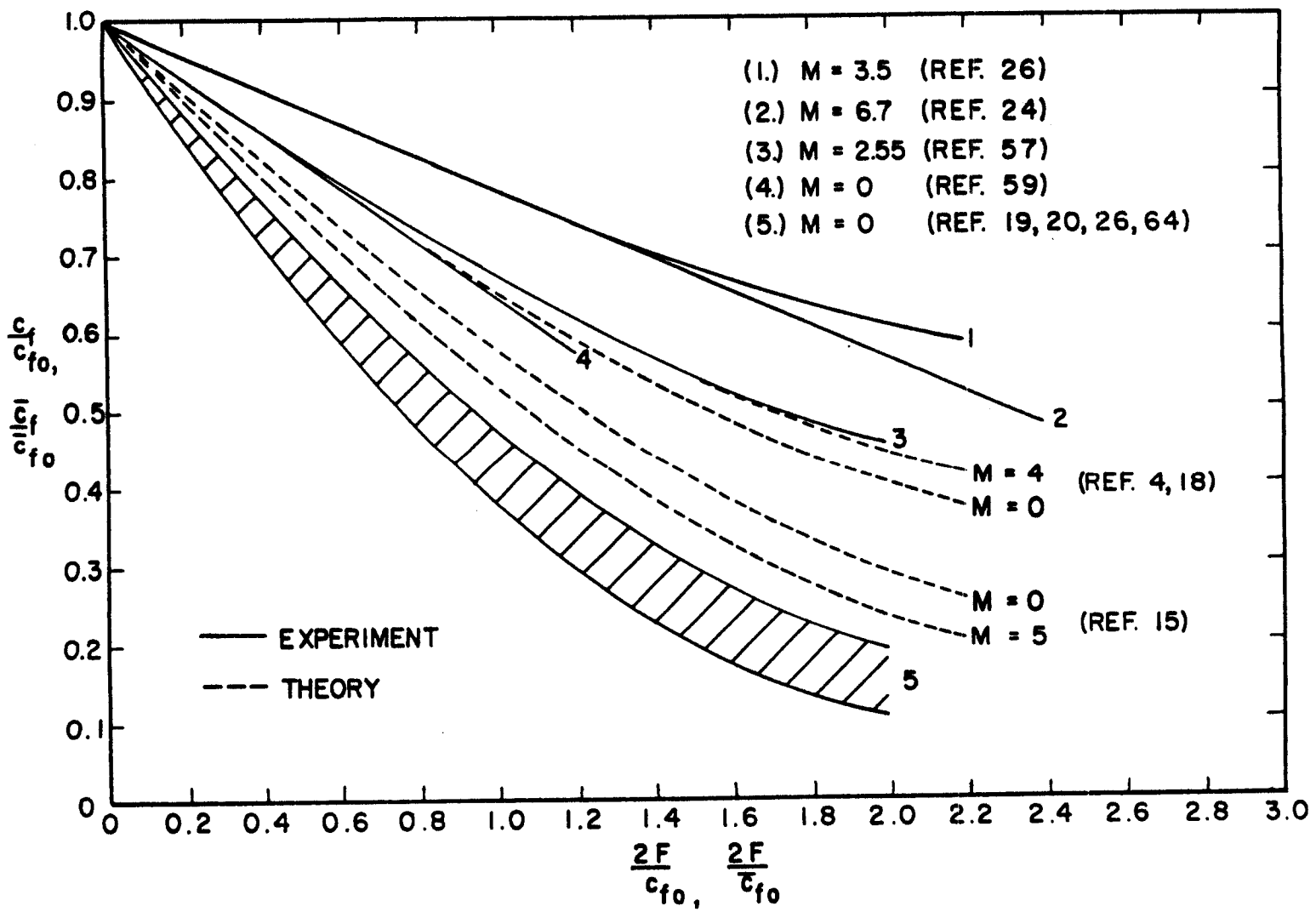

FIGURE 3.7 COMPARISON OF THEORETICAL PREDICTIONS WITH EXPERIMENTAL RESULTS FOR THE REDUCTION IN SKIN FRICTION

The results for evaluating all variables influencing the heat transfer in transpiration cooling have been more successful. The experimental results of References 19, 24, 27 and 28 for the reduction in the Stanton number ratio with mass addition are presented in Figure 3.8 and compared with the theoretical analyses of References 4 and 18. Though there is some scatter in the data, it can be seen that the analyses of Rubesin and van Driest agrees with the experimental results to within 15 percent. The analysis of Dorrance and Dore gives a somewhat lower prediction though it displays the same general trends.

As discussed earlier, it has been shown (14, 19, 26) that gases having a relatively low molecular weight are more effective coolants than the "heavier" gases. Furthermore, the results of Brunner (27) indicate that light gases are also more desirable than water. However, the experimental data obtained in the laminar flow investigation by Sparrow, Minkowycz, and Eckert (97) demonstrated that the foregoing conclusion may not always be valid. To clarify this point, it should be kept in mind that the term "cooling effectiveness" generally refers to the effect of blowing on reducing the heat transfer to the porous material; i.e., the effect of blowing on the temperature and velocity profiles and the influence of the coolant on the properties of the boundary layer. In this context, hydrogen and helium are the most "effective". However, the energy capacity of the coolant in flowing from the reservoir to the point of injection is also an important factor in determining the coolant flow rate required to maintain a specified wall temperature. Consequently, in some cases, it may be desirable to take advantage of the added energy capacity afforded by using a liquid

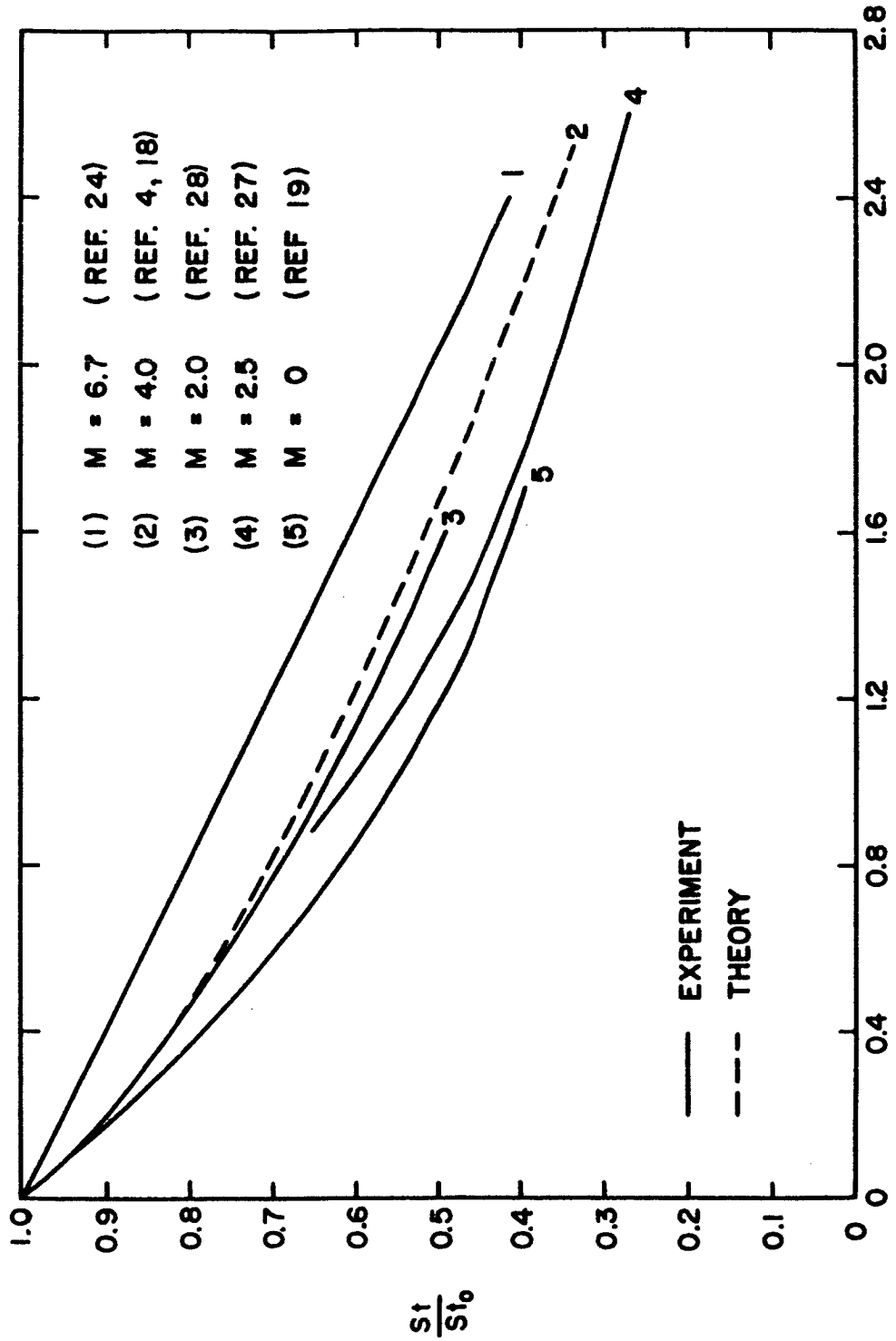

FIGURE 3.8 COMPARISON OF THEORETICAL PREDICTIONS WITH EXPERIMENTAL RESULTS FOR THE REDUCTION IN STANTON NUMBER

coolant that evaporates prior to injection. Preliminary calculations indicate that the cooling effectiveness of gaseous hydrogen is superior to that of water even when the heat of vaporization of the water is taken into consideration. However, when helium and water is compared, calculations indicate that the flow rate of water required to maintain a wall temperature between its saturation temperature and approximately 1000 F may be less than the required flow rate of gaseous helium. The practical difficulties of using water as a transpiration coolant are serious, but some success has been achieved by Evans, Crossland, and Boginski (96) in developing a controllable system of transpiration with water.

4. POROUS MATERIALS

4.1 Desirable Properties

Porous materials have been used or are potentially suitable for numerous applications, e.g., filtration of impurities in gaseous or liquid flow systems, distillation and gas absorption in petroleum refineries, boundary layer control by suction, and transpiration cooling. Fortunately, the most important design and performance criteria are basically the same for each of the foregoing applications. All porous materials presently available possess certain inherent disadvantages depending upon their structure and physical properties and consequently, for selection purposes, it is necessary to consider first environmental factors and then decide what characteristics are the most important.

Glenny (73) made an extensive study of commercially available materials for gas turbine applications and Debeau (74) made a similar but less thorough evaluation of materials for boundary layer control. Hawkins, et. al. (75) investigated porous wall structures for use in transpiration cooled components in solid propellant rocket motors. On the basis of these studies the most desirable characteristics of porous materials for transpiration cooling applications are summarized below.

Permeability Requirement The permeability of a porous material may be qualitatively defined as a proportionality factor between the flow rate per unit area and the pressure gradient across the material.

There are actually two desirable characteristics related to this property: (1) a minimum permeability must be obtainable without jeopardizing the structural integrity of the material; and (2) a uniform flow rate must be possible for any cross-section of the material. The first specification will be discussed below under the subject heading "Strength Requirement." The second is particularly critical for the successful application of liquid transpiration cooling. At points within the material where the permeability is abnormally low, smaller coolant flow rates will result. Evaporation of the liquid is then likely to occur before the coolant reaches the surface with a subsequent "vapor locking" effect and a further reduction in the local coolant flow rate. The lower rate of mass injection into the boundary layer will cause the local material temperature to increase which, in turn, increases the amount of evaporation; thus, the phenomena becomes self-propagating with disasterous results. Qualitatively then, it can be said that the greater the homogeneity of the porous structure, the less will be the opportunity for the foregoing to occur.

Strength Requirement The large stresses imposed by high pressure rocket engines has proven to be a critical factor in the design of transpiration cooled systems. The ratio of the permeability to the porosity[1] of a porous material has been found (73) to be an important criterion in assessing its strength. Although, in general, the foregoing ratio should be as large as possible, the minimum allowable strength of a material can only be evaluated by considering a particular application.

Studies have recently been conducted (76, 77, 78) to determine the required thicknesses of porous nozzle inserts on the basis of the various strength considerations. It was found that steady state thermal and mechanical stresses are of equal importance for typical environmental conditions (2000 F $< T_\infty <$ 7000 F). Since for a given heat flux to the surface, the temperature difference across a porous material increases with the thickness, the thermal stresses will likewise increase with wall thickness. As a consequence, there is an optimum thickness for a particular application. The optimum thickness has been determined by means of a force balance which accounts for both thermal and mechanical stresses and which employs the von Mises criteria for obtaining the yield strength of the material (76, 77, 78).

Critical Pore Density The microstructure of a specimen should be such that the coolant will coalesce upon injection into the hot gas stream to form a continuous blanket over the porous surface. The high cooling efficiency of transpiration cooling is due to two effects - highly efficient heat transfer from the wall to the coolant as it passes through the material, and the so-called "blanketing" effect of the coolant over the surface. Thus, in order to achieve a continuous layer of fluid, the number of pores per unit surface area should be as large as possible so that the individual jets of coolant will coalesce upon injection. Reference 47 concludes that materials with a large number of divergent surface pores per unit area accomplish this end most effectively. However, a very important

---

1 Total volume of voids per total volume of porous material

limit exists on the minumum pore size since the smaller the average pore diameter, the greater will be the tendency for the material to be clogged by impurities in the coolant, causing reduced flow and material failure due to localized hot spots.

Thermal Shock Requirement Experiments on transpiration cooled rocket nozzles have been conducted which indicate that the first few seconds after ignition are critical if damage due to thermal shock of the porous material is to be avoided. The nozzle material is instantaneously exposed to a high temperature environment and cracking is sometimes unavoidable. Attempts to prevent such problems from occurring have involved the infiltration of tungsten samples with a liquid metal (76, 77, 78) which at room temperatures, is in the solid state, but which melts when exposed to typical wall temperatures. The primary objective of this "porous matrix"[1] is to maintain an initial lower temperature differential by increasing the conductivity of the wall, thus minimizing the possibility of damage due to thermal shock. An additional advantage of composite structures is the added strength over that of the porous material during the initial critical period. Silver and tungsten are typical materials used as infiltrants. During the transient heating period, the infiltrant is melted and expelled in the liquid state by the pressurized coolant contained in the annulus surrounding the porous insert.

---

[1] Also frequently referred to as "composite materials"

PAGE 105

MISSING

or what is commonly called the supericial velocity (74, 82), or seepage velocity (80), defined by

$$Q = \frac{\dot{m}}{A} \tag{4.1}$$

The proportionality factor depends on both the porous material and the fluid. Nutting (80) altered Darcy's solution slightly to account for the variation in the viscous properties of different fluids by dividing the constant by the dynamic viscosity of the fluid. Duwez and Wheeler (45) performed experiments on sintered metal compacts and verified that this constant, called by some the permeability coefficient, was not significantly affected by the fluid properties. The slight deviations of the values they obtained were attributed to experimental error rather than to a difference in fluids.

Darcy's equation in modified form is

$$Q = \frac{K_p}{\mu} \frac{dP}{dy} \tag{4.2}$$

where K_p is the permeability coefficient and μ the dynamic viscosity of the fluid. In arriving at equation 4.2, Darcy assumed that the following were true for his experimental investigation:

(1) the flow is isothermal

(2) the flow is laminar and steady

(3) the porous media is homogeneous

Rearranging the above form of Darcy's law (4.2) gives the definition

the transition region separating the two is reasonably well defined by the Reynolds number. However, for flow through porous materials, three different regimes have been observed and unfortunately, distinct lines of demarcation do not exist. The explanation usually offered for this problem is that the transition from one regime to another does not take place at a definite point but instead, a "mixed" laminar and turbulent flow occurs (79, 80); i.e., the flow may be laminar in some regions of the material and turbulent in others. Physically, the flow pattern can be interpreted as being a superposition of one regime upon another. For the above reasons, the mathematical analysis of fluid flow through porous materials relies heavily on empirical results.

The three regimes encountered in flow through porous materials may be categorized as follows:

(1) slip or creeping

(2) viscous or laminar

(3) inertial

The flow rates most requently observed in transpiration cooling experiments have resulted in flow regimes characteristic of types (2) and (3) and the analysis of both is presented in the following section.

4.2.1 Darcy's Law

In 1856, H. Darcy (81) laid the foundations for the analysis of fluid flow through porous materials with his now classic experiment on water seepage through sand filters. He discovered that for the range of velocities encountered under gravity flow conditions, the pressure gradient is directly proportional to the mass flow rate per unit area

or what is commonly called the supericial velocity (74, 82), or seepage velocity (80), defined by

$$Q = \frac{\dot{m}}{A} \tag{4.1}$$

The proportionality factor depends on both the porous material and the fluid. Nutting (80) altered Darcy's solution slightly to account for the variation in the viscous properties of different fluids by dividing the constant by the dynamic viscosity of the fluid. Duwez and Wheeler (45) performed experiments on sintered metal compacts and verified that this constant, called by some the permeability coefficient, was not significantly affected by the fluid properties. The slight deviations of the values they obtained were attributed to experimental error rather than to a difference in fluids.

Darcy's equation in modified form is

$$Q = \frac{K_p}{\mu} \frac{dP}{dy} \tag{4.2}$$

where K_p is the permeability coefficient and μ the dynamic viscosity of the fluid. In arriving at equation 4.2, Darcy assumed that the following were true for his experimental investigation:

(1) the flow is isothermal

(2) the flow is laminar and steady

(3) the porous media is homogeneous

Rearranging the above form of Darcy's law (4.2) gives the definition

of permeability coefficient most frequently used (74, 79, 82, 83, 84)

$$K_p = \frac{Q\ \mu}{d\ P/dy} \tag{4.3}$$

The main problem arising out of such an expression for determining K_p for a particular porous material is that the flow is not always laminar and consequently, the permeability coefficient will not always be constant for flow rates outside the viscous regime. To obtain a valid expression for the mixed and inertial regime, the equation for K_p must be modified. This will be described in Section 4.2.2.

Upon integrating this modified form (2.3) of Darcy's law, Muskat (79) arrived at a form more useful for experimental work. For isothermal perfect gas flow, the following relationship was obtained.

$$\frac{Q}{(P_i^2 - P_e^2)/L} = \frac{K_p\ \rho_e}{2\ P_e\ \mu} \tag{4.4}$$

The "i" and "e" subscripts denote inlet and exit conditions respectively. For liquids, a similar relationship results

$$\frac{Q}{(P_i - P_e)/L} = \frac{K_p\ \rho_e}{\mu} \tag{4.5}$$

For laminar flow through a given porous media, equation 4.4 will yield the same value of permeability coefficient for a gas that equation 4.5 will give for a liquid permitting the generalizations of the value for the permeability coefficient.

4.2.2 Empirical Correlations

Becuase of the inability of accurately describing the irregular nature of the flow through unconsolidated porous structures, such flow may never admit to a complete analytical solution. By examining the microstructure of a sintered metal, the need for empirical relations can perhaps be seen more vividly. The compact is composed of variable diameter metal spheres and random open and dead end pores preventing even a statistical approach. This has forced many to resort to a semi-empirical means. Attempts at analytical solutions for the flow through the more uniform woven wire cloth have been comparatively more successful. But even with wire cloth, when successive layers are joined together, pores become easily clogged due to the bonding material.

Since the analysis due to Green (49, 82) is simple and not limited to a uniform porous media, it is the most commonly accepted. Nevertheless, it relies heavily upon the experimental determination of two constants[1] for the predictions of flow rates. Thus, more data is required for any porous structure manufactured from a new material, by a different technique, or with a different porosity. This problem led to the solution by Grootenhuis (85) which also has a limitation for it is restricted to flow through homogeneous materials with continuous pores.

Solution by Green From 1945 to about 1950, work was conducted at the California Institute of Technology (42, 43, 45, 46, 47, 48, 49) on flow through porous materials to elucidate the laws governing such flow.

---

[1] Inertial and viscous resistance factors

The experiments were performed with sintered compacts of iron, stainless steel and porex[1] with porosities ranging from 25 to 60 percent. Flow rates were obtained in both the laminar and inertial regimes and consequently, Darcy's law expressed earlier by equation 4.2 was ruled out. The metals were studied microscopically and were found non-uniform. Attempts at finding a single characteristic curve for relating flow rate as a function of pressure drop were futile.

The only feasible approach was dimensional analysis. Neglecting gravitational effects, Green (49) was able to deduce the relation

$$-\frac{dP}{dy} = \text{constant}\ \frac{\mu^2}{\rho L^3}\ J \tag{4.6}$$

where J is some function of the parameter "$L\rho v/\mu$" and "L" is a length characterizing pore openings. In the viscous region where low flow rates are observed, this equation reduces to Darcy's law with

$$J = \frac{L\rho v}{\mu} \tag{4.7}$$

and thus

$$-\frac{dP}{dy} = \text{constant}\ \frac{\mu v}{L^2} \tag{4.8}$$

i.e., the function J is equal to its argument. At high flow rates, it was shown experimentally (49, 82) that

---

[1] Porous bronze

$$-\frac{dP}{dy} = (\text{constant})\left(\frac{\rho v^2}{L}\right) \tag{4.9}$$

and thus

$$J = \left(\frac{L\rho v}{\mu}\right)^2 \tag{4.10}$$

In the region of transition from laminar to turbulent flow, an expression for the net dP/dy can be obtained by adding the right hand side of equation 4.8 to the right hand side of equation 4.9 if the singular effects of the regimes can be considered superposable. This form of the expression has been shown to give a good representation in the transition regime. Since "L" is a constant for a particular porous material, it may be absorbed by defining two new constants, α and β, which are resistance factors characteristic of the given material. Thus the final expression, which is valid for any flow rate in the laminar or inertial regime (49, 79, 82) becomes for a liquid or an incompressible gas

$$-\frac{dP}{dy} = \alpha\mu v + \beta\rho v^2 \tag{4.11}$$

When the velocity is sufficiently low, the second term on the right hand side of equation 4.11 is negligible compared to the first and the equation reduces to Darcy's form (4.3) for laminar flow. In the inertial regime, which results at high velocities, the first term may be neglected in comparison to the second and equation 4.11 reduces to the form given by 4.9.

Before attempting to apply equation 4.11, it must be emphasized that it is restricted to an incompressible fluid. Since most of the work in transpiration cooling deals with gases at high pressures, the effects of compressibility should be (49, 82) accounted for by an additional term and then the result integrated to obtain a workable expression. A similar result can be found for liquids by again beginning with equation 4.11[1] and integrating.

Considering compressible fluids first, Green (49, 82) made the following additional assumptions: (1) the porous material is composed of a bundle of constant area capillaries; and (2) the flow is one-dimensional. With the foregoing model and using equation 4.11, a momentum balance can be written for the pores as follows

$$dp + \alpha\mu v dy + \beta\rho v^2 dy + \rho v dv = 0 \qquad (4.12)$$

In fact, equation 4.12 is identical with 4.11 except for the last term on the left hand side which was introduced to account for the change in momentum due to density gradients. If the coolant is assumed to be an isothermal perfect gas, equation 4.12 becomes

$$\frac{P}{bT}\, dP + \alpha\mu Q dy + \beta Q^2 dy + \frac{Q^2 P}{bT}\, d\left(\frac{bT}{P}\right) = 0 \qquad (4.13)$$

where "b" is defined

$$b = \frac{R_u}{W}$$

---

[1] Further modification of equation 4.11 is not necessary for liquids

R_u is the universal gas constant and W is the molecular weight. Integrating between the inlet and exit surfaces of the porous material gives upon simplification

$$\frac{P_i^2 - P_e^2}{L} = \alpha(2bT\mu)Q + \left(\beta + \frac{1}{L} \ln \frac{P_i}{P_e}\right) (2bT)\, Q^2 \qquad (4.14)$$

Now experimentally, it was found (49) that

$$\frac{1}{L} \ln \frac{P_i}{P_e} << \beta$$

Thus, the flow rate equation for an isothermal, perfect gas is

$$\frac{P_i^2 - P_e^2}{L} = \alpha(2bT\mu)Q + \beta(2bT)Q^2 \qquad (4.15)$$

It has been shown (49) that a plot of the pressure difference per unit length against mass flow rate on a log-log graph for several porous materials yields a series of nonparallel curves. This suggests that an equivalent capillary diameter cannot correlate the data and, in fact, two characteristic dimensions are required.

However, if equation 4.11 is nondimensionalized in terms of Reynolds number and friction factor, the data can be forced to fit a single universal curve for any porous material (49, 82). Reynolds number can be interpreted as the ratio of inertial to viscous forces and an examination of equation 4.15 reveals that the two terms on the right hand side represent those

quantities. Thus, an equivalent Reynolds number can arbitrarily be defined as

$$Re_\lambda = \frac{\beta \rho V}{\alpha \mu} = \frac{\lambda Q}{\mu} \tag{4.16}$$

where λ represents the characteristic length, β/α. Similarly an effective friction factor for the pores can be defined in terms of the ratio of dissipative forces to inertial forces. Thus

$$c_f = \frac{1}{\beta}\left(\frac{\Delta p^2/L}{2bTQ^2}\right) \tag{4.17}$$

Using the definitions 4.16 and 4.17, equation 4.15 can be rearranged to give

$$c_f = \frac{2}{Re_\lambda} + 2 \tag{4.18}$$

where the quantity $2/Re_\lambda$ is the contribution to the friction factor due to inertial forces and "2" the contribution due to viscous forces. Equation 4.18 is a good approximation for a Reynolds number less than 10^{-1} but because the logarithmic term was dropped from equation 4.14, considerable error is incurred beyond this region.

It is imperative to recognize that though equation 4.18 represents a universal curve of friction factor as a function of Reynolds number similar to Moody's curve for pipe flow, its usefulness is severely limited. The "constants" α and β are not universal constants but depend on many

material properties such as porosity, surface roughness, number of "dead" end pores, i.e., the geometry of the material, and they must be determined experimentally. Whether the viscous and inertial coefficients (α, β) are limited in their dependence to the aforementioned characteristics of the porous media is still an unanswered question. Green studied the problem experimentally and concluded that α and β are virtually independent of the fluid properties, but this data was not extensive. Greenberg and Weger (83) conducted a more recent study of the effects of changing selected fluid and porous material properties on α and β. The results of this study are listed below.

(1) Up to 2000 psi, the resistance coefficients for a given porous material are virtually independent of pressure.

(2) The viscous coefficient (α) decreases with increasing temperature.

(3) The greater the surface roughness of the individual particles forming the porous material, the greater the change in permeability with temperature.

Extensive research is still required to assess the variations of viscous resistance with temperature.

Many investigators (74, 56, 82, 83) do not believe that the inertial resistance term is due to the onset of turbulence as originally proposed by Fancher and Lewis (86). Green concurs with Bakmeteff and Feodoroff (87) that at high flow rates (Reynolds number greater than 1), the anomalous increase in resistance to flow is due to the continuous expansion and contraction of fluid through the pores causing separation and eddy formation. Other mechanisms have been proposed for the deviations from Darcy's law but the above is the most commonly accepted.

Returning again to equation 4.11, it is somewhat easier to integrate that expression for the flow of a liquid. For with the hypothesis (82) that all variables including density, velocity and viscosity are constant except for pressure and distance y, the equation becomes a linear, first order differential equation in P and y, giving upon integration

$$\frac{P_i - P_e}{L} = \alpha\left(\frac{\mu Q}{\rho}\right) + \beta\left(\frac{Q^2}{\rho}\right) \qquad (4.19)$$

the foregoing assumption of constant velocity again theoretically restricts the pores to constant area capillaries. Thus, compatible equations are obtained for the flow of both a gas (equation 4.15) and a liquid (equation 4.19). Brunner[1] (27) demonstrated the use of these equations and found that the resistance coefficients for a gas can be used for a liquid and vice-versa.

Solution by Grootenhuis The solution due to Grootenhuis (85) for gas flow is restricted to more uniform materials and consequently, is less applicable than Green's. Experiments were performed on sintered gauze packs manufactured from phosphur bronze wire. Because these packs had continuous pores, the analysis permitted the introduction of a characteristic dimension, called the hydraulic diameter, which could be determined as a function of the wire diameter and material structure. As a consequence, a more useful correlation resulted, the main advantage being the elimination for the need of empirical resistance coefficients.

The following assumptions were made:

---

[1] His experimental work on transpiration cooling was reviewed in Chapter 3

(1) The pressure drop is due solely to frictional effects and the change in momentum of the fluid entering and leaving.

(2) The shear stress at any point along the porous surface is the same.

(3) The fluid enters the media with a uniform normal (y) component of velocity.

(4) The flow is one-dimensional and isothermal.

(5) The fluid is a perfect gas.

A Further basic assumption made, though not stated explicitly by Grootenhuis, was that the flow through porous materials can be related in terms of friction factor and Reynolds number; in fact, it will be seen that this is the whole basis of his derivation. Beginning with the definitions

$$c_f = \frac{R}{\rho v^2}$$

$$Re_d = \frac{\rho v d_e}{\mu}$$

where R is the frictional force per unit surface area of passage exposed to flow and d_e the hydraulic mean diameter, the momentum equation expressed by

change in momentum = wall shear force + pressure force becomes for a differential length dy and cross-sectional area "A"

$$\rho v A \frac{\partial v}{\partial y} dy = - R c dy - A \frac{\partial P}{\partial y} dy \qquad (4.20)$$

The parameter "c" is the perimeter of a square passage. Upon integrating, the above relation gives

$$\frac{P_i^2 - P_e^2}{2P_i} = R\left(\frac{cL}{A}\right)\frac{\rho}{\rho_i} + \frac{Q^2}{\rho_i}\ln\left(\frac{P_i}{P_e}\right) \tag{4.21}$$

Grootenhuis discovered, like Green, that the last term on the right hand side of equation 4.21 was negligible and thus the equation can be simplified to the form

$$R = \frac{\rho_i}{\rho}\,\frac{(P_i^2 - P_e^2)}{2P_i}\,\frac{1}{a} \tag{4.22}$$

where the quantity cL/A has been replaced by its definition "a" (the surface area of an internal passage per unit total of frontal cross-sectional area). For incompressible fluids, equation 4.22 can be reduced to

$$R = \frac{\Delta P}{a} \tag{4.23}$$

if the pressure differential $P_i - P_e$ is sufficiently low.

When the specific frictional force "R" is substituted into the friction factor expression (4.22), the only variable remaining that depends on the porous structure is the hydraulic diameter, i.e., the ratio of cross-sectional open to flow to the total cross-sectional area per unit length. By considering the geometrical structure, the hydraulic diameter can be related to porosity, wire diameter, and mesh per unit width.

Grootenhuis analyzed these form factors and arrived at the following:

(1) friction factor

(i) compressible flow

$$c_f = \frac{(P_i^2 - P_e^2)\,\rho_i d w^2}{8\,P_i\,Q^2 L\,(1-w)} \tag{4.24}$$

(ii) incompressible flow

$$c_f = \frac{\Delta P\,\rho_i\,dw^2}{4\,Q^2\,L\,(1-w)} \tag{4.25}$$

(2) Reynolds number

$$Re_d = \frac{Qd_e}{\mu w} \tag{4.26}$$

where

d = wire diameter

L = length of pore

w = porosity

Plotting friction factor against Reynolds number, he obtained a universal curve valid for any porous material of uniform construction and square pores. Fitting an equation to the curve he found

$$\log c_f = 1.75\,(Re_d)^{-0.203} - 1.76 \tag{4.27}$$

Experiments were conducted for air flow only, but by recalling the results of Green, it may be assumed that equation 4.27 may be generalized to all fluids. The range of Reynolds numbers for which equation 4.27 is valid is

$$0.1 < Re_d < 5000$$

Thus, it may be used in both the viscous and inertial regimes. It is interesting to note that although equations 4.18 and 4.27 cannot be easily compared due to the different characteristic lengths employed, the two curves display the same trend when plotted on a log-log graph.

4.3 Reduced Flow Rates

One of the primary reasons transpiration cooling has not been used in actual rocket vehicles is due to the erratic and irreproducible coolant flow rates. Anomalous flows have been observed in virtually all work performed with porous materials and the causes have never been completely explained. Since the mass flow rate in transpiration cooling is so critical, small perturbations in the flow rate can result in complete failure of the cooling system. Experiments have shown that liquids are much harder to control than gases.

The basic reasons for low permeability are known but separating the various causes quantitatively so that surface temperatures can be adequately predicted has proven impossible. The problem arises from the fact that the causes of low permeability can exist simultaneously and they all tend to reduce mass flow rate. The problems relating to lower mass flow rates are outlined below.

4.3.1 Clogging of Pores

Engineers who have experimented with transpiration cooling models generally attribute a decrease in flow rate with time (all other conditions being the same) to the clogging of pores with impurities in the coolant. In addition to serving as an injector, the porous material unfortunately acts as a filter by removing most of the impurities from the fluid. As discussed in Section 4.1, it is desirable for the material to have small pores for more efficient operation but, to minimize clogging, large pores are preferable. Thus an optimum size must be found so that clogging is avoided and the wall jets coalesce immediately after injection. For the above reasons, the coolant should be filtered before reaching the injector to remove as much of the foreign matter as possible. Generally all particles with diameters greater than the minimum pore diameter should be filtered out.

Filtering is particularly a problem for gas turbine operation where atmospheric air is used as the coolant. Over industrial areas, the atmosphere contains large amounts of carbon siliceous materials and pollen. Thus, in addition to continuous filtering of the coolant, the porous mass should be purged after extended use by periodically reversing the flow.

Another form of blocking is due to deposition on the external porous surface. For example, in solid propellant rockets or in gas turbine operation in which a heavy fuel oil is burned, solid and liquid particles contained in the gas stream readily adhere to the bounding surface. Grootenhuis (2) found that, contrary to what many anticipated, this is not critical if transpiration cooling is used. He exposed two cylinders

to the products of fuel oil combustion for 150 hours. One cylinder was constructed of stainless steel sheet while the other was made from a permeable material. The latter was cooled so that it had the same surface temperature of 1000 F as the solid sheet. He discovered that the solid steel surface had collected considerable scale while the porous material remained clean. The only observable change to the porous surface was a slight discoloring.

4.3.2 Two Phase Flow

Two phase flow in transpiration cooling invariably occurs when liquids are used as the coolant because gases are always present to some degree. Gases not in solution with the coolant may be due to one of two causes -- either they can be entrained in the liquid or vaporization can take place within the pores. Most of the experimental work with two phase flow has been concerned with entrained and dissolved gases; few tests have dealt with liquid boiling in capillaries. In either case, the gas causes what is commonly known as "vapor locking" of the pores with reduced flow rates as an inevitable consequence.

Eisenklam (89, 90) conducted an extensive three part survey on the retardation of liquid flow rates in porous materials. His primary objective was to evaluate the effect of entrained and dissolved gases on coolant flow under both steady state and transient starting conditions. Carbon dioxide and air were dissolved in both kerosene and water coolants, and steel, bronze and glass were used as the porous material. The glass was included so that the flow could be observed visually. The pressure gradients were varied up to a maximum of eighty psi per inch but unfortunately

the tests were performed under isothermal conditions, the temperature being atmospheric. Nevertheless, the flow was two phase and to a degree, simulates conditions similar to those when boiling occurs within the material.

Part I of Eisenklam's report presents experimental evidence of the erratic flow rates frequently observed for liquids. Part II, which is the major and most important contribution of his work, discusses the effect of gases dissolved or entrained in the liquid. Thus his investigation must be considered pertinent since two phase flow for transpiration cooled surfaces can result from entrainment of gases during pumping, high negative pressure gradients through the porous material, or nucleation due to high temperatures.

Before summarizing the results of his study, some terminology must be reviewed to gain some familarization with the subject. Eisenklam (91) used the phrase "dead fluid flow rate" to define the flow rate occurring under conditions when no gases are entrained in the liquid and thus a maximum permeability is realized. By moisture content, he meant the percentage of liquid contained in the pore spaces of a permeable mass. Relative permeability of a liquid was defined as the ratio of "permeability for a liquid entrained with gas" to the "dead fluid flow rate." This quantity is usually expressed as a percent.

It was discovered that the relative permeability depended upon the initial condition of the porous mass. For a plate which is flooded with the coolant before the flow begins, the length of the transient period before the steady state flow rate is obtained is a minimum. To obtain

the highest or dead fluid flow rate with no initial transient period, the gas concentration in the liquid coolant must be less than that corresponding to saturation conditions at exit. On the other hand, for the flow of super-saturated fluids, a steady but lower mass flow results because of the blocking of pores by entrained gases.

Tests were also conducted on permeable plates which were initially dry, i.e., did not contain any coolant and as predicted, the length of the transient period was less. The saturated liquid was again superior as it dissolved the gases contained within the dry mass and removed them almost immediately. A 100 percent relative permeability was achieved in the steady state portion of the experiment. For kerosene, the transient time was negligible while for water, a constant flow rate was realized after fifty seconds of run time. In contrast, with liquids supersaturated with gas, a constant maximum permeability was possible but the initial period was twice as long. Thus for water, the transient period would require a hundred seconds.

From the data obtained, Eisenklam plotted moisture content against relative permeability and he discovered that the curve drops abruptly at first. For example, a decrease in moisture content of 10 percent for water lowered the permeability by 68 percent. As expected there is a minimum or critical content at which liquids will cease to flow. Also, it was concluded that the permeability is influenced not only by moisture content by also by pore structure and surface wettability.

Obviously, the only manner in which retarded flow rates can be completely eliminated is by maintaining the liquid at a saturated or

undersaturated condition and the porous medium flooded. Quantitative prediction of flow rates has met with little success due to a dearth of experimental data. A qualitative understanding of reduced flows exists but until correlations are obtained, prediction of mass flow rates will be impossible.

4.4 Comparison of Commercially Available Materials

On the basis of the most desirable properties discussed in Section 4.1, the materials available today will be compared. It will be seen that no material presently available meets all specifications but a couple are considered to be potential candidates for transpiration cooling applications.

Glenny (73) made the most extensive survey of porous materials to date. His work was performed at the National Gas Turbine Establishment in England and though he had gas turbines specifically in mind, his survey pertains to any application of transpiration cooling; for he had not only considered the cooling of blades, but flame tubes and inlet ducting.

The permeable materials considered by Glenny can be categorized as follows:

(1) permeable materials prepated by the sintering of powders

(2) perforated sheet

(3) woven wire cloth

(4) sheet prepared by metal spraying

(5) permeable ceramics

(6) wire wool

Although all six types were mentioned in his report, only the first three were thought to be adequate by him. Those three will be discussed below.

Sintered metals There are essentially two ways of preparing sintered porous material from metallic powders. One method, developed by Duwez in 1945 (48), involves the addition of an agent such as ammonium bicarbonate to the powder mixture. This agent decomposes at high temperatures and sublimes into the gaseous phase; thus after the material is compacted at pressures up to 80,000 psi, it is sintered and the additive escapes as a gas, forming pores as it leaves. The material shrinks during sintering closing some of the pores but enough remain open to meet the specified permeability. By varying the amount of pore producing agent, the porosity, permeability and mechanical strength can be altered though not necessarily independently. For a zero to 15 percent addition of ammonium bicarbonate, an 18 to 52 percent change in porosity can be obtained. For that reason, this method is usually preferred. The other alternative requires more discrimination in the selection of the powder so that the desired void space will exist after packing in the mould (88).

Lenel, Reddy and Reen (84) did extensive work at Rensselaer Polytechnic Institute on sintered metals and found that the method of manufacture does not significantly alter the permeability-mechanical strength ratio. The limitations on the size of sheet that can be produced by these techniques are the sintering furnace and pressing tool or mould. To form a hollow cylindrical material from a porous sheet, it is common to proceed by cutting a number of rings from flat sheet and to assemble them by any one of a number of techniques such as brazing, welding or tie rods.

These methods are particularly preferable when the cylinder desired is less than 6 in. in diameter for cracking normally occurs if sheet rolling is attempted.

When transpiration cooling was first investigated, sintered compacts were the only porous material used; but because of its low strength and poor permeability characteristics, it is less desirable than woven wire and perforated materials. The only advantages are a high cooling efficiency and good rigidity, the latter being a property not easily realized with woven wire cloth. Glenny (73) found that sintered bronze compacts gave a better cooling efficiency than any other material. It is believed (73) that porous metal compacts made from traditional powder metallurgical techniques will never have a practical use because at high temperatures in rocket motor environments, impermeable refractory metals possess higher strength and ductility.

Perforated Sheet As with the powder metallurgy, there are two ways of manufacturing perforated sheet. The most ovbious way of course is by drilling holes. The approximate diameter of the minimum size which can be drilled in stainless steel sheet is 0.026 in. (71). This dimension of course depends upon the thickness of the sheet. Using the foregoing hole size, about four holes per inch would be all that would be necessary to obtain a typical permeability for adequate cooling. With such a distribution, the wall jets would not coalesce and the cooling efficiency would be extremely low.

An alternate method is the one preferred and the one actually used in experiments. By a process called electroforming, a hole

distribution of 300 per inch is realized with uniform permeability. The required hole size is obtained by deposition of metal onto a square grid matrix of interwoven wires. The material can be manufactured in both cylindrical and flat sheet form. The electroformed sheet has the same strength characteristics as the drilled sheet with the added advantage of a superior hole distribution. Glenny found that the tensile strength of perforated sheet was a function of the aperture area density. On one sheet, a tensile strength of 44,000 psi and a 30 percent elongation was obtained. The ductility of electroformed sheet is superior to the sintered stainless steel.

Woven Wire Cloth For approximately the last ten years, woven wire cloth has been preferred over the aforementioned varieties of porous material because of better characteristics in virtually every respect. The cloth manufactured with trade names of Poroloy[1] and Rigimesh[2] have become commonly accepted as two of the best materials available today.

Basically there are three ways woven wire cloth can be constructed. Glenny classified these methods as plain, twilled, and Hollander. The first or plain weave is loom woven from strands of wire of constant thickness. The strands are interwoven at right angles with an over-under type pattern. The twilled weave is similar but instead of crossing alternately over and under, each wire crosses over two wires running perpendicular to it then under two. The twilled cloth is preferred over

---

1 Manufactured by Porology Equipment Col; Pocoima, California

2 Manufactured by Aircraft Porous Media Co.; Glen Cove, New York

the plain because heavier gauge wire may be used, offering added strength. The Hollander cloth is constructed from both heavy warp waires and thin weft wire. The warp wire is spaced at regular intervals while the weft is woven with no spacing between adjacent strands. The pattern can be either plain or twilled.

The cloth from any pattern can be strengthened by joining two or more together, one on top the next. Successive plies are oriented so that their axis of symmetry is turned 45^{0} to the preceding ply which diminshes chance of aperture blocking. The sheets can be bonded together by sintering or copper brazing in a furnace. The resulting material is called multiply sheet.

The metal for these sheets is usually phosphor bronze, monel (68 percent nickel, 29 percent copper, 1.5 percent iron, and 1 percent manganese) and stainless steel. The sheet has the same corrosion and heat conductivity as the material from which the ply is constructed.

One of the ostensible advantages of the woven wire gauze is that no limits exist on size. The tensile strength is also excellent, Hollander cloth possessing a higher strength in the direction of the weft wires than any other material. The only disadvantage of wire cloth is its inherent lack of rigidity. This though can be improved by using thick multiply cloth or a very porous rib as a support.

5. CONCLUSIONS AND RECOMMENDATIONS

From the foregoing discussion of the literature on or related to transpiration cooling, the following conclusions have been drawn.

(1) The numerous theoretical analyses for predicting the influence of mass injection on the heat transfer and skin friction coefficients have exhibited qualitative agreement with the trends indicated by experimental data but there is no theory which adequately accounts for the influence of all variables of importance. The disagreement can be attributed to:

(a) inherent limitations of necessarily simplified theoretical analyses; and

(b) the limited accuracy and scope of existing experimental data.

(2) The semi-empirical analysis of Spalding, et. al. (5) provides the most readily applied method for predicting the reduction in heat transfer or skin friction due to mass injection. In view of the fact that this analysis is based upon and representative of the majority of the existing experimental data, the use or development of more refined theoretical analyses is not warranted at this time. The predictions obtained from this analysis are are as accurate (or more so) than those obtainable from any other existing theories.

(3) The theoretical analysis of Rubesin and Pappas (14), as well as that of Spalding, et. al. (5), and the experimental data of Brunner (27) and Romanenko and Kharchenko (19) demonstrate the superior cooling effectiveness of gases with low molecular weights over those with higher

molecular weights. However, if the added energy capacity of a liquid (heat of vaporization) is included, the overall cooling effectiveness of a liquid such as water may be superior to that of a light gas such as helium.

(4) If the experimental data for the Stanton number and the skin friction coefficient are presented in terms of the ratios St/St_o and c_f/c_{fo} as a function of the dimensionless blowing rate parameter (F/c_{fo} or F/St_o), then the influence of the independent variables, Re_∞ and T_w/T_∞, and the flow geometry (flat plate, cone, etc.) is satifactorily eliminated from those correlations. However, the influence of the Mach number on the reduction of St and c_f has not been adequately established. It can be concluded though that the effect of Mach number on St/St_o is less significant than its effect on c_f/c_{fo}.

(5) In regard to the foregoing conclusion, at high supersonic Mach numbers ($2 < M < 7$), the influence of Mach number on St/St_o or c_f/c_{fo} has been observed to be minor and the correlation of Spalding, et. al. (5) as well as the theories of van Driest (18) and Rubesin (4) are in good agreement with existing data. On the other hand, there is considerable disagreement among the data regarding the influence of Mach number in the low supersonic and subsonic regimes; the results of Tewfik (59) indicate a negligible influence of Mach number on c_f while the data of Mickley and Davis (20), Pappas and Okuno (26), Hacker (64), and Romanenko and Kharchenko (19) exhibit a pronounced influence of Mach number.

(6) The effects of a free stream pressure gradient on skin friction and

heat transfer have been evaluated experimentally by Romanenko and Kharchenko (19). Again, though a significant influence of a moderate longitudinal pressure gradient on the skin friction ratio was demonstrated, it has only a negligible influence on the relative reduction in Stanton number.

(7) The effectiveness and potential use of transpiration cooling has been well established by the work which has preceded this report. However, the practical application of transpiration for rocket motor cooling has been for the most part, unsuccessful to date. The difficulties, which are in general related to the use of porous materials, may be summarized as follows:

(a) The theories which have been derived for the prediction of flow rates through porous materials are severely limited by the assumptions involved in the analyses, and furthermore, experimental testing of a given specimen is required for determining the empirical flow coefficients.

(b) The establishment and maintenance of a predetermined coolant flow rate is, in most cases, extremely difficult due to nonuniformities in porosity introduced by the manufacturing process (see conclusion (7) (c)), pore blocking by impurities contained in the coolant, and the "vapor locking" effect encountered with liquid coolants. Each of the aforementioned problems can be sufficient cause for localized reductions in mass flow rate and hot spots that subsequently lead to excessive wall temperatures and catastrophic failure of the cooling system.

(c) One of the major problems related to the use of porous materials is the manufacturing of unusual shapes (i.e., rocket nozzles

and nose cones). Since a pressure gradient will exist along the exposed surface of the material for most practical applications of transpiration cooling, a specific permeability distribution is required to obtain a uniform mass injection rate. If this distrbution is not obtained, then failure of the system is likely to occur.

(8) Of the commercially available porous materials, woven wire cloth (e.g., Rigimesh and Poroloy) appears to be the most desirable from the standpoint of its relatively high strength characteristics and its ability to be fabricated into cylindrical shapes.

The following recommendations are also offered on the basis of the foregoing discussion.

(1) Since, in general, the various theories for transpiration cooling and flow through porous materials have reached the point where further refinements are only possible if more precise data become available, it is suggested that future work be primarily of an experimental nature. Additional data obtained by means of boundary layer measurements under closely controlled and well defined conditions would always be of value in establishing (or verifying) the dependence of the skin friction and heat transfer coefficients upon the blowing rate and other variables of importance. It is recommended that future work be concentrated on the following:

(a) Determine the effect of Mach number (particularly in the subsonic and low supersonic regimes) on the functional relationship between the skin friction or heat transfer coefficients and the blowing rate.

(b) Experimentally determine the effects of severe negative pressure

gradients (typical of nozzle flows) on the heat transfer with blowing to establish the range of validity of the findings of Romanenko and Kharchenko (19) and to access the capabilities of the theoretical analyses (4, 5, 15, 18) for predicting those effects.

(c) Determine the influence of the properties of the freestream upon the correlations for c_f/c_{fo} and St/St_o in view of the preliminary indications (27, 56) that such influence may not be adequately accounted for in a correlation such as proposed by Stewart (56).

(d) Investigate further the feasibility of using water as a coolant in view of its desirable volumetric and containment storage characteristics.

(2) In conjunction with the preceding recommendation, it is suggested that the equations due to Spalding, et. al. (5) be used to tabulate the necessary functions for predicting injection rates for free stream gases other than air and for additional coolants such as water.

BIBLIOGRAPHY

6. BIBLIOGRAPHY

1. Leadon, B. M., "The Status of Heat Transfer Control by Mass Transfer for Permanent Surface Structures," Aerodynamically Heated Structures, Edited by P. E. Glaser, Prentice-Hall, Inc., 1962, pp. 171-196.

2. Grootenius, P., "The Mechanism and Application of Effusion Cooling," Journal Royal Aeronautical Society, February 1959.

3. Rannie, W. D., "A Simplified Theory of Porous Wall Cooling," Progress Report No. 4-50 Jet Propulsion Laboratory, California Institute of Technology, Pasadena, California, November 1947.

4. Rubesin, M. W., "An Analytical Estimation of the Effect of Transpiration Cooling on the Heat Transfer and skin Friction Characteristics of a Compressible, Turbulent Boundary Layer," NACA Tn 3341, December 1954.

5. Spalding, D. B., D. M. Auslander, and T. R. Sundarum, "The Calculation of Heat and Mass Transfer Through the Turbulent Boundary Layer on a Flat Plate at High Mach Numbers, with and without Chemical Reaction," Supersonic Flow, Chemical Process and Radiative transfer, Edited by D. B. Olfe and V. Zakkay, Pergamon-MacMillan, 1964, pp. 211-276.

6. Knuth, E. L., and H. Dershin, "Use of Reference States in Predicting Transport Rates in High Speed Turbulent Flows with Mass Transfer," Journal Heat and Mass Transfer, December 1963.

7. Schlicting, H., "Boundary Layer Theory," Fourth Edition, McGraw Hill, Inc., New York, 1960.

8. Townsend, A. A., "The Structure of the Turbulent Boundary Layer," Proceedings of the Cambridge Philosophical Society, V. 47, pt. 2, April 1951.

9. Friedman, J., "A Theoretical and Experimental Investigation of Rocket-Motor Sweat Cooling," Journal American Rocket Society, December 1949.

10. Crocco, L., "An Approximate Theory of Porous, Sweat, or Film Cooling with Reactive Fluids," Journal American Rocket Society, November-December 1952.

11. Goldstein, S., (editor), "Modern Developments in Fluid Dynamics," v. 2, Oxford: University Press, 1938.

12. Duwez, P., and Wheeler, Jr., H. L., "Heat Transfer Measurements in a Nitrogen Sweat Cooled Porous Tube," Progress Report No. 4-48, Jet Propulsion Laboratory, California Institute of Technology, Pasadena, California, November 1947.

13. Wheeler, H. L., Jr., "An Empirical Equation for Heat Transfer in a Tube Sweat-Cooled with a Gas," Progress Report No. 4-49, Jet Propulsion Laboratory, California Institute of Technology, Pasadena, California, November 1947.

14. Rubesin, M. W., and C. C. Pappas, "An Analysis of the Turbulent Boundary Layer Characteristics on a Flat Plate with Distributed Light-Gas Injection," NACA TN 4149, February 1958.

15. Dorrance, W. H., and F. T. Dore, "The Effect of Mass Transfer on the Compressible Turbulent Boundary Layer SKin Friction and Heat Transfer," Journal Aeronautical Sciences, June 1954.

16. Clarke, J. H., H. R. Menkes, and P. A. Libby, "A Provisional Analysis of Turbulent Boundary Layers with Injection," Journal Aeronautical Sciences, April 1955.

17. Lapin, Y. V., "Friction and Heat Transfer in a Compressible Turbulent Boundary Layer on a Plate with the Injection of Matter," Soviet Phys. Tech. Phys., 1960.

18. Van Driest, E. R., "On Mass Transfer near the Stagnation Point," North American Aviation Inc. Report No. AL-2553, June 1957.

19. Romanenko, P. N., and V. N. Kharchenko, "The effect of Transverse Mass Flow on Heat Transfer and Friction Drag in a Turbulent Flow of Compressible Gas Along an Arbitrary Shaped Surface," Journal Heat and Mass Transfer, June 1963.

20. Mickley, H. W., and P. S. Davis, "Momentum Transfer for Flow over a Flat Plate with Blowing," NACA TN 4017, November 1957.

21. Turcotte, D. L., "A Sublayer Theory for Fluid Injection into the Compressible Turbulent Boundary Layers," Journal Aerospace Sciences, September 1960.

22. Rannie, W. D., "Heat Transfer in Turbulent Shear Flow," Journal Aeronautical Sciences, May 1956.

23. Rubesin, M. W., "A Modified Reynolds Analogy for the Compressible Turbulent Boundary Layer on a Flat Plate," NACA TN 2917, 1953.

24. Danberg, J. E., "Characteristics of the Turbulent Boundary Layer with Heat and Mass Transfer at M = 6.7," United States Naval Ordance Laboratory, NOL TR 64-99, October 1964.

25. Kreith, F., "Principles of Heat Transfer," International Textbook Company, Scranton, Pennsylvania, 1958.

26. Pappas, C. C., and A. F. Okuno, "Measurements of Skin Friction of the Compressible Turbulent Boundary Layer on a cone with Foreign Gas Injection," Journal Aero/Space Sciences, May 1960.

27. Brunner, M. J., "Transpiration Cooling Test of a Sharp, Sphere-Cone in a Rocket Exhaust Using N_2, He, and H_2O Coolants," ASME paper No. 64-WA/HT-50 (1964)

28. Bartle, E. R., and B. M. Leadon, "The Compressible Turbulent Boundary Layer on a Flat Plate with Transpiration Cooling," Convair Scientific Research Laboratory, Research Report 11, May 1961.

29. Wilke, C. R., "A Viscosity Equation for Gas Mixtures," Journal Chemistry and Physics, April 1950.

30. Pappas, C. C., "Effect on Injection of Foreign Gases on the Skin Friction and Heat Transfer of the Turbulent Boundary Layer," IAS-59-78, January 1959.

31. Denison, R.M., "The Turbulent Boundary Layer on Chemically Active Ablating Surfaces," Journal Aero/Space Sciences, June 1961.

32. Tennekes, H., "Similarity Laws for Turbulent Boundary Layers with Suction or Injection," Journal Fluid Mechanics, V. 21, part IV, 1965.

33. Stevenson, T. N., "A Law of the Wall for Turbulent Boundary Layers with Suction or Injection," CoA. Report Aero No. 166, 1963.

34. Leadon, B. W., "Comments on 'A Sublayer Theory for Fluid Injection,'" Journal Aerospace Sciences, October 1961.

35. Black, T. J., and A. J. Sarnecki, "The Turbulent Boundary Layer with Suction or Injection," Aeronautical Research Council R. and M. No. 3387, 1965.

36. Brunk, W. E., "Experimental Investigation of Transpiration Cooling for a Turbulent Boundary Layer in Subsonic Flow Using Air as a Coolant," NACA TN 4091, October 1957.

37. Spalding, D. B. and S. W. Chi, "The Drag of a Compressible Turbulent Boundary Layer on a Flat Plate with and without Mass Transfer," Journal Fluid Mechanics, January 1964.

38. Spalding, D. B., "Convective Mass Transfer," McGraw-Hill Book Company, New York, 1963

39. Oberth, H. "Methods of Space Travel," Oldenburg, Munchen, 1929.

40. Goddard, R. H., "Rocket Development," Prentice Hall Inc., New York, 1948

41. Meyer-Hartwing, F., "Sweat Cooling of Nozzle Surfaces Under High Thermal Stresses," USAF Translation F-TS-2067, September 1948.

42. Duwez, P., and H. L. Wheeler, Jr., "Experimental Study of Cooling by Injection of a Fluid Through Porous Material," Journal Aeronautical Sciences, September 1948.

43. Green, J. L. and P. Duwez, "Fluid Flow Through Porous Material," Journal Applied Mechanics, March 1951.

44. Wheeler, Jr., H. L., and P. Duwez, "Heat Transfer Through Sweat Cooled Porous Tubes," Jet Propulsion, October 1955.

45. Duwez, P. and Wheeler, Jr., H. L., "An Experimental Study of the Flow of Gas Through Porous Metals," Progress Report No. 1-66 Jet Propulsion Laboratory, California Institute of Technology, Pasadena, California, August 1947.

46. Wheeler, Jr., H. L., "The Influence of Wall Material on the Sweat-Cooling Process," Progress Report No. 4-90, Jet Propulsion Laboratory, California Institute of Technology, Pasadena, California, May 1949.

47. Wheeler, Jr., H. L., and F. O. Myers, "The Pattern of Flow of Gases Leaving Porous Metal Surfaces," Progress Report No. 4-83, Jet Propulsion Laboratory, California Institute of Technology, Pasadena, California, November 1948.

48. Duwez, P., and Martens, H. E., "The Powder Metallurgy of Porous Metals and Alloys Having a Controlled Porosity,: Transactions AIME, 1948.

49. Green, L., "Fluid Flow Through Porous Metals," Progress Report NO. 4-111 Jet Propulsion Laboratory, California Institute of Technology, Pasadena, California, August 1949.

50. Young, D. A., "Various Bureau of Aeronautics Projects," Aerojet Engineering Corporation, 1946-1948.

51. Chauvin, L. T., and H. S. Carter, "Exploratory Tests of Transpiration Cooling on a Porous 8 Degree Cone at M = 2.05 Using Nitrogen Gas, Helium Gas and Water as Coolants," NACA RM-L55-C29, June 1955.

52. Meyer-Hartwing, F. "Sweat Cooling of Nozzle Surfaces Under High Thermal Stress," USAF Translation F-TS-2067, September 1948.

53. Jakob, M., and I. B. Fieldhouse, "Cooling by Forcing a Fluid Through a Porous Plate in Contact with a Hot Plate in Contact with a Hot Gas Stream," Heat Transfer and Fluid Mechanics Institute, University of California, Berkeley, June 1949.

54. Radcliffe, W. F., and E. W. Schwartz, "Vapor Phase Heat Transfer in Porous Media," Convair, Division of General Dynamics, S-51, 20-1, June 1957, (CONFIDENTIAL)

55. Grootenhuis, P. and N. P. W. Moore, "Sweat Cooling--A Review of Present Knowledge and its Application to the Gas Turbine," Iron and Steel Institute, Special Report 43, 1951.

56. Stewart, J. D., "Transpiration Cooling: An Engineering Approach," General Electric, Missile and Space Vehicle Department, GE-TIS R59SD-338, May 1959.

57. Tendeland, T., and A. F. Okuno, "The Effect of Fluid Injection on the Compressible Turbulent Boundary Layer--The Effect on Skin Friction of Air Injected into the Boundary Layer of a Cone at M = 2.7," NACA RM A56D05, June 1956.

58. Barrow, H., "An Experiment on Flat Plate Turbulent Boundary Layer Flow--The Effect of Local Fluid Addition on Friction and Velocity Distribution," Journal Royal Aeronautical Society, February 1958.

59. Tewfik, O. E., "Some Characteristics of the Turbulent Boundary Layer with Air Injection," AIAA Journal, June 1963.

60. Olson, R. M., and E. R. G. Eckert, "Experimental Studies of Turbulent Flow in a Porous Circular Tube with Uniform Fluid Injection Through the Tube Wall," ASME Paper No. 65-APM-29, (1965).

61. Rubesin, M. W., C. C. Pappas, and A. F. Okuno, "The Effect of Fluid Injection on the Compressible Turbulent Boundary Layer--Preliminary Tests on Transpiration Cooling of a Flat Plate at M = 2.7 with Air as the Injected Gas," NACA RM A55I19, December 1955.

62. Rubesin, M. W., "The Influence of Surface Injection on Heat Transfer and Skin Friction Associated with the High--Speed Turbulent Boundary Layer," NACA RM A55L13, February 1956.

63. Mickley, H. S., R. C. Ross, A. L. Squyers, and W. E. Stewart, "Heat, Mass,and Momentum Transfer for Flow over a Flat Plate with Blowing or Suction, NACA TN 3208, July 1954.

64. Hacker, D. S., "Empirical Prediction of Turbulent Boundary Layer Instability Along a Flat Plate with Constant Mass Addition at the Wall," Jet Propulsion, September 1956.

65. Hartnett, J. P., D. J. Masson, J. F. Gross, and C. Grazley Jr., "Mass Transfer Cooling in a Turbulent Boundary Layer," IAS Paper No. 60-66 (1960).

66. Van Driest, E. R., "The Turbulent Boundary Layer for Compressible Fluids on a Flat Plate with Heat Transfer," North American Aviation Rep. AL-1006, February 1950.

67. Leadon, B. M., and C. J. Scott, "Transpiration Experiments in Turbulent Boundary Layer at M = 3.," Journal Aeronautical Sciences, August 1956.

68. Bernicker, R. P., "On Experiment with a Transpiration Cooled Nozzle," AFOSR TN 60-1484, July 1960.

69. Librizzi, and R. J. Cresci, "Transpiration Cooling of A Turbulent Boundary Layer in an Axisymmetric Nozzle," AIAA Journal, April 1964.

70. Hatch, J. E. and S. S. Papell, "Use of a Theoretical Flow Model to Correlate Data for Film Cooling or Heating an Adiabatic Wall by Tangential Injection of Gases of Different Fluid Properties," NASA TN D-130, November 1959.

71. Rashis, B., "Exploratory Investigation of Transpiration Cooling of a 40° Double Wedge Using Nitrogen and Helium as Coolants at Stagnation Temperatures from 1,295° F to 2,910° F," NASA TN D-721, May 1961.

72. Leadon, B. M., and C. J. Scott, "Measurement of Recovery Factors and Heat Transfer Coefficients with Transpiration Cooling in a Turbulent Boundary Layer at M = 3.0 Using Air and Helium as Coolants," Rosemont Aernautical Report 126, University of Minnesota, February 1956.

73. Glenny, E., "The Development of Permeable Materials Potentially Suitable for Effusion Cooled Gas Turbine Components," National Gas Turbine Establishment, Great Britain, NGTE Memo 218, May 1954.

74. Debeau, D. E., "Evaluation of Porous Materials for Boundary Layer Control," Air Material Command, WADC-TR-56-486, November 1956.

75. Hawkins, T. D., Et. Al. "Transpiration and Film Cooling for Solid Propellant Rocket Nozzles," United Nuclear Corporation, Development Division, NDA 2150-1, February 1961.

76. Electromechanical Division, Thompson Ramo Wooldridge Inc., "Feasibility Demonstration of a Transpiration Cooled Nozzle System," First Interim Report, RPL-TDR-63-1036, September 1963.

77. Electromechanical Division, Thompson Ramo Wooldridge Inc., "Feasibility Demonstration of a Transpiration Cooled Nozzle System," Second Interim Report, RPL-TDR-63-1074, December 1963.

78. Electromechanical Division, Thompson Ramo Woldridge Inc., "Feasibility Demonstration of a Transpiration Cooled Nozzle System," Third Interim Report, RDL-TDR-64-42, March 1964.

79. Muskat, M., "The Flow of Homogeneous Fluids Through Porous Media," McGraw-Hill, Inc., New York, 1937.

80. Scheidegger, A. E., "The Physics of Flow Through Porous Media," The MacMillan Company, New York, 1957.

81. Darcy, H., "Les fontaines publiques de la ville de Dijon," 1856.

82. Green, Jr., L., "Heat, Mass and Momentum Transfer in Flow Through Porous Media," ASME Paper 57-HT-19 (1957).

83. Greenberg, D. B., and E. Weger, "An Investigation of the Viscous and Inertial Coefficients for the Flow of Gases through Porous Sintered Metals with High Pressure Gradients," Chemical Engineering Science, March 1960.

84. Lenel, F. V., R. L. Reddy, and O. W. Reen, "Production of Porous Metal Compacts," Powder Metallurgy Laboratory, Rensselaer Polytechnic Institute, November 1954.

85. Grootenhuis, P., "A Correlation of the Resistance to Air Flow of Wire Gauzes," Proceedings of the Institution of Mechanical Engineers, March 1954.

86. Fancher, G. H., and J. A. Lewis, Industrial and Engineering Chemistry, v. 25, 1933, p. 1139.

87. Bakhmeteff, B. A., and N. V. Frodoroff, "Flow Through Granular Media," Transactions ASME, v. 57, 1937.

88. Yuan, S. W., "Cooling by Protective Fluid Films," High Speed Aerodynamics and Jet Propulsion, v. 5, Edited by L. C. Lin, Princeton University Press, New Jersey, 1959, pp 428-481.

89. Eisenklam, P., and L. H. Ford, "Flow Through Porous Materials, Pt. III, Flow Rates at Commencement of Liquid Flow Through Porous Materials," Imperial College of Science and Technology, London, DGGW, EMR-58-9, May 1958.

90. Eisenklam, P., "Flow through Porous Materials. The Retardation of Liquid Flow Rates in Porous Materials. Pt II. The Effect of Gases Dissolved or Entrained in the Liquid," Imperial College of Science and Technology, London, DGGW EMR-55-6, Marcy 1955.

91. Eisenklam, P. "Porous Masses," Chemical Engineering Practice, v. 2, Edited by H. W. Cremer and T. Davies, Butterworths Scientific Publications, London, 1956, pp 342-463.

92. Walton Jr., T. E., and B. Rashis, "Measurement and Empirical Correlation of Transpiration Cooling Parameters on a 25° Cone in a Turbulent Boundary Layer in Both Free Flight and A Hot-Gas Jet," NASA TN D-967, October 1961.

93. Eckert, E. R. G., A. J. Diaguila, and P. L. Donoughe, "Experiments on Turbulent Flow Through Channels Having Porous Rough Surfaces With or Without Air Injection," NACA TN 3339, February 1955.

94. Duwez, P. and H. L. Wheeler, "Experimental Study of Cooling by Injection of a Fluid Through a Porous Material," Journal Aeronautical Sciences, September 1948.

95. Brunner, M. J. (Private communication, April 1966).

96. Evans, R. W., F. J. Crossland, and W. A. Baginski, "Development of Practical Water/Stream Transpiration Cooled Systems," AIAA Paper 65-290 July 1965.

97. Sparrow, E. M., W. J., Minkowycz, and E. R. G. Eckert, "Mass-Transfer Cooling of a Flat Plate with Various Transpiring Gases, AIAA Journal, July 1965.

6.1 General References

1. Bartle, E. R., and B. M. Leadon, "Experimental Evaluation of Heat Transfer with Transpiration Cooling in a Turbulent Boundary Layer at M = 3.2," Journal Aerospace Sciences, January 1960.

2. Bernicker, R. P., "An Investigation of Porous Wall Cooling," AFOSR TN-59-878, June 1959.

3. Donoughe, P. L, and R. A. McKinnon, "Experimental Investigation of Air-Flow Uniformity and Pressure Level on Wire Cloth for Transpiration Cooling Application," NACA TN-3652, January 1956.

4. Duwez, P. and H. L. Wheeler, "Experimental Study of Cooling by Injection of a Fluid Through a Porous Material," Journal Aeronautical Sciences, September 1948.

5. Eckert, E. R. G., and J. B. Livingood, "Comparison of Effectiveness of Convection-, Transpiration- and Film Cooling--Methods with Air as a Coolant," NACA 1182, 1954.

6. Eisenklam, P., P. Grootenhuis, and H. Ziebland, "Transpiration Cooling," Chemical Engineering Practice, V. 2, Edited by H. W. Cremer, and T. Davies, Butterworths Scientific Publications, London, 1956, pp. 609-632.

7. Goddard, R. H., "Combustion Chambers for Aircraft," U.S. Patent 2,183,313 (1938)

8. Grootenhuis, P., "The Flow of Gases Through Porous Metal Compacts," Engineering, April 1949.

9. Grootenhuis, P., "Theoretical and Experimental Studies in Transpiration Cooling," University of London, Ph. D. Thesis, 1957.

10. Hill, J. A. F., "The Permeability of Porous Walls," Massachusetts Institute of Technology, Naval Supersonic Laboratory, MTP-TM-4, September 1956.

11. Leadon, B. M., C. J. Scott, and G. E. Anderson, "Mass Transfer Cooling At Mach Number 4.8," Journal Aeronautical Sciences, 1958.

12. Moore, N. P. W., and P. Grootenhuis, "Improvements Relating to Internal Combustion Turbines and Like Apparatus Working with Gases at High Temperatures," Patent 619,634 (Great Britain), May 1950.

13. Newman, G., "An Investigationsof the Non-adiabatic Flow of Fluids Through a Porous Wall," Ph.D. Thesis, London University, (1958).

14. Spalding, D. B., "Single Formula for the Law of the Wall," Journal of Applied Mechanics, E28, No. 3, 455, 1961.

APPENDICES

APPENDIX A

NOTATION

a	internal surface area of a pore per unit total of frontal cross-sectional area
A	total cross-sectional area
A_1	denotes a function (equation 3.13)
b	free demensionless parameter
B_1, B_2	constants in equation 2.43
B_h	driving force for heat transfer = F/St
B_u	driving force for mass transfer = $\dot{m}u_\infty/\tau_w$
c	perimeter of square pore
c_f	local skin fricition coefficient
$\bar{c}_f$	average skin friction coefficient
c_p	specific heat at constant pressure
d	tube diameter
d_e	hydraulic mean diameter
D_{12}	molecular diffusion coefficient for binary diffusion
E'	a constant in equation 2.67
f	mass fraction of foreign gas
F	blowing rate = $(\rho v)_w/(\rho u)_\infty$
F_c	denotes a function (equation 2.66)
F_{Rx}	denotes a function (equation 2.66)
g	denotes a function (equation 2.66)

h	heat transfer coefficient
J	denotes a function (equation 4.6)
k	thermal conductivity
K	mixing length constant
K_p	permeability coefficient
L	characteristic length
L_p	Prandtls mixing length
M	Mach number
Nu	Nusselt number = hL/k
P	static pressure
Pr	Prandtl number = $c_p\mu/k$
Pr'	turbulent Prandtl number = $\varepsilon_M c_p/\varepsilon_k$
Pr^*	equivalent Prandtl number = $c_{pc}u_\infty/k$
q	heat transfer per unit area
Q	superficial velocity of coolant through porous material
r	recovery factor
R	frictional force per unit surface area of passage exposed to flow
Re_L	Reynolds number = $u_\infty L/\mu_\infty$
Re	Reynolds number per unit length
R_u	universal gas constant
Sc	Schmidt number = $\mu/(\rho D_{12})$
Sc'	turbulent Schmidt number = $\varepsilon_v/(\rho\ \varepsilon_d)$
St	Stanton number for heat transfer = $h/(\rho_\infty\ u_\infty\ c_p)$
St_o	St evaluated in the absence of mass transfer

T	static temperature
T_r	recovery temperature
T^o	stagnation temperature
u	streamwise component of velocity
u^+	demensionless velocity (equation 2.32)
u^*	friction velocity = $(\tau_w/\rho_w)^{0.5}$
W	molecular weight
x	distance downstream measured from leading edge
y	distance normal to the wall
y^+	demensionless distance from the wall (equation 2.32)
z	velocity ratio = u/u_∞

Greek

α, β	resistance coefficients of a porous material
ε_k	eddy thermal conductivity
ε_M	eddy viscosity
δ	turbulent boundary layer thickness
δ^*	displacement thickness
Θ	momentum thickness
ϕ	energy defect of boundary layer
ρ	density
μ	dynamic viscosity
ν	kinematic viscosity
τ	shear stress

Subscripts

o	coolant reservoir condition
l	denotes light gas
i	inlet conditions
e	exit conditions
w	inner wall (exposed to flow)
∞	mainstream condition
a	evaluated at sublayer interface with turbulent boundary layer

APPENDIX B

SAMPLE CALCULATIONS

The calculations presented below are included to illustrate the determination of the following: (1) the mass flow rate required to cool a surface to a typical wall temperature according to the predictions of Rannie (3), Rubesin (4), Spalding, Auslander, and Sundarum (5), and Bartle and Leadon (28); and (2) the change in the mass flow rate which would be necessary to cool the surface to the same temperature if a different freestream temperature were specified.

The following conditions are given:

flow geometry: flat plate

coolant: air

freestream gas: air

$M = 0.3$

$Re_x = 1 \times 10^7$

$P = 1000$ psia

$T_o = 70$ F

$T_w = 2000$ R

First, the mass flow rate necessary to cool a surface to a temprature of 2000 R for a freestream static temperature of 3000 R will be determined.

Rannie's Solution

The final equation obtained from Rannie's analysis is:

$$\frac{T_\infty - T_w}{T_\infty - T_o} = 1 - \frac{\exp\left(-37\ Pr\ F\ Re^{0.1}\right)}{1 + \left(1.18\ Re^{0.1} - 1\right)\left(1 - \exp\left(-37\ F\ Re^{0.1}\right)\right)}$$

The above equation must be solved using a trial and error solution; therefore, assume $F = 0.63 \times 10^{-3}$. Substituting the appropriate values into Rannie's equation gives

$$\frac{3000 - 2000}{3000 - 530} = 0.404$$

$$0.040 \stackrel{?}{=} 1 - \frac{\exp(-37 \times 0.765 \times 0.63 \times 10^{-3} \times 10^{0.7})}{1 + (1.18(10^{0.7}) - 1)\ (1 - \exp(-37 \times 0.63 \times 10^{-3} \times 10^{0.7}))}$$

$$0.404 = 0.404$$

Thus

$$F = 0.63 \times 10^{-3}$$

Rubesin's Solution

The solution due to Rubesin is also simple to employ since the resulting equations of his analysis have been solved and plotted graphically. However, a trial and error solution is required again.

From Figures 4 and 10 in Reference 4, $St_o = 1.5 \times 10^{-3}$ and $r \approx 0.93$ for $Re_x = 1 \times 10^7$. Using the estimated value of recovery factor, the recovery temperature can be found as follows:

$$T_r = T_\infty + \frac{r\ u_\infty^2}{2\ c_p}$$

where

$$u_\infty = M\,(\gamma\, R_u\, T/W)^{0.5}$$

$$= 0.3\,(1.4 \times 53.3 \times 32.2 \times 3000)^{0.5} = 806 \text{ fps}$$

$$T_r = 3000 + \frac{0.93 \times 806^2}{2 \times 0.297 \times 778 \times 32.2} = 3041 \text{ R}$$

The definition of the Stanton number is

$$St = \frac{F\,(T_w - T_o)}{(T_r - T_w)}$$

Assume $F = 0.84 \times 10^{-3}$

$$St = \frac{0.84 \times 10^{-3}\,(2000 - 530)}{(3041 - 2000)} = 1.185 \times 10^{-3}$$

$$\frac{St}{St_o} = \frac{1.185 \times 10^{-3}}{1.5 \times 10^{-3}} = 0.79$$

$$\frac{F}{St_o} = \frac{0.84 \times 10^{-3}}{1.5 \times 10^{-3}} = 0.56$$

From Figure 11 in Reference 28, $St/St_o = 0.79$ when $F/St_o = 0.56$.

Thus

$$F = 0.84 \times 10^{-3}$$

Spalding, Auslander, and Sundarum's Solution

The procedure for calculating the mass transfer rate was outlined in Chapter 2 and is illustrated below. The driving force for heat transfer (B_h) must be calculated first.

$$B_h = \frac{c_{p\infty}(T_\infty - T_w) + r\, u_\infty^2/2}{c_{pc}(T_w - T_o)}$$

Assume r = 0.89.

$$B_h = \frac{0.293 \times 778 \times 32.2\ (3000 - 2000) + 0.89 \times 806^2/2}{0.277 \times 778 \times 32.2\ (2000 - 530)}$$

$$= 0.756$$

To verify the assumed value of the recovery factor, the equation (5)

$$r = (Pr)^{0.33}\ (1 + B_h)^{-0.04}$$

is used. Thus

$$r = (0.765)^{0.33}\ (1 + 0.756)^{-0.04} = 0.89$$

Knowing B_h, the driving force for mass transfer can be determined.

$$B_u = (Pr)^{-0.67}\ B_h$$

$$= (0.765)^{-0.67}\ (0.756) = 0.905$$

The function F_c is taken directly from Table 2(a) for B_u =0.905, M = 0.3, and T_w/T_∞ = 0.67. Thus

$$F_c = 1.067$$

$$F_{Rx} = \frac{\mu_\infty (1 + B_u)^{-0.5}}{\mu_w F_c}$$

$$= \frac{3.69\times10^{-5} (1 + 0.0.905)^{-0.5}}{3\times10^{-5}\times1.067} = 0.836$$

$$F_{Rx}\ Re_x = 0.836\times10^{7} = 8.36\times10^{6}$$

From Table 3 in Reference 5, for $F_{Rx}\ Re_x = 8.36\times10^{6}$,

$$\frac{c_f F_c}{2} = 1.27\times10^{-3}$$

$$\frac{c_f}{2} = \frac{1.27\times10^{-3}}{1.067} = 1.19\times10^{-3}$$

$$\rho_\infty = \frac{P_\infty W}{R_u T} = \frac{1000\times144}{53.3\times3000} = 0.9 \text{ lb/cu ft}$$

$$F = B_u\ c_f/2 = 0.905\times1.19\times10^{-3} = 1.07$$

Bartle and Leadon's Solution

The design temperature ratio function, determined experimentally by Bartle and Leadon, can be used to obtain the desired wall temperature. The function is plotted in Figure 3.4 and the appropriate equation for that curve is

$$R = \frac{T_w - T_o}{T_{ro} - T_w} = (1 + F/3\ St_o)^{-3}$$

It was shown earlier that $T_{ro} = 3041$. Thus

$$R = \frac{2000 - 530}{3041 - 530} = 0.586$$

$$\frac{F}{St_o} = \frac{3}{R^{0.33}} - 3$$

$$= \frac{3}{(0.586)^{0.33}} - 3 = 0.58$$

From the solution due to Rubesin, $St_o = 1.5 \times 10^{-3}$. Thus

$$F = 0.58\ St_o = 0.58 \times 1.5 \times 10^{-3} = 0.87 \times 10^{-3}$$

The second series of calculations were performed for the same set of conditions except for the freestream temperature which was changed to 6000 R. Since the calculation procedures are the same for both cases, they will not be repeated here. The results are compared below.

Table B.1 Comparison of Predicted Blowing Rates for $T_w = 2000$ R, $Re_x = 10^7$, and M = 0.3

Reference	F ($T_\infty = 3000$ R)	F ($T_\infty = 6000$ R)
Rannie	0.63×10^{-3}	2.3×10^{-3}
Rubesin	0.84×10^{-3}	2.2×10^{-3}
Spalding, et. al.	1.07×10^{-3}	3.41×10^{-3}
Bartle and Leadon	0.87×10^{-3}	2.51×10^{-3}

The discrepancy between the results of Spalding, et. al. and the results of Rubesin, and Bartle and Leadon in Table B.1 is due to the use of the Reynolds analogy by the latter two. If the Colburn analogy, as recommended by Spalding, et. al. ($St\ Pr^{0.67} = c_f/2$), had been used for evaluating St_o in the solutions due to Rubesin, and Bartle and Leadon instead of the more simplified form, $St = c_f/2$, then the percent error between any two methods (except Rannie's) would have been less than four percent for $T_\infty = 3000$ and twenty three percent for $T_\infty = 6000$ R.

at this time, enable the most accurate predictions of mass injection rates for a specified surface temperature are recommended and sample calculations are presented in the appendix to illustrate a typical application.

The experimental investigations are discussed from the standpoint of establishing the influence of the various independent parameters on the skin friction coefficient and the rate of heat transfer. A correlation procedure based on the data is shown to agree with the analyses, the problems due to experimental error being considered. A table summarizing over twenty experimental investigations is included.

A solution for the prediction of mass flow rates through porous materials is recommended and the causes of deviations from these predictions are described qualitatively. The various types of porous materials available are discussed and compared on the basis of the most desirable properties.

14. KEY WORDS	LINK A		LINK B		LINK C	
	ROLE	WT	ROLE	WT	ROLE	WT
Transpiration cooling						
Heat Transfer						
Porous Materials						

INSTRUCTIONS

1. ORIGINATING ACTIVITY: Enter the name and address of the contractor, subcontractor, grantee, Department of Defense activity or other organization *(corporate author)* issuing the report.

2*a*. REPORT SECURITY CLASSIFICATION: Enter the overall security classification of the report. Indicate whether "Restricted Data" is included. Marking is to be in accordance with appropriate security regulations.

2*b*. GROUP: Automatic downgrading is specified in DoD Directive 5200.10 and Armed Forces Industrial Manual. Enter the group number. Also, when applicable, show that optional markings have been used for Group 3 and Group 4 as authorized.

3. REPORT TITLE: Enter the complete report title in all capital letters. Titles in all cases should be unclassified. If a meaningful title cannot be selected without classification, show title classification in all capitals in parenthesis immediately following the title.

4. DESCRIPTIVE NOTES: If appropriate, enter the type of report, e.g., interim, progress, summary, annual, or final. Give the inclusive dates when a specific reporting period is covered.

5. AUTHOR(S): Enter the name(s) of author(s) as shown on or in the report. Enter last name, first name, middle initial. If military, show rank and branch of service. The name of the principal author is an absolute minimum requirement.

6. REPORT DATE: Enter the date of the report as day, month, year, or month, year. If more than one date appears on the report, use date of publication.

7*a*. TOTAL NUMBER OF PAGES: The total page count should follow normal pagination procedures, i.e., enter the number of pages containing information.

7*b*. NUMBER OF REFERENCES: Enter the total number of references cited in the report.

8*a*. CONTRACT OR GRANT NUMBER: If appropriate, enter the applicable number of the contract or grant under which the report was written.

8*b*, 8*c*, & 8*d*. PROJECT NUMBER: Enter the appropriate military department identification, such as project number, subproject number, system numbers, task number, etc.

9*a*. ORIGINATOR'S REPORT NUMBER(S): Enter the official report number by which the document will be identified and controlled by the originating activity. This number must be unique to this report.

9*b*. OTHER REPORT NUMBER(S): If the report has been assigned any other report numbers *(either by the originator or by the sponsor)*, also enter this number(s).

10. AVAILABILITY/LIMITATION NOTICES: Enter any limitations on further dissemination of the report, other than those imposed by security classification, using standard statements such as:

(1) "Qualified requesters may obtain copies of this report from DDC."

(2) "Foreign announcement and dissemination of this report by DDC is not authorized."

(3) "U. S. Government agencies may obtain copies of this report directly from DDC. Other qualified DDC users shall request through _____."

(4) "U. S. military agencies may obtain copies of this report directly from DDC. Other qualified users shall request through _____."

(5) "All distribution of this report is controlled. Qualified DDC users shall request through _____."

If the report has been furnished to the Office of Technical Services, Department of Commerce, for sale to the public, indicate this fact and enter the price, if known.

11. SUPPLEMENTARY NOTES: Use for additional explanatory notes.

12. SPONSORING MILITARY ACTIVITY: Enter the name of the departmental project office or laboratory sponsoring *(paying for)* the research and development. Include address.

13. ABSTRACT: Enter an abstract giving a brief and factual summary of the document indicative of the report, even though it may also appear elsewhere in the body of the technical report. If additional space is required, a continuation sheet shall be attached.

It is highly desirable that the abstract of classified reports be unclassified. Each paragraph of the abstract shall end with an indication of the military security classification of the information in the paragraph, represented as *(TS)*, *(S)*, *(C)*, *or (U)*.

There is no limitation on the length of the abstract. However, the suggested length is from 150 to 225 words.

14. KEY WORDS: Key words are technically meaningful terms or short phrases that characterize a report and may be used as index entries for cataloging the report. Key words must be selected so that no security classification is required. Identifiers, such as equipment model designation, trade name, military project code name, geographic location, may be used as key words but will be followed by an indication of technical context. The assignment of links, roles, and weights is optional.

UNCLASSIFIED

Security Classification

DOCUMENT CONTROL DATA - R&D

(Security classification of title, body of abstract and indexing annotation must be entered when the overall report is classified)

1. ORIGINATING ACTIVITY *(Corporate author)*

Jet Propulsion Center
School of Mechanical Engineering
Purdue University, Lafayette, Indiana

2a. REPORT SECURITY CLASSIFICATION

UNCLASSIFIED

2b. GROUP

N/A

3. REPORT TITLE

Transpiration Cooling--Its Theory and Application

4. DESCRIPTIVE NOTES *(Type of report and inclusive dates)*

N/A

5. AUTHOR(S) *(Last name, first name, initial)*

Kelley, John B.

6. REPORT DATE	7a. TOTAL NO. OF PAGES	7b. NO. OF REFS
June 1966	153	111

8a. CONTRACT OR GRANT NO.	9a. ORIGINATOR'S REPORT NUMBER(S)
NsG 592	TM-66-5
b. PROJECT NO.	
c.	9b. OTHER REPORT NO(S) *(Any other numbers that may be assigned this report)* JPC-422
d.	

10. AVAILABILITY/LIMITATION NOTICES

NO RESTRICTIONS

11. SUPPLEMENTARY NOTES	12. SPONSORING MILITARY ACTIVITY
N/A	National Aeronautics and Space Administration

13. ABSTRACT

Transpiration from a porous surface is one of several mass transfer cooling concepts considered for applications in propulsion and related fields. The merits and feasibility of the concept have been demonstrated in numerous theoretical and experimental investigations. The material presented herein comprises a literature review of the various theories proposed and the experimental results obtained in the field of transpiration cooling of turbulent boundary layers.

The over-all objective of the review was to examine the extensive literature pertaining to transpiration cooling and to access the state of the art of this cooling scheme in the following subject areas:

(1) the theoretical analyses pertaining to the correlation of mass injection rates with surface temperature;

(2) the experimental investigations relating to the verification of existing theories and the development of empirical correlations for determining the effects of mass injection on surface heat transfer and skin friction;

(3) the theoretical and experimental studies regarding the characteristics of, and flow through, conventional porous materials.

The more prominent and applicable theories for the turbulent boundary layer with distributed injection are described and compared with the pertinent experimental data. Special emphasis is placed on the physical processes involved in the reduction of heat transfer and skin friction due to transpiration from a porous surface. The theoretical and empirical solutions which,

DD FORM 1 JAN 64 1473

UNCLASSIFIED

Security Classification